

**THE EFFECTS OF MOISTURE AND ASH CONTENT ON
THE PYROLYSIS OF A WOOD DERIVED MATERIAL**

Thesis by
Murray Ross Gray

In Partial Fulfillment of the Requirements
for the Degree of
Doctor of Philosophy

California Institute of Technology
Pasadena, California

1984

(Submitted September 28, 1983)

For W. H. Corcoran, 1920-1982

For Dinah Ann and Ross William

How then am I so different from the first men through this way ?
Like them I left a settled life, I threw it all away
To seek a Northwest Passage at the call of many men
To find there but the road back home again.

Stan Rogers, 1981.

Copyright © by

Murray R. Gray

1983

ACKNOWLEDGEMENTS

I would like to thank Dr. George Gavalas for his thoughtful suggestions and guidance through the second half of this project. He stepped into a difficult situation and gave of his time and energy without stint. The late Dr. William Corcoran was of tremendous assistance during the first half of this project, and gave me insight into not only the work at hand but research in general. His ideas on professional and personal conduct will always guide me. Both men gave me considerable latitude in my investigations and were a pleasure to work with. I am grateful for the chance to have learned from both of them. I would also like to acknowledge Dr. Shaik Qader of JPL for his ongoing interest in my work. George Griffith was a great help in constructing my equipment.

I gratefully acknowledge the financial support of the Natural Science and Engineering Research Council of Canada and the Bechtel Corporation.

Many people helped to make my time at Caltech not only instructive but enjoyable as well. My fellow graduate students contributed suggestions and advice and helped to make my life outside the laboratory happy and stimulating. In particular I thank Teri, Dave, Brian, Puvin, Karl, and Bill. I gratefully acknowledge my mother for her support during my time in California, and for helping me get away from the rigors of research for vacations in Canada.

Most of all I want to thank Dinah for her love and support throughout our time in Pasadena. In a very real way this thesis is hers as well as mine.

ABSTRACT

Moisture and ash are always present in wood to some extent, but their affect on its chemical behavior is not fully known. The influence of moisture and ash on the thermal degradation of wood was investigated by pyrolyzing samples of ground wood waste in a batch fluid-bed reactor at between 320 and 470 ° C in helium at 101-104 kPa. The wood samples were heated at about 300 ° C/ min. so that drying and pyrolysis were simultaneous. Woodex[®] pellets were used in this study because their density was suitable for fluid-bed tests.

In ash-free samples moisture suppressed the formation of pyrolysis tar at temperatures above 390 ° C and increased the yield of char, relative to dry samples. A model for the behavior of free radicals during pyrolysis is proposed which gives qualitative agreement with the observed effect of temperature. The ion-exchange capacity of wood was used to disperse calcium atoms in the polymer matrix, which increased the formation of aqueous product during pyrolysis at the expense of tar by enhancing dehydration and fragmentation reactions. The native mineral components in the wood waste gave effects equivalent to calcium.

The effect of moisture on char yield was independent of the ash components, but the yield of tar from Woodex containing moisture and ash exhibited a minimum at 390 ° C. Below 390 ° C the water hydrated catalyst sites to reduce reactivity. A kinetic model for hydration gave qualitative agreement with the observed effects of temperature. Above 390 ° C the degradation of tar became independent of the availability of catalyst sites, and was suppressed by the effect of water on the concentration of tar within the particles, and on the equilibrium of dehydration reactions.

CONTENTS

ACKNOWLEDGEMENTS(iii)

ABSTRACT (iv)

CONTENTS..... (v)

LIST OF TABLES..... (xi)

LIST OF FIGURES(xiv)

1. INTRODUCTION..... 1

2. WOOD COMPOSITION, CHEMISTRY, AND PHYSICS..... 5

 2.1 Wood Composition..... 5

 2.2 Woodex Chemical Analysis 5

 2.2.1 Polymer Composition..... 5

 2.2.2 Ash Analysis..... 7

 2.2.3 Carboxylate Determination 8

 2.2.4 Infra-red Spectrophotometry..... 9

 2.3 Chemical Properties of Woodex 11

 2.3.1 Reduction in Ash Content 11

2.3.2 Air-Oxidation of Woodex	12
2.4 Woodex Physical Analysis.....	16
2.4.1 Surface Area Determination.....	16
2.4.2 Electron Microscopy and EDAX	20
2.4.3 Swelling of Wood by Water	21
2.4.4 Solvent Exchange of Woodex	23
2.4.5 Glass Transition of Wood Polymers	24
REFERENCES.....	26
3. PYROLYSIS OF WOOD AND RELATED MATERIALS.....	45
3.1 Mechanisms of Pyrolysis.....	46
3.2 Kinetics of Pyrolysis Reactions.....	47
REFERENCES.....	53
4. EFFECT OF MOISTURE ON THE PYROLYSIS OF WOOD EX.....	55
4.1 Introduction and Background	55
4.1.1 Physical Effects of Moisture.....	56
4.1.2 Chemical Effects of Moisture	57
4.2 Experimental	59

4.2.1 Material.....	59
4.2.2 Apparatus and Procedure.....	59
4.3 Results	62
4.4 Discussion.....	63
4.4.1 A Mechanism for the Effect of Moisture on Free Radicals in Wood.....	63
4.4.2 Surface Area of Chars.....	72
4.4.3 Simultaneous [*] Drying and Pyrolysis of Wood.....	73
4.5 Summary.....	76
REFERENCES.....	77
Appendix - Rate of Reaction of Water with Radicals.....	78
5. EFFECT OF INORGANIC COMPONENTS ON THE PYROLYSIS OF WOODEX.....	93
5.1 Introduction and Background	93
5.1.1 Observed Effects of Inorganic Compounds on Pyrolysis of Solids.....	94
5.1.2 Effects of Moisture on Pyrolysis.....	95

5.2 Experimental	96
5.3 Results	98
5.3.1 Effects of Inorganic Components.....	98
5.4 Discussion	100
5.4.1 Effect of Inorganic Components	100
5.4.2 Relative Yields of Products from Woodex and Wood.....	103
5.4.3 Interactions Between Water and Inorganic Compounds	103
5.4.4 Pyrolysis in Carbon Dioxide.....	112
5.5 Summary.....	113
REFERENCES	115
Appendix - Regression Analysis of Tar Data	117
6. CONCLUSIONS AND RECOMMENDATIONS.....	130
6.1 Conclusions.....	130
6.2 Recommendations	133
6.3 Suggestions for Further Research	134

APPENDIX A: KINETIC MODELS OF PYROLYSIS REACTIONS	135
A.1 Two-Reaction Model.....	135
A.1.1 Isothermal Reaction Conditions.....	136
A.1.2 Application of Model to the Data of Iatridis and Gavalas (1979)	137
A.2 Three-Reaction Model	139
A.3 Modified-Three-Reaction Model	142
REFERENCES	146
APPENDIX B: VARPRO SUBROUTINE.....	161
B.1 Description of VARPRO Algorithm	161
B.2 Test Calculation	163
REFERENCES	165
APPENDIX C: REACTOR DESIGN AND PRELIMINARY TESTS	169
C.1 Reactor Design.....	169
C.2 Reactor Operation - Slow Pyrolysis	172
C.2.1 Gas Analysis.....	173

C.2.2 Aqueous Condensate Analysis	174
C.2.3 Tar Analysis	174
C.3 Slow Pyrolysis of Woodex in Nitrogen	174
C.3.1 Products of Woodex Pyrolysis	175
C.3.2 IR Spectra of Char from Pyrolysis of Woodex.....	175
C.3.3 Composition of Condensate Samples	176
C.4 Effect of Heating Rate on Pyrolysis of Woodex	177
C.5 Effect of Initial Composition on Pyrolysis of Woodex.....	179
C.5.1 Effects of Calcium on the Pyrolysis of Woodex.....	179
C.5.2 Effect of Moisture Content on the Pyrolysis of Woodex	180
C.5.3 Effect of Air-Oxidation on the Pyrolysis of Woodex.....	180
REFERENCES	182
APPENDIX D: FLUIDIZATION TESTS AND MATERIAL SELECTION	192
D.1 Prediction of Fluidization Velocity in Reactor	192
D.2 Experimental	193
D.3 Results and Material Selection	194
REFERENCES	196

LIST OF TABLES

Table	Title	Page
Table 2.1	Composition of Whole Woodex Pellets	28
Table 2.2	Woodex Ash Analysis	28
Table 2.3	Woodex Infra-red Absorption Peaks	29
Table 2.4	Ash form Acid Washed Woodex	30
Table 2.5	Composition of Acid Washed Woodex	30
Table 2.6	Effect of Acid Wash and Extraction on Carboxylate Content of Woodex	31
Table 2.7	Woodex Oxidation	31
Table 2.8	Analysis of Oxidized Sample 3	32
Table 2.9	Carboxylate and Ash Content of Air-Oxidized Woodex	32
Table 2.10	Infra-red Absorbance of Air-Oxidized Woodex	33
Table 2.11	Infra-red Absorbance of Air-Oxidized Woodex after Ca Exchange	33
Table 2.12	Woodex Surface Area	33
Table 3.1	Aqueous Products from Pyrolysis of Wood	54
Table 4.1	Variation Between Replicate Samples	81
Table 4.2	Yields of Products from Dry Ash-free Woodex	81
Table 4.3	Yields of Products from 16%-Moist Ash-free Woodex	82
Table 4.4	Yields of Liquid Products from Ash-free Woodex	83
Table 4.5	Yields of Products from Moist Ash-free Woodex at 396°C	84
Table 4.6	Nitrogen Surface Areas of Chars	84
Table 4.7	Rate Constants for Pyrolysis	84
Table 4.8	Hop Ratio for Douglas Fir Wood	85

Table	Title	Page
Table 4.9	Aqueous Condensate from Woodex Pyrolysis at 390°C	85
Table 4.10	Gas and Condensate from Woodex at 390°C	86
Table 4.11	Time Constants for Heating of Woodex	86
Table 4.12	Rate Constants for Reaction of Water with Free Radicals	87
Table 4.13	Rate of Reaction of Water with Free Radicals	87
Table 5.1	Ash Content of Samples	119
Table 5.2	Variation Between Replicate Samples	119
Table 5.3	Yield of Char from Woodex at Different Ash Levels	120
Table 5.4	Yields of Products from Woodex at Different Ash Levels	120
Table 5.5	Yield of Liquid Products from Woodex at Different Ash Levels	121
Table 5.6	Yields of Products from Untreated Dry Woodex	122
Table 5.7	Product Yields from Untreated 16%-Moist Woodex	122
Table 5.8	Yields of Products from Untreated 28%-Moist Woodex	123
Table 5.9	Yields of Gaseous Compounds	123
Table 5.10	Yield of Products from Untreated Woodex	124
Table 5.11	Effect of Fluidizing Gas on Pyrolysis of Woodex at 460°C	125
Table 5.12	Hydrate Behavior in Moist Wood	125
Table A.1	Fractional Yields from the Pyrolysis of Lignin	147
Table A.2	Kinetic Parameters for Pyrolysis of Lignin (from Two-Reaction Model)	148

Table	Title	Page
Table A.3	Kinetic Parameters for Pyrolysis of Lignin (from Modified Three-Reaction Model)	148
Table B.1	Data for Test of VARPRO Routine	166
Table B.2	Optimum Parameters from VARPRO Test Case	167
Table C.1	Reaction Conditions for Pyrolysis of Woodex in N ₂	183
Table C.2	Yields of Products from the Pyrolysis of Untreated Woodex in Nitrogen	183
Table C.3	IR Absorbance Ratios of Char from Pyrolysis of Woodex	184
Table C.4	Condensate Analysis from Pyrolysis of Woodex in N ₂	184
Table C.5	Reaction Operating Conditions- Compositional Tests	185
Table C.6	Material Balance for Ca-Exchanged Woodex	185
Table C.7	Composition of Condensate from Ca-Exchanged Woodex	186
Table C.8	IR Absorbance Ratios of Char from Pyrolysis of Woodex	186
Table C.9	Material Balance for Moistened Woodex	187
Table C.10	Composition of Condensate from Moistened Woodex	187
Table C.11	Material Balance for Oxidized Woodex	188
Table C.12	Composition of Condensate from Oxidized Woodex	189
Table D.1	Fluidization Velocities in Nitrogen at NTP	196

LIST OF FIGURES

Figure	Title	Page
Figure 2-1	Infra-red Spectrum of Woodex	34
Figure 2-2	Infra-red Spectra of Woodex Components	35
Figure 2-3	Effect of Oxidation in Air at 195°C on Carboxylate Content of Woodex	36
Figure 2-4	Effect of Oxidation in Air at 195°C on Weight of Woodex	37
Figure 2-5	Effect of Ca-Exchange on Ash-free Weight of Air-Oxidized Woodex	38
Figure 2-6	Effect of Oxidation in Air at 195°C on Ash Content of Ca-Form Woodex	39
Figure 2-7	IR Spectra of Oxidized Woodex	40
Figure 2-8	Effect of Air Oxidation on Absorbance of Woodex at 1725 cm. ⁻¹	41
Figure 2-9	Effect of Air Oxidation on Absorbance of Woodex at 3400 cm. ⁻¹	42
Figure 2-10	Effect of Air Oxidation on Absorbance of Woodex at 1615 cm. ⁻¹	43
Figure 2-11	Gas Adsorption Apparatus	44
Figure 4-1	Pyrolysis Reaction Apparatus	88
Figure 4-2	Details of Reactor	89
Figure 4-3	Effect of Moisture on Yield of Tar from Ash-free Woodex	90
Figure 4-4	Effect of Moisture on Yield of Char from Ash-free Woodex	91
Figure 4-5	Cleavage of Cellulose Linkage	92

Figure	Title	Page
Figure 4-6	Reaction of Water with Radicals	92
Figure 4-7	Reaction of Water with Molecular Groups	92
Figure 5-1	Effect of Temperature on Products of Untreated Woodex	126
Figure 5-2	Effect of Moisture on Yield of Char from Untreated Woodex	127
Figure 5-3	Effect of Moisture on Yield of Tar from Untreated Woodex	128
Figure 5-4	Yield of Aqueous Product from Untreated Moist Woodex	129
Figure A-1	Gas from Pyrolysis of Lignin (Data of Iatridis and Gavalas) Curves from Two-Reaction Model Equal wts.	149
Figure A-2	Gas from Pyrolysis of Lignin (Data of Iatridis and Gavalas) Curves from Two-Reaction Model Gas Only	150
Figure A-3	Gas from Pyrolysis of Lignin (Data of Iatridis and Gavalas) Curves from 3-Reaction Model Gas Only	151
Figure A-4	Char from Pyrolysis of Lignin (Data of Iatridis and Gavalas) Curves from 3-Reaction Model Gas Only	152
Figure A-5	Gas from Pyrolysis of Lignin (Data of Iatridis and Gavalas) Curves from 3-Reaction Model Gas and Char	153

Figure	Title	Page
Figure A-6	Char from Pyrolysis of Lignin (Data of Iatridis and Gavalas) Curves from 3-Reaction Model Gas and Char	154
Figure A-7	Volatiles from Pyrolysis of Lignin (Data of Iatridis and Gavalas) Curves from 3-Reaction Gas and Char	155
Figure A-8	Arrhenius Plot for Pyrolysis of Lignin, Model to Fit Gas Data, 3-Reaction Model	156
Figure A-9	Arrhenius Plot for Pyrolysis of Lignin, Model to Fit Gas and Char Data, 3-Reaction Model	157
Figure A-10	Char from Pyrolysis of Lignin (Data of Iatridis and Gavalas) Curves from Mod. 3-Reaction Model Gas and Char	158
Figure A-11	Gas from Pyrolysis of Lignin (Data of Iatridis and Gavalas) Curves from Mod. 3-Rxn. Model Gas and Char	159
Figure A-12	Arrhenius Plot fro Pyrolysis of Lignin, Model to Fit Gas and Char Data, 3-Reaction Model	160
Figure B-1	Convergence of VARPRO Routine	168
Figure C-1	Fluid-Bed Reactor System	189
Figure C-2	Details of Reactor	190
Figure C-3	Effect of Temperature on Product of Pyrolysis of Woodex	191
Figure D-1	Fluidization Test Apparatus	197

1. INTRODUCTION

Waste biomass materials such as sawmill and crop wastes are currently burned or buried for disposal. Given appropriate technology such potential raw materials could be utilized to provide fuel gas or chemical feedstocks. Two conversion pathways are currently under development, but both types of process have been used in one form or another throughout recorded history. The first, thermal conversion, is rapid and energy efficient for feedstocks with a relatively low water content. The second, biological conversion of biomass proceeds more slowly with lower degrees of conversion but with greater selectivity for a given product. Wastes which contain a high fraction of water and which are easily attacked by microorganisms or enzymes are the most suitable. Each biomass material has certain characteristics which render it suitable for one or the other approach. Wood wastes such as sawdust, wood chips, and bark have an equilibrium water content of at most about 40% at room conditions. The cellulose fraction of wood is attacked only very slowly by microorganisms due to the presence of lignin, so that pretreatment steps are required. The lignin polymers which constitute a large fraction of wood wastes are only attacked over long periods of time by molds and fungi. Wood is much more suited to thermal conversion processes where the low initial water content is exploited. The thermal processes such as pyrolysis produce a dry char that is easily burned in conventional boilers.

Thermal processes seek to decompose the wood structure into useful products or intermediate products. All such processes involve pyrolysis reactions to some extent. The term *pyrolysis* denotes thermal degradation of an organic compound in either an inert atmosphere or, if air is present, under very fuel-rich conditions so that combustion is not initiated. When any solid material

is pyrolyzed, physical and chemical effects influence the course of the reactions. When a biological material such as wood is pyrolyzed, a whole range of factors can affect the process. The solid can contain minerals which exert catalytic effects. The moisture content could vary considerably from sample to sample. Weathering of the wood by oxidants can introduce chemical changes which could alter the course of the reactions. At the present time such fundamental effects are poorly understood. An understanding of the influence of mineral content, moisture content, and exposure to oxidants is important for the development of processes for the thermal conversion of biomass.

The present work concentrates on the behavior of wood waste, which is produced in large quantities as a byproduct of pulp and paper and lumber production. A particular wood waste product called Woodex was selected for experimental use because of its convenient pellet form. Wood wastes contain large amounts of inorganic salts and minerals and have a high moisture content. The wastes are high in bark components, because the bark of the tree has little value in any conversion process. Although the makeup of wood waste is different from wood itself, its chemical composition and behavior are not dissimilar, as we shall see later. The terms *wood*, *wood waste*, and *Woodex* will be used interchangeably throughout this report.

The purpose of the present work was to determine the impact of mineral and moisture content on the pyrolysis of wood waste by measuring the product distribution over a range of temperatures. Using a fluid-bed reactor it was possible to react well mixed samples at uniform temperatures and achieve an overall material balance of better than 95% on average. Previous investigations were restricted in scope because of several limitations: material balances were not reported, analyses of the starting material and products were not

performed, or only one or two aspects of pyrolysis were analyzed, normally the weight of solid residue or the composition of the gas. The fluid-bed reactor allowed collection and analysis of samples of all of the pyrolysis products of wood. The polymer and ash content of the starting material was measured, as were the compositions of the gas and aqueous products. The infra-red absorbance and surface areas of the wood and the char residue were measured to check for physical and chemical changes. Electron and visible light microscopy were employed to view physical changes directly.

Chapter 2 presents the results of a series of analyses and tests on the chemical and physical composition and behavior of Woodex. Important properties such as ion-exchange capacity and swelling by solvents are considered. Chapter 3 covers the mechanisms and kinetics of the pyrolysis reactions, using material drawn from the literature. The effects of moisture on the pyrolysis of ash-free Woodex are presented in Chapter 4. A speculative mechanism is proposed to explain the observed yields of tar with temperature, wherein the moisture serves to facilitate free-radical reactions. The effects of ash constituents in dry and moist samples are covered in Chapter 5. The chemical effects of the ash are discussed in terms of the chemistry of analogous base catalysts. The effects of moisture on the catalytic ash reactions are explained in terms of hydration of active sites and reaction equilibrium. Chapter 6 lists the conclusions and recommendations from this work.

The appendices present supplementary information on kinetic modelling and development of the experimental methods that were used in this study. In Appendix A a series of kinetic models were applied to data on lignin pyrolysis (from the literature) to determine whether simple lumped models could predict the yields of char, tar, and gas. The trial models showed that the approach was

of quantitative use in predicting yields but that any inference to the actual kinetic mechanisms had to be approached with caution. This work served as a background for the simple kinetic model in Chapter 4. Appendix B describes a mathematical routine for fitting experimental data to non-linear models in a least squares sense. Appendix C presents the results of early experiments on the fluid-bed reactor and is intended to show how the final experimental techniques were developed. Appendix D describes the fluidization experiments that preceded the design of the reactor apparatus.

2. WOOD COMPOSITION, CHEMISTRY, AND PHYSICS

2.1 Wood Composition

Woody plants contain three structural polymers (Grabowski and Bain, 1979; Sarkanen and Ludwig, 1971) :

cellulose - a polysaccharide of repeating glucose units

hemicellulose - a polysaccharide containing monomers such as xylose glucose and glucuronic acid. Xylose polymers are called xylans.

lignin - a random polymer of substituted methoxyphenols joined by ether and carbon-carbon linkages.

Cellulose and hemicellulose chains are mixed in the cell wall which is bonded to an encrusting layer of lignin. Cellulose and hemicellulose together are often referred to as holocellulose. Wood also contains extractives such as mineral salts, oils, tannins, and starches. The composition of bark is similar to wood, with smaller amounts of polysaccharides and larger amounts of salts and extractives. The polyphenol portion of bark is lower in methoxy groups than "true" lignins from wood.

2.2 Woodex Chemical Analysis

2.2.1 Polymer Composition.

2.2.1.a Method The polymer composition of the feed material must be known in order to understand its behavior under reaction conditions. The extractives were removed by following *ASTM D-1105-56 Standard Method for Preparation of Extractive Free Wood*. A 5 gram sample was placed in a Soxhlet extraction apparatus and extracted with a 1:1 mixture of benzene and 95% ethanol for four hours. The sample was washed with ethanol to remove the benzene and

extracted for four hours in 95% ethanol. The sample was then extracted for one hour with each of three one-liter portions of water at 100 ° C. The sample was dried overnight at 105 ° C and weighed.

The lignin content was determined by the Klason lignin method, with modifications suggested by Sarkanen and Ludwig (1971). 72% sulfuric acid decomposed the holocellulose content of the wood to simple sugars and dissolved some lignin. The lignin was precipitated by refluxing the sample in dilute sulfuric acid. The raw lignin was filtered out of the dilute acid, and treated with a sodium hydroxide solution to remove polyphenols, giving Klason lignin.

Holocellulose was determined in two ways. In one, the weights of lignin, ash, and extractables were subtracted from the total weight of the wood sample to give the weight of holocellulose. The holocellulose content was obtained directly by a chlorine dioxide-bleach technique given by Hagglund (1951). A sample of extract-free Woodex was slurried in 0.5N HCl at 80 ° C, and 1-2 grams of sodium chlorite were added to generate chlorine dioxide. The ClO₂ reacted with the aromatic lignin structures to form carbon dioxide and HCl, leaving behind the holocellulose.

The cellulose content of the holocellulose was determined by *ASTM D1103-60 Standard Test Method For α -Cellulose in Wood*. The holocellulose from the ClO₂ bleach was treated with 17.5% NaOH to remove the hemicellulose and cellulose containing less than 100 glucose units. The sample was then washed with 8.3% NaOH solution followed by distilled water, 10% acetic acid, and finally distilled water. The sample was dried overnight at 105 ° C and weighed.

Ash content was determined by heating samples in flowing oxygen at 1200 ° C in a Leco furnace . The ash content of untreated Woodex was measured as well as the ash content of the separated lignin and cellulose.

2.2.1.b Results The analyses given in Table 2.1 for whole Woodex pellets indicate excellent agreement between the Kraft-lignin and chlorite-bleach determinations so that either may be used with confidence. Table 2.5 shows the results of an analysis of 60-100 mesh ground Woodex. The 80-100-mesh-size fraction which was analyzed had a higher polyphenol content and a lower holocellulose content than did the whole pellets. Clearly some fractionation of the polymers took place when the pellets were sieved and ground. The particles which were larger than 60 mesh were more resistive to grinding and were higher in holocellulose.

2.2.2 Ash Analysis.

2.2.2.a Method Woodex ash was analyzed by following *ASTM D-2795-69 Standard Methods of Analysis of Coal and Coke Ash*. One ash sample was fused with NaOH and then dissolved to make a solution which was used for the spectrophotometric determination of Al and Si. Another ash sample was dissolved in hydrofluoric acid, treated with concentrated sulfuric and nitric acids and then diluted to make the solution which was employed to determine the Ca, Mg, and Fe contents of the ash. The Ca and Mg contents of the solution were determined by an EDTA (ethylenediamine-tetra-acetic acid) titration, using calcein and phtalein purple indicators. The Fe content was determined spectrophotometrically using the complex of iron and phenanthroline.

2.2.2.b Results An analysis of Woodex ash is listed in Table 2.2. Woodex is much higher in minerals than is wood which typically contains 0.8 to 2.2% ash, depending on the tree species and bark content of the sample (Mills and Rowan, 1889). Wood ash is about 50% calcium oxide. The composition of the Woodex ash suggests that some soil minerals were included in the pellets.

2.2.3 Carboxylate Determination

2.2.3.a Method A procedure developed by Schafer (1970) for determining the carboxylic-acid- group content of lignite was applied to Woodex. A 125-mg. sample of ground 60-100 mesh Woodex was refluxed for 4 hours with 50 ml. of 1N-calcium-acetate solution which had been adjusted to pH 8.3 with dilute NaOH. The refluxed mixture was titrated back to pH 8.3. The carboxylic acid groups in the wood preferentially picked up calcium ions and released acid to the solution. The carboxylate content of the wood was calculated from the volume of titrant as follows:

$$n_c = \frac{V_{\text{NaOH}} N_{\text{NaOH}}}{1000 w} \quad (2.1)$$

n_c = carboxylate content, gram-equivalent/gram sample

V_{NaOH} = volume of NaOH titrant, cm^3

N_{NaOH} = normality of NaOH solution, g. mole/liter

w = weight of sample, grams.

Special care was taken to ensure that the pH measurements were reproducible. The pH was measured with a calomel-glass- electrode pair and a Beckman SS-20 pH meter. The calomel electrode was kept filled with saturated-KCl solution in the presence of KCl crystals. The electrode was stored in saturated-KCl solution when not in use. Prior to a determination, the electrodes were placed in a pH 7 buffer solution for half an hour to equilibrate. At the end of the half hour the meter was calibrated to pH 7. The electrode pair was then immersed in a buffer solution of pH 4 to check the response of the meter. The pH of the sample solution was then determined.

Each sample was filtered from the solution after the potentiometric titration and dried overnight at 105 ° C. The samples were then weighed to

determine how much soluble material was lost during the determination.

2.2.3.b Results The carboxylate content of untreated Woodex was 0.77 mg.equivalent/gram. The calcium-acetate solution became colored when the sample was refluxed because some of the wood components were dissolved. After the potentiometric titration, the wood sample was filtered, washed, dried overnight, and weighed. The sample showed a net loss in weight of 7.5%, despite the uptake of calcium ions. The ash content of the dried sample was 11.8%, up from 6.86% before Ca exchange.

2.2.4 Infra-red Spectrophotometry

2.2.4.a Method Dried samples of Woodex or derivatives of Woodex were ground with dry potassium bromide. The powdered mixture was compressed to 10,000 psi in an evacuated press to form a disk. A Beckman IR4240 Spectrophotometer scanned the infra-red spectrum between wave numbers 4000 cm^{-1} and 500 cm^{-1} to record the % transmission for each disk. The absorption for the major peaks between 4000 cm^{-1} and 1500 cm^{-1} was calculated by means of the baseline method, which is illustrated in Figure 2-1 for a typical Woodex spectrum (Kagler,1973). Table 2.3 lists the locations of the major peaks which appear in Figure 2-1 and gives the origin of each peak. The peak assignments are from Hergert (1971). The peak at 1725 cm^{-1} was of the greatest interest because it derived from the carboxylic acid groups in the sample.

The absorption was calculated from the measured peak heights using the following equation, which was derived from Beer's law:

$$A = \ln(D_{100\%} / D_p) = \epsilon c d \quad (2.2)$$

A = absorption at a given wavelength

$D_{100\%}$ = distance from baseline to 0% transmission line

D_p = distance from 0% transmission line to tip of peak

ϵ = molar extinction coefficient, grams/(g.mole-cm.)

c = concentration of functional species, g.moles/gram of KBr disk

d = path length of light through the sample, cm.

As the size of a given peak in the infra-red spectrum increases, the value of the absorption for the peak will increase. Equation (2.2) demonstrates that the absorption of a band is proportional to the concentration of the sample. Due to the difficulty in assigning values to the concentration of a given species in a solid mixture, ratios of absorbances from a given Woodex spectrum were related to ratios from other spectra. In some cases a band was unaffected by the reactions of interest and was used as an internal standard. The absorption of the standard band was divided into the other absorption values in the same spectrum to eliminate the effect of variations in sample weight. The ratio of the absorbances of the two peaks will be the ratio of the molar extinction coefficients (a constant) times the ratio of the concentrations.

2.2.4.b Results Figure 2-2 depicts the spectra of the cellulose, lignin, and extractive fractions of Woodex. All of the components exhibited absorption in the 3400 cm^{-1} and 2800 cm^{-1} bands due to C-H and O-H groups. The spectrum of the extractives exhibited significant absorption at 1700 cm^{-1} due to carboxylic acid groups. The other samples exhibited no evidence of carboxylic acid content. The spectra of the lignin and the extractives contained major peaks due to aromatic groups in the $1400\text{-}1600\text{ cm}^{-1}$ range. Cellulose exhibited only a small absorbance in the same region due to residual water and lignin groups.

The above results confirm the assigned identity of the peaks in the infra-

red spectrum of Woodex, since the structure of cellulose and lignin are known. An interesting observation was the significant aromatic nature of the extractives which revealed that polyphenols such as tannins and humic acids were predominant in the extractive portion of Woodex.

2.3 Chemical Properties of Woodex

2.3.1 Reduction in Ash Content

2.3.1.a Method The standard techniques for demineralizing coal cannot be applied to wood because concentrated acids would hydrolyze all of the polysaccharides in the sample. Consequently, dilute solutions of HCl at room temperature and pressure were used to determine the extent of ash removal. Samples of ground 60-100 mesh Woodex were stirred with 0.5N, 1.0N, and 2.0N HCl solutions in the ratio of 50 ml. of acid/gram of wood at 25 ° C for 7 hours. Each sample was weighed before and after the acid treatment, and burnt to determine the ash content. Acid concentration had little effect on the extent of removal of ash, so 0.5N HCl was used to prepare all further samples.

2.3.1.b Results An analysis of ash from acid-washed Woodex is listed in Table 2.4. The treatment with dilute HCl removed almost all of the Ca, Mg, Na, and K, and over half of the iron. The resistance of iron to acid leaching indicated that a large fraction of the iron was in discrete mineral particles.

A sample of acid-washed Woodex was analyzed for its polymer constituents, and the results are given in Table 2.5. The main effects were a reduction in the extractive content from 11.49% to 6.98%, due to the removal of water-soluble material, and a reduction in the ash content from 6.86% to 4.83%.

When samples of holocellulose which had been acid-washed were viewed under an optical microscope, opaque mineral particles were clearly visible and

were enmeshed in strands of holocellulose fiber. The particles of mineral matter were distinct but held by the strands on a microscopic scale.

The carboxylate and ash contents of Woodex before and after acid treatment are listed in Table 2.6. The acid wash increased the carboxylate content from 0.77 to 0.88 mg. equiv./gram., presumably by removing metal cations and freeing sites for exchange. Extract-free Woodex had a carboxylate content between the values for untreated and acid-washed Woodex. From the infra-red spectra of the wood components, we would expect extraction to reduce the carboxylate content, because only the extractives exhibit the characteristic absorption of the carbonyl group. The carboxylate contents from Table 2.6 show that the holocellulose and lignin fractions must also contain a significant number of acid groups. Consequently the *isolated* cellulose and lignin must differ in carbonyl content from the polymers in the wood, due to chemical changes induced by the reagents used in the separation of the polymers.

The hot-water wash used in the ASTM extraction procedure was more effective for demineralizing the Woodex than was stirring in 0.5N HCl but it dissolved more of the wood as well. All of the samples lost weight during the Ca-exchange procedure, but the extract-free sample lost the least weight because the soluble constituents had already been removed.

The carboxylate determinations showed that while the acid removed cations from the wood, the wash also removed phenolic acids. Hence the net effect of an acid-wash on the carboxylate content was small.

2.3.2 Air-Oxidation of Woodex

2.3.2.a Method Reactions between wood samples and oxygen were carried out in an oven at atmospheric pressure which was controlled with a thermocouple sensor and equipped with a circulating fan to give uniform temperatures.

Ground samples of Woodex were placed in covered crucibles in the oven and allowed to react with the oxygen in the air. The samples were weighed at timed intervals to determine the weight loss due to oxidative reactions. One gram samples were used to prevent overheating and autoignition of the wood. The exothermic oxidation reactions cause local heating which can ignite the sample.

A series of one-gram samples of 60-100 mesh Woodex which had been vacuum dried were oxidized in air at 195 ° C for measured times. The carboxylate content of each sample was determined. After the carboxylate determination for each sample, the Ca-exchanged wood was filtered on sintered glass and washed with deionized water. A portion of each Ca-exchanged sample was saved for an IR spectrum measurement, and the remainder was ashed. A replicate sample filtered on cellulose exhibited a reduction in ash content due to the removal of calcium from the wood to the filter paper. A second replicate sample was washed with deionized water which had been adjusted from the usual pH 7.8 to pH 8.5. No difference in the ash content was detected.

The nature of the ion-exchange groups in the wood and how they were affected by reaction with oxygen were investigated by infra-red spectrophotometry. Spectra were recorded of dried samples of air-oxidized Woodex and air-oxidized Woodex which had been Ca-exchanged. The absorption of the peak at 2920 cm^{-1} which was due to stretching of the C-H bond in methyl and methylene groups was used as an internal standard to correct for sample size (Hergert, 1971). The methylene and methyl groups were associated with lignin in the sample and were unaffected by exposure to oxygen at relatively low temperature and atmospheric pressure.

2.3.2.b Results Samples of Woodex pellets that were heated in air for several days gradually lost weight until a relatively constant weight was reached (see

Table 2.7.). The amount of moisture initially present in the samples had a measurable effect on the weight loss. The vacuum dried sample which was heated at 121 ° C lost 5% less weight than did a similar sample which had not been dried.

Sample 3 was analyzed to determine the effect of the weight loss on the chemical composition. The ClO₂- bleach method was used for the analysis, and results are given in Table 2.8. The data indicated that the weight loss was due to evaporation of the extractables and to decomposition of the holocellulose. The degree of polymerization of the cellulose was significantly reduced as indicated by the small percentage of cellulose.

Table 2.9 summarizes the results for the samples oxidized at 195 ° C. The major effect was the increase in the carboxyl content from 0.88 mg. equiv./g. to 2.68 mg. equiv./g. after 23.5 hours of heating in air. The change in carboxylate content with reaction time is shown graphically in Figure 2-3. The carboxylate content increased linearly with reaction time within the accuracy of the data.

As the Woodex was heated it lost mass due to the evolution of water and carbon dioxide. Figure 2-4 shows the downward trend of the sample weight with reaction time. When the oxidized samples were refluxed with calcium-acetate solution, some of the sample dissolved and colored the solution. The color ranged from light brown for untreated Woodex to dark gray for the Woodex oxidized for 23.5 hours. Figure 2-5 shows that the weight of Woodex recovered from the reflux procedure appears to pass through a maximum after about ten hours of reaction.

When the Ca-exchanged samples were ashed, the weight of ash was lower than expected based on the assumption that all of the calcium picked up by ion exchange would be present in the ash as CaO. Figure 2-6 shows that there was a

significant difference between the measured and predicted ash contents. When the holocellulose in the Woodex was oxidized in air, the polysaccharide polymer chains broke down into short segments and monomers and the individual monomer sugars were attacked at the C-O linkage. Reaction of oxygen at the C-O bond gave rise to uronic acids, which tended to dissolve when not attached to a polymer chain. Thus the acid sites generated by air-oxidation were distributed between soluble and insoluble entities. The former were lost in the Ca-exchange procedure while the latter remained in the solid matrix.

Table 2.10 gives the adjusted absorption measurements for the major identifiable peaks in the infra-red spectra of oxidized Woodex. Figure 2-1 shows the locations and relative sizes of the important peaks. The peak at 2920 cm^{-1} , which was due to C-H bond, was used to eliminate the effect of sample size. The absorptions corrected by dividing by A_{2920} are designated A' . The values of A'_{1510} show little change with the extent of oxidation. The peak at 1510 cm^{-1} was due to aromatic skeletal vibrations which would not be affected by the oxidation conditions; hence the lack of change in A'_{1510} was an internal confirmation of the method used. The IR spectra before and after oxidation are depicted in Figure 2-7, and illustrate the trends in the absorption.

Figures 2-8, 2-9, and 2-10 show the effect of oxidation on the absorption of Woodex at 3400 , 1725 and 1615 cm^{-1} . As would be expected the absorption at 1725 cm^{-1} increased with the time of oxidation because this peak was due to carboxyl groups. Absorption at 3400 and 1615 cm^{-1} went through a maximum relative to A_{2920} . These peaks were influenced by water and OH groups. The appearance of a maximum in the absorption indicated that the total OH content was determined by competing reactions which added and removed OH groups.

Table 2.11 lists the corrected absorbances for the air-oxidized samples

after Ca exchange. The addition of calcium to the carboxyl groups eliminated the absorption at 1725 cm^{-1} . The formation of the salt shifted the peak to the $1590\text{-}1560\text{ cm}^{-1}$ range of C=O stretching (Hergert, 1971). This shift contributed to the increase in the absorption of the peak at 1615 cm^{-1} and to the broadening of this peak. The peak at 1725 cm^{-1} was not eliminated by the formation of the calcium salt, indicating that unconjugated ketone groups were present. The same effect was observed by Schafer (1970). The increase in absorption at 1725 cm^{-1} with oxidation showed that some ketone groups were formed by the oxidation reactions. The effect of ion exchange on the spectra is illustrated in Figure 2-7. The addition of calcium increased the equilibrium water content of the Woodex due to hydration of the metal ions (Schafer, 1972). An increase in the amount of hydrated water was responsible for the increase in the absorption at 3400 cm^{-1} and for a part of the increase at 1615 cm^{-1} . The reduction in absorption at 1510 cm^{-1} with the time of reaction indicated that the formation of a salt influenced the vibrations of aromatic groups in the sample.

2.4 Woodex Physical Analysis

2.4.1 Surface Area Determination

2.4.1.a Method Surface areas were determined by gas adsorption in the apparatus depicted by Figure 2-11. The apparatus consisted of two dosing volumes and a sample cell, with associated gas supplies, gauges and a vacuum pump. The pressure of the gas in the primary-dosing volume was measured by a Wallace and Tiernan gauge or by a Pirani gauge. The Pirani-type gauge was useful only at very low pressures when the sample was being evacuated.

The volume of the primary-dosing volume was measured by gas exchange with a sample bulb of known volume. The volume of the sample bulb was

determined by evacuating it to less than 0.001 torr and then filling it with methanol at 23.5° C. The weight of the bulb after filling with methanol, less the initial weight of the bulb when evacuated, divided by the density of methanol at 23.5° C, gave the bulb volume of 1128.1 cm³. The sample bulb was attached to the primary-dosing volume, and the whole assembly was evacuated to less than 0.001 torr. The volume of the primary-dosing volume was measured by allowing helium gas to expand from the dosing volume into the sample bulb. With the assumption of ideal-gas behavior, the volume of the dosing volume may be calculated from the measured pressures:

$$V_d = \frac{P_2 V_b}{P_1 - P_2} \quad (2.3)$$

V_d = primary-dosing volume

V_b = sample-bulb volume

P_1 = initial pressure

P_2 = final pressure

The volume of gas adsorbed onto a solid sample was determined by introducing gas into the primary-dosing volume and then opening the valve to the sample cell and allowing the system pressure to equilibrate. More gas was then added to the dosing volume, and the process was repeated. The volume of adsorbate was given by a balance on the gas in the sample cell and the primary-dosing volume.

$$v_{ads,i} = (P_{1,i} V_d + P_{eq,i-1} V_{dv} - P_{eq,i}(V_d + V_{dv})) \frac{T_s}{T_r P_r W} + v_{ads,i-1} \quad (2.4)$$

$v_{ads,i}$ = volume adsorbed in the i^{th} step, cc/gram

$P_{1,i}$ = initial pressure, i th step

$P_{eq,i}$ = final pressure, i th step

V_{dv} = sample-cell dead volume

T_s = standard temperature, 273° C

T_r, P_r = room temperature and pressure

w = weight of sample

The dead volume of the sample cell was determined by gas exchange of helium between the sample cell and the primary-dosing volume.

2.4.1.b BET Surface Area Determination The theory of Brunauer, Emmet and Teller (1938) was employed to interpret data from nitrogen adsorption. The BET theory as applied to surface area determinations is discussed fully elsewhere (Kralik, 1981, Clark, 1970, Browning, 1963). The fundamental equation is:

$$\frac{P}{v_{ads}(P_o - P)} = \frac{1}{c x_m} + \frac{c-1}{c x_m} \frac{P}{P_o} \quad (2.5)$$

P = system pressure at equilibrium

P_o = adsorbate vapor pressure

v_{ads} = volume adsorbed at pressure P (cm^3 at STP/gram of sample)

x_m = volume of adsorbate in monolayer (cm^3 at STP/gram of sample)

A least-squares fit of a plot of $\frac{P}{v_{ads}(P_o - P)}$ vs $\frac{P}{P_o}$ for the range $0.05 < \frac{P}{P_o} < 0.35$ gives a slope of $\frac{c-1}{c x_m}$ and an intercept of $\frac{1}{c x_m}$. The value of x_m is given by:

$$x_m = \frac{1}{\text{slope} + \text{intercept}} \quad (2.6)$$

The area is then calculated:

$$S_a = \frac{x_m N_o A_a}{V_a} \quad (2.7)$$

S_a = surface area (cm² / gram)

N_o = Avogadro's number

V_a = 22, 414 cm³ at STP / mole

A_a = molecular-cross-sectional area

= 16.2 x 10⁻¹⁶ cm² /molecule for N₂

Seven to ten adsorption points between 5 and 35% of atmospheric pressure were taken. Fifteen minutes were allowed at each step for the system to achieve equilibrium, and each time the dewar was filled to overflowing with liquid nitrogen to ensure a consistent liquid level around the sample cell.

2.4.1.c DPR Surface Area Determination Surface areas for several samples were calculated by applying the Kaganer modification of the Dubinin-Polanyi-Radushkevich (DPR) theory to CO₂ -adsorption data measured at room temperature (Kralik, 1981). The relevant equation is:

$$\ln(a) = \ln(a_m) - k_1 R^2 T^2 \ln^2 \frac{P}{P_o} \quad (2.8)$$

a = moles adsorbate/gram adsorbent

a_m = moles adsorbate/gram adsorbent in a monolayer

k_1 = a constant which characterizes the

Gaussian distribution of adsorption potentials

A least-squares fit of $\ln a$ vs $\ln^2 \frac{P}{P_o}$ calculated from the adsorption data yielded $\ln(a_m)$ as the intercept. The surface area was calculated from Equation (2.7) using a value of 23.4 x 10⁻¹⁶ cm² for the cross-sectional area of a molecule of CO₂.

Approximately ten adsorption points were measured per sample at pressures up to 1 atm. Five minutes were allowed at each step for equilibration to take place.

2.4.1.d Measured Surface Areas The surface area of Woodex was determined by both N₂ and CO₂ adsorption. Using the BET equation on the nitrogen adsorption isotherm a surface area of 2.75 m²/gram was calculated. The use of the DPR equation on the CO₂ adsorption isotherm gave a value of 98.7 m²/gram. As in the case of coal, the surface area determined by carbon dioxide adsorption was greater than the BET area (Kralik, 1981). The Woodex area was greater than the value of 0.22 m²/gram for sugar pine reported by Stamm and Millett (1944), from stearic acid absorption, or the value of 1.59 m²/gram for the surface area of paper measured with N₂ adsorption by Emmett and DeWitt (1941).

2.4.2 Electron Microscopy and EDAX

2.4.2.a Method A sample of Woodex which had been acid-washed and then Ca-exchanged was examined with a Tracor Northern Model TN-1700 EDAX probe attached to an International Scientific Instruments Model Super II electron microscope. EDAX is an acronym for Energy Dispersive Analyzer of X-rays. The probe detected the x-rays which were emitted by the Woodex sample when bombarded with electrons. The EDAX probe can map the location of a given element in two-dimensions. A window of x-ray energies was selected which corresponded to the emissions of a given element. The area of view was then scanned, and whenever x-rays of the selected energies were detected, a blip appeared on the screen. A map of the area resulted which indicated a concentration of an element in a zone.

A sample such as wood must be protected from a buildup of static electricity. A layer of conducting material was laid down over the sample to

prevent such problems. Either gold or carbon may be used. Gold shows up as a strong peak in the EDAX spectrum, but does not obscure the peaks of any other elements of interest in this case.

2.4.2.b Results A sample of Woodex, which had been acid-washed and then Ca-exchanged, was examined with the Energy Dispersive Analyzer of X-Rays (or EDAX) probe of a scanning electron microscope (SEM). The EDAX probe measured the X-rays emitted when electrons bombarded a sample.

The EDAX probe was used to scan areas of the surface of the Woodex and to determine the composition at selected points. Scans of silicon, iron, and aluminum energies showed that these elements were concentrated in discrete grains. Point measurements on these areas showed that little calcium was associated with the other minerals. Scans of calcium energies showed an even distribution of the metal. Point measurements on wood particles showed only calcium.

The above results confirm that aluminum and silicon (with iron to a lesser extent) occurred together in discrete particles of mineral material. Calcium was easily detected and was well distributed through the the Woodex sample so that no concentrated regions were observed in EDAX maps of calcium. We expect that similar scans on Woodex that had not been washed with acid would show calcium, iron, sodium, magnesium, and aluminum associated with the wood, as well as the mineral particles.

2.4.3 Swelling of Wood by Water The moisture content of cellulosic materials has a direct bearing on their physical characteristics. Wood polymers are hygroscopic and swell upon the absorption of water. Dry-wood fiber typically has a surface area of $0.4 \text{ m}^2/\text{g}$. as measured by nitrogen adsorption while water-swollen fibers have a surface area of $100\text{-}300 \text{ m}^2/\text{g}$.(Browning,1963). Other polar

solvents also cause swelling, depending on the degree of hydrogen bonding. When water-swollen wood is dried, the expanded structure collapses, and the surface area returns to its former value. The surface area is largely preserved when the fibers are successively extracted with solvents of decreasing polarity and then dried.

The swelling of wood is not completely reversible. When green wood is dried, the original adsorption isotherm for water can never be regained. Some of the hygroscopic capacity of the wood is lost (Browning, 1963). Gorbaty (1978) observed a similar irreversible loss of structure when a sample of subbituminous coal was dried.

The amount of surface area available for gas-solid reactions and the pore structure of the carbonaceous material will have a large effect on the course of pyrolysis reactions. The fact that moisture content can have a significant effect on the surface areas of biomass materials has not yet been fully recognized in the gasification literature.

2.4.4 Solvent Exchange of Woodex

2.4.4.a Method A sample of 60-100 mesh ground Woodex was solvent exchanged to prepare a dry sample which retained the swollen structure of water saturated wood. The sample was slurried with deionized water and allowed to stand for 24 hours. The slurry was then poured into a separatory funnel, and the water was drained off. Anhydrous methanol was added to the sample in 15 ml.-aliquots and drained off at a rate of 2 ml./min. until a total of 200 ml. of methanol had been used. The methanol displaced the water while maintaining the wood structure. Anhydrous n-pentane was added in the same manner to displace the methanol. The sample was dried by flowing dry nitrogen through the funnel for three hours. The sample was then stored over activated, 4-angstrom molecular sieves. Moisture was excluded from the sample during and after the solvent exchange in order to maintain the swollen wood structure.

Anhydrous methanol was prepared by reacting 5 g. of magnesium turnings with 40 ml. of methanol to form the Grignard reagent, magnesium methoxide. The reaction was started by heating the mixture with a heat gun and adding a crystal of iodine to initiate the reaction. When all of the magnesium had reacted, a liter of methanol was added to the Grignard reagent, and the methanol was distilled into a flask containing activated 4 angstrom -molecular sieves. Anhydrous n-pentane was prepared by shaking pentane with activated molecular sieves. The 4-angstrom -molecular sieves were activated by heating to 400 ° C for 48 hours.

2.4.4.b Results The effect of solvent exchange on surface areas is given in Table 2.12. While solvent exchange increased the N₂ area from 2.75 m²/gram to 4.2 m²/gram , the CO₂ surface was essentially unchanged. The CO₂ surface area did not quantify the accessible surface area of the wood.

The increase in the surface area of Woodex due to solvent exchange was much less than other workers have found for similar materials. Thode et al. (1958) found that the N_2 -surface area of cellulose fibers exchanged with methanol and n-pentane increased from less than $1 \text{ m}^2/\text{gram}$ to $100 \text{ m}^2/\text{gram}$. Stamm and Millett (1944) reported that the surface area of sugar-pine wood increased from $0.22 \text{ m}^2/\text{gram}$ when measured by stearic acid absorption from benzene solution to $400 \text{ m}^2/\text{gram}$ when measured by water absorption from glycerol solution. The former area would be the collapsed surface area, while the latter would approach the fully swollen surface area. The absence of such dramatic increases in the surface area of Woodex after solvent exchange could be due to the high lignin content of the Woodex or the pelletizing procedure.

2.4.5 Glass Transition of Wood Polymers Any amorphous polymer, such as lignin, polyphenol, or hemicellulose can undergo a glass transition. Above the glass transition temperature the polymer becomes a plastic material. Lignins soften in the range of $125 - 200^\circ \text{C}$, depending on the molecular weight and water content of the polymer (Goring, 1971). Addition of moisture to the polymer lowers the glass transition temperature. The presence of 27% moisture in a spruce lignin lowered the softening temperature to 90°C as compared to 195°C for a dry sample. The drop in the glass transition temperature was linearly proportional to the water content of the sample. Polyphenols, xylans, and mannans all exhibited similar behavior due to their amorphous structure. Cellulose softened above 230°C , but its glassy transition was unaffected by moisture because of its crystalline structure (Goring, 1971).

Molecular weight influenced the glassy transition temperature. The lower the molecular weight, the lower the softening temperature of wood polymers. Such results were in accord with observations on synthetic amorphous polymers

(Goring, 1971).

2.4.5.a Optical Microscopy of Woodex Chars Several samples of char from Woodex were examined under a microscope at 100-150x magnification. The chars were prepared at temperatures ranging from 330 ° C to 470 ° C in helium. The particles of char were viewed by reflected light.

The particles of char were very smooth and glossy in appearance, resembling an anthracite coal. Two trends were noted with temperature:

- [1] The number of fibrous particles decreased with increased temperature. The char which had been prepared at 470° C contained no fibres. Some particles showed surface striations which resembled fibrils encased in a glossy plastic material.
- [2] At higher temperatures some particles were glassy and translucent, with evidence of gas bubbles and glass-like fracture faces.

At pyrolysis temperatures the amorphous polymers softened and melted. Such behavior would be more pronounced in Woodex than in wood samples because of its high bark content and small cellulose fraction. Indeed, the thermoplastic behavior of the polymers was exploited in forming Woodex into pellets, by the application of heat and pressure.

In considering the mechanism for the evolution of gases from Woodex during pyrolysis, we should think largely in terms of bubble formation and evolution. Fibers of cellulose would be surrounded by molten organic material. The molten Woodex would not be a simple fluid, because the fibers would hinder the evolution of bubbles. Nevertheless the best description for the Woodex particles above 300 ° C is a fluid, similar to a caking coal.

REFERENCES

- [1] Browning, B.L., in *The Chemistry of Wood*, ed. B.L. Browning, Wiley, New York, 1963.
- [2] Brunauer, S., Emmett, P.H., and Teller, E.J., *J. Am. Chem. Soc.* **60**, 309, 1938.
- [3] Clark, A., *The Theory of Adsorption and Catalysis*, Academic Press, New York, 1970.
- [4] Emmett, P.H., and DeWitt, T., *Ind. Chem. Eng. Anal. Ed.* **13(1)**, 28-33, 1941.
- [5] Gorbaty, M. L., *Fuel* **57**, 796-797, 1978.
- [6] Goring, D. A. I., in *Lignins*, eds. Sarkanen, K.V., and Ludwig, C.H., Wiley, New York, 1971.
- [7] Graboski, M., and Bain, R., in *A Survey of Biomass Gasification Vol II- Principles of Gasification*, Solar Energy Research Inst., July, 1979.
- [8] Hagglund, E., *Chemistry of Wood*, Academic Press, New York, 1951.
- [9] Hergert, H.L., in *Lignins*, eds. Sarkanen, K.V., and Ludwig, C.H., Wiley, New York, 1971.
- [10] Kagler, S.H., *Spectroscopic and Chromatographic Analysis of Mineral Oil*, Halsted Press, London, 1973.
- [11] Kralik, J.G., *An Investigation of the Applied Chemistry of the Reactions of Coal and Nitrogen Dioxide with a Particular Emphasis on Oxidative Desulfurization*, Ph.D. Thesis, California Institute of Technology, 1981.
- [12] Mills, E.J., and Rowan, F.J., *Fuel and Its Applications, Vol.1 of Chemical Technology*, C.E. Groves and W. Thorp eds., P. Blakiston & Son Co., Philadelphia, 1889.

- [13] Sarkanen, K.V., and Ludwig, C.H. in, *Lignins*, eds. Sarkanen, K.V., and Ludwig, C.H., Wiley, New York, 1971.
- [14] Schafer, H. N. S., *Fuel* **49**, 8-13, 1970.
- [15] Schafer, H.N.S., *Fuel* **51**, 4-9, 1972.
- [16] Stamm, A.J. and Millett, M.A., *J. Phys. Chem.* **45**, 43-54, 1944.
- [17] Thode, E.F., Swanson, J.W., and Becher, J.J., *J. Phys. Chem.* **62**, 1036-1039, 1958.

Table 2.1. Composition of Whole Woodex Pellets		
Component	Klason Lignin Detn. (weight %)	ClO ₂ Cellulose Detn. (weight %)
Extractables	11.49	11.49
Polyphenols	37.26	37.82
(Lignin)	(23.72)	-
Holocellulose	44.99	44.43
(Cellulose)	-	(21.44)
Ash	6.26	6.26
Total	100	100

Table 2.2. Woodex Ash Analysis	
Compound	Weight %
SiO ₂	46.73
Al ₂ O ₃	31.5
Fe ₂ O ₃	9.46
CaO	9.56
MgO	1.86
Na ₂ O,K ₂ O	0.89
Total	100

Peak	Wavenumber, cm^{-1}	Origin
1	3400	Hydrogen-bonded OH groups
2	2920	C-H bonds
3	1725	Carboxylic acid groups
4	1610	Aromatic skeletal vibration, carboxylate groups and water
5	1510	Aromatic skeletal vibration coupled to C-H stretch

Table 2.4. Ash From Acid-Washed Woodex			
	Initial	Acid-Washed	Fraction Removed
Total ash, wt.%	7.83	4.83	0.38
Component	wt.% of Initial Ash		
Removed by acid	-	38.31	-
SiO ₂	46.73	30.32	0.35
Al ₂ O ₃	31.5	27.50	0.13
Fe ₂ O ₃	9.46	3.57	0.62
CaO	9.56	0.30	0.97
MgO	1.86	-	1.0
Na ₂ O,K ₂ O	0.89	-	1.0
Total	100	100	

Table 2.5. Composition of Acid-Washed 60-100 mesh Woodex		
Component	Untreated Woodex (weight %)	Acid-Washed Woodex (weight %)
Extractables	11.49	6.98
Polyphenols	48.00	50.93
Holocellulose	33.66	37.26
(Cellulose)	(20.17)	-
Ash	6.86	4.83
Total	100	100

Table 2.6 Effect of Acid Wash and Extraction on Carboxylate Content of Woodex			
	Untreated Woodex	ASTM-Extractive-Free Woodex	Acid-Washed Woodex
Carboxylate, mg.equiv./g.	0.77	0.81	0.88
% Recovery from Ca-exch.	93.5	96.2	95.5
% Ash before Ca-exch.	6.86	4.51	4.63
% Ash after Ca-exch.	8.47	5.51	7.25
% Ash Predicted	11.17	7.76	9.56

Table 2.7. Woodex Oxidation				
Sample	T ° C	Time (hr)	Final Wt.(% of initial)	Sample Preparation
1	121	235	89.8	none
2	121	315	94.4	vacuum dried
3	172	113	89.7	same

Table 2.8. Analysis of Oxidized Sample 3		
Component	Initial Wt.%	Wt.% After Heating
Lost Weight	0	10.28
Extractables	11.49	6.17
Polyphenols	37.82	37.46
Holocellulose	44.43	40.61
(Cellulose)	(21.44)	(8.26)
Ash	6.26	5.48
Total	100	100

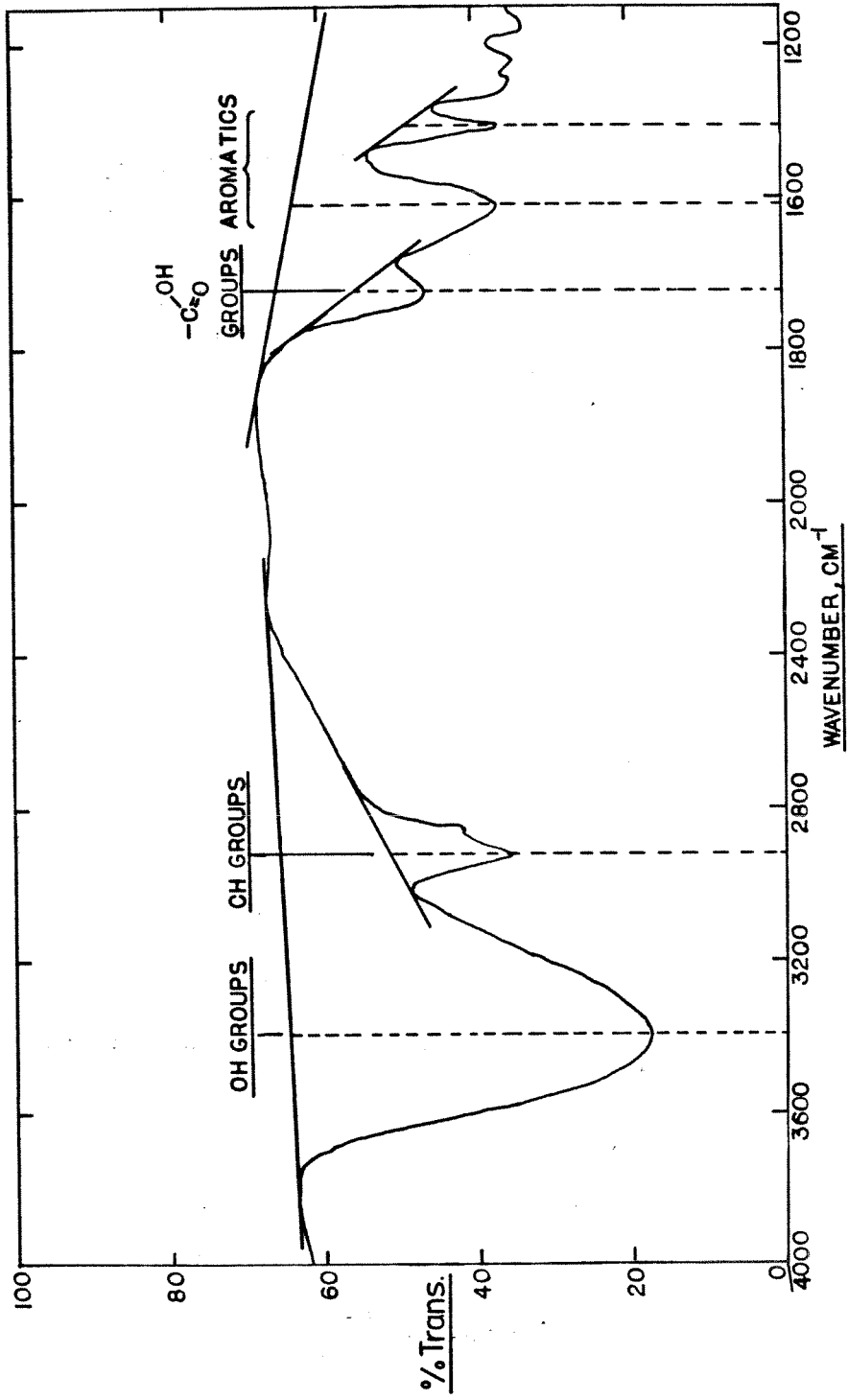
Table 2.9 Carboxylate and Ash Content of Air-Oxidized Woodex Reaction at 195 ° C and Atmospheric Pressure						
Reaction time,hr.	0	5	10	10.5	17.5	23.5
Carboxylate,mg.equiv./g.	0.88	1.36	1.62	1.63	1.82	2.68
% of Initial Wt.	100.	95.2	88.9	88.9	86.2	79.2
% Recovery from Ca-exch.	92.5	93.6	95.4	91.1	93.2	88.5
Ash-free Basis						
% Cumulative Recovery	92.5	89.1	84.9	-	-	70.1
% Ash before Ca-exch.	4.63	4.87	5.11	5.20	5.37	5.85
% Ash after Ca-exch.	7.25	9.26	9.90	-	-	15.02
% Ash Predicted	9.56	12.49	14.18	-	-	20.86

Table 2.10 Infra-Red Absorbance of Air-Oxidized Woodex				
Reaction at 195 ° C and Atmospheric Pressure				
Reaction time,hr.	0	10.5	17.5	23.5
A' ₃₄₀₀	3.55	5.07	6.34	4.82
A' ₁₇₂₅	0.489	1.30	1.43	1.51
A' ₁₆₁₅	1.52	2.48	3.11	2.53
A' ₁₅₁₀	0.78	0.94	0.70	0.69

Table 2.11 Infra-Red Absorbance of Air-Oxidized Woodex after Ca Exchange				
Reaction at 195 ° C and Atmospheric Pressure				
Reaction time,hr.	0	10.5	17.5	23.5
A' ₃₄₀₀	3.44	5.54	6.92	8.88
A' ₁₇₂₅	0.19	0.30	0.62	0.67
A' ₁₆₁₅	1.92	3.25	4.60	6.39
A' ₁₅₁₀	0.62	0.41	0.42	0.19

Table 2.12 Woodex Surface Area, m ² /gram		
Dry Samples	Untreated Woodex	Solvent-Exchanged Woodex
N ₂ Adsorption	2.75	4.2
CO ₂ Adsorption	98.7	103.3

FIGURE 2-1 INFRA-RED SPECTRUM OF WOODDEX



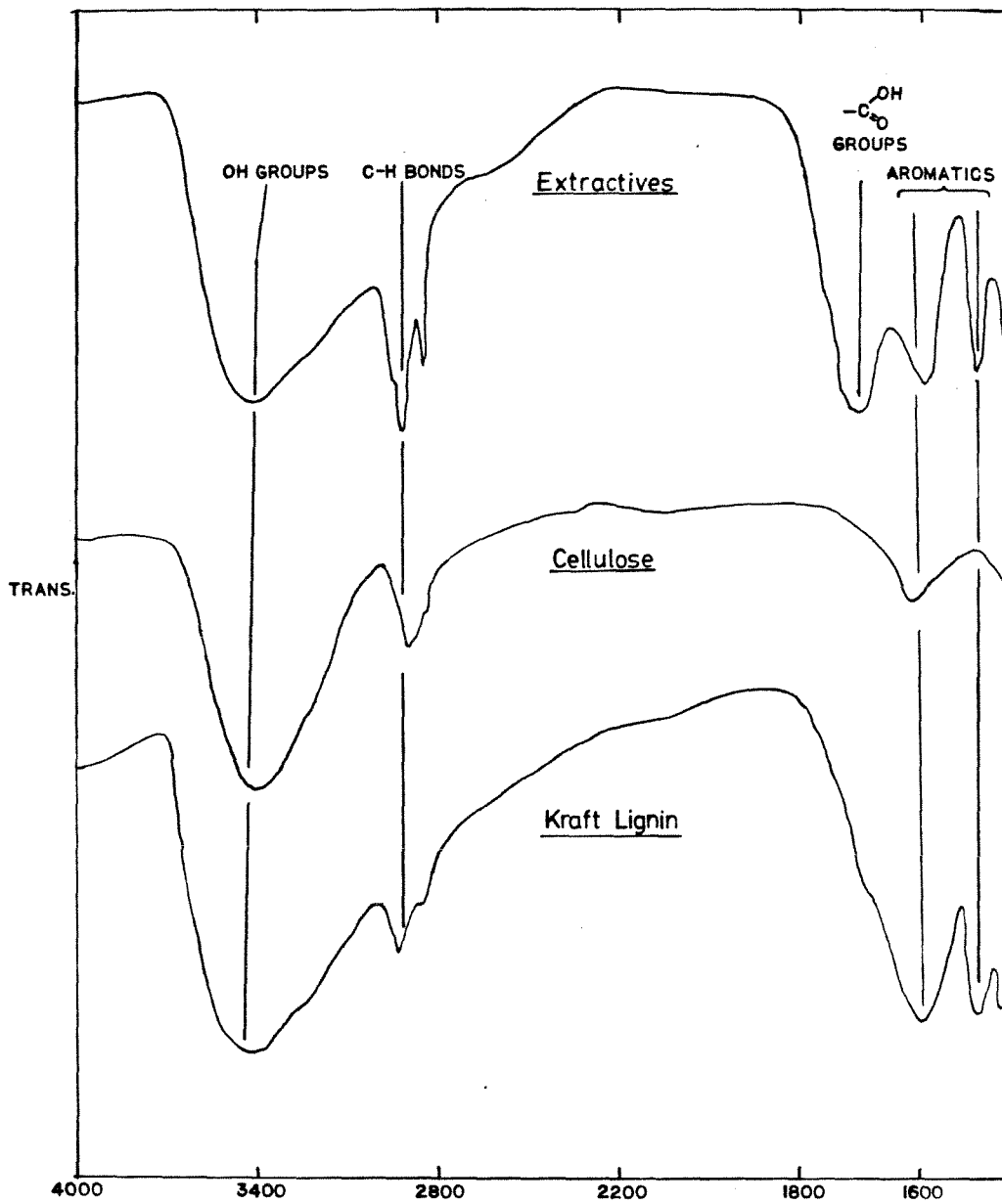


FIGURE 2-2 INFRARED SPECTRA OF
WOODEX COMPONENTS

(SAMPLES IN KBr WAFERS)

FIGURE 2-3
EFFECT OF OXIDATION IN AIR AT 195C
ON CARBOXYLATE CONTENT OF WOODDEX

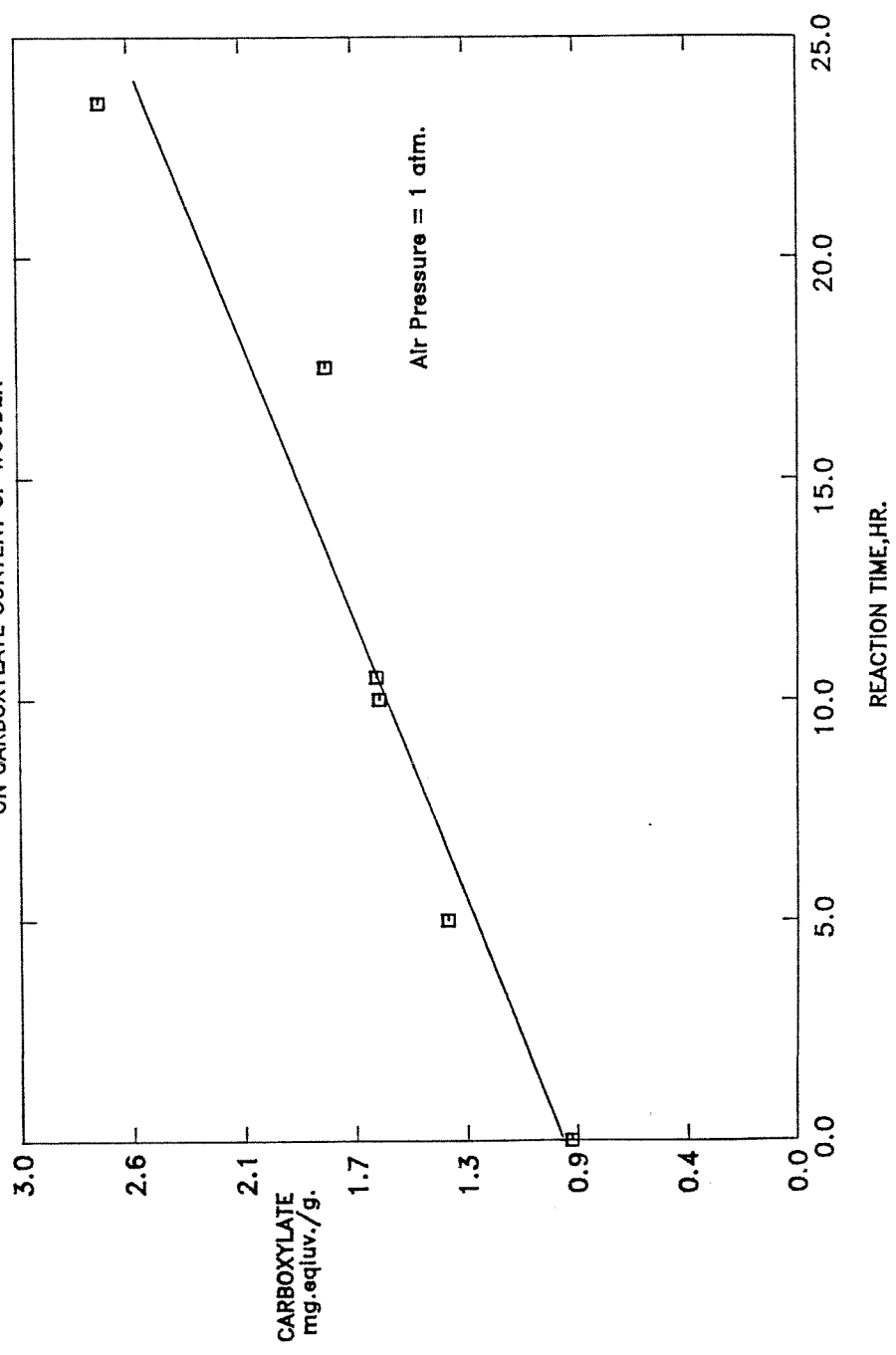


FIGURE 2-4
EFFECT OF OXIDATION IN AIR AT 195C
ON WEIGHT OF WOODDEX

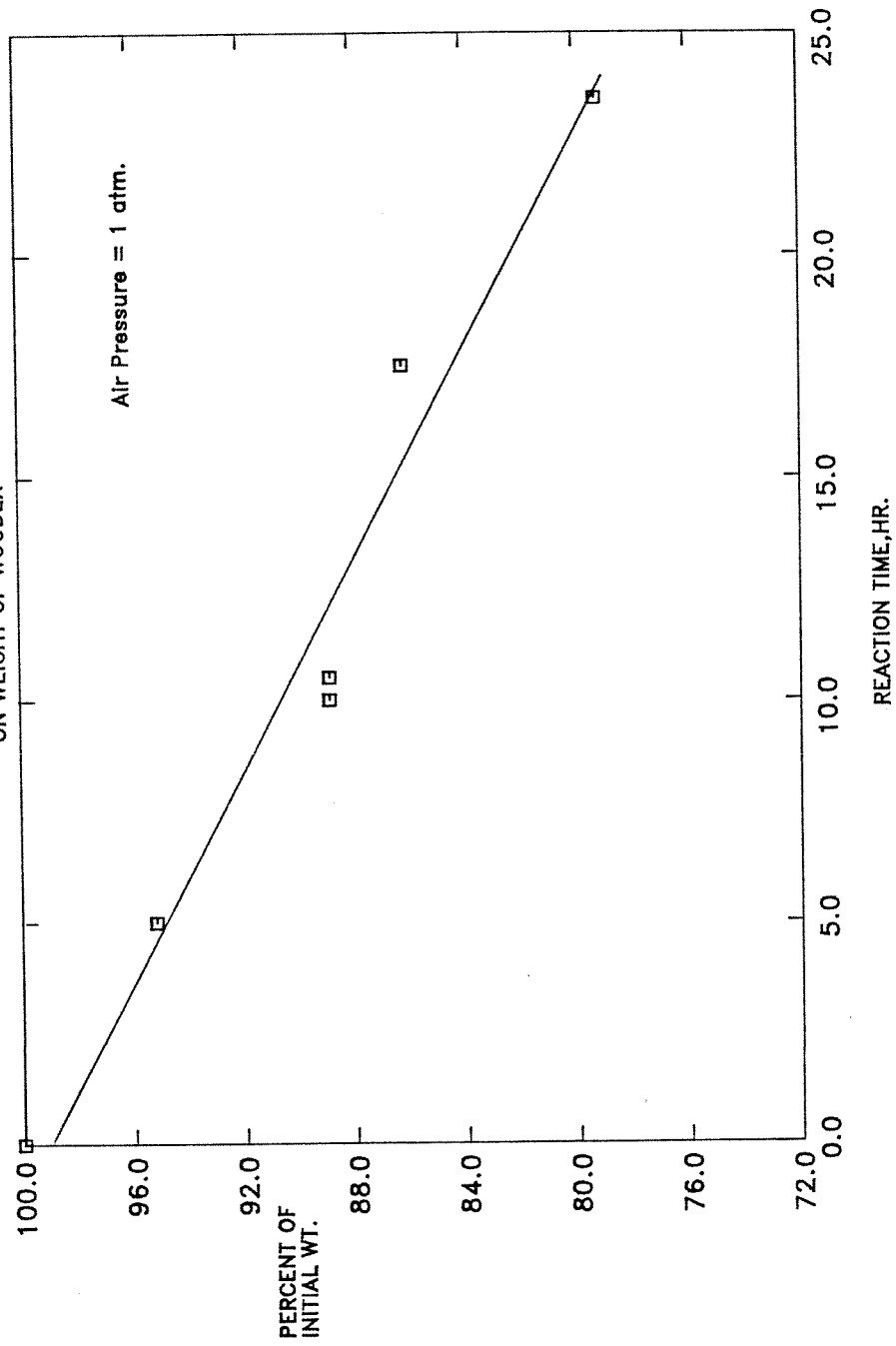


FIGURE 2-5
EFFECT OF CA-EXCHANGE ON ASH-FREE
WEIGHT OF AIR-OXIDIZED WOODDEX

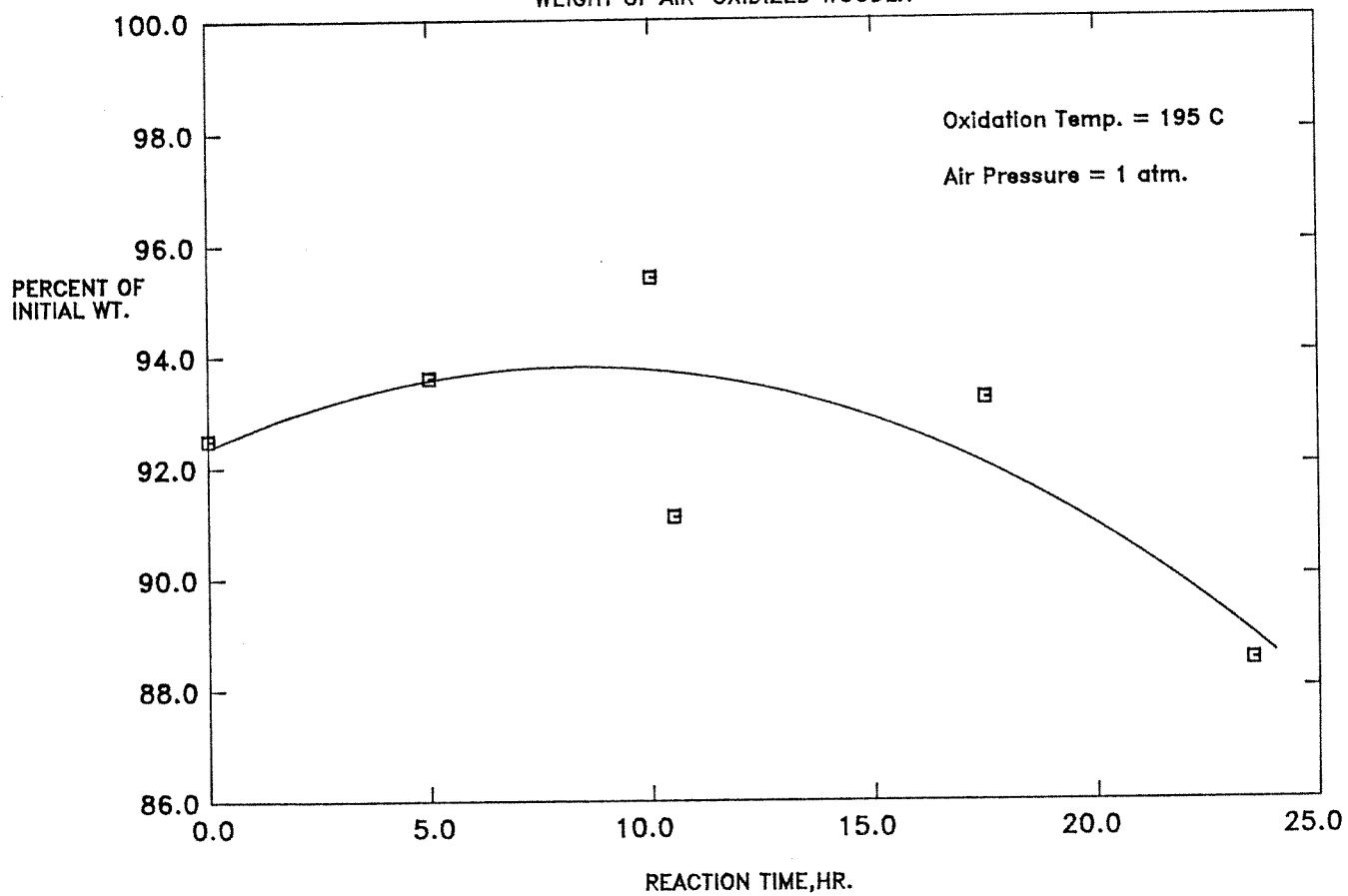
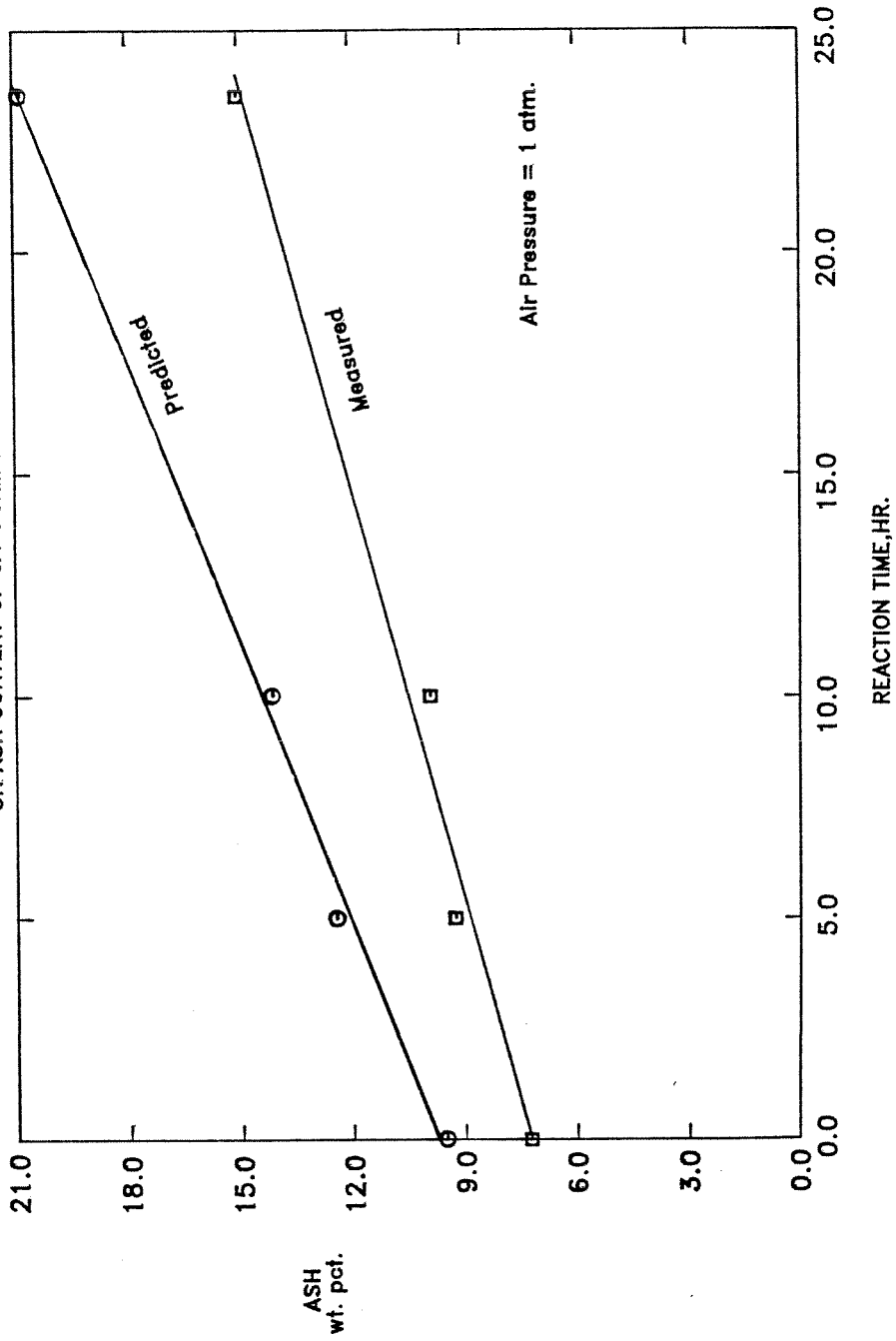


FIGURE 2-6
EFFECT OF OXIDATION IN AIR AT 195C.
ON ASH CONTENT OF CA-FORM WOODDEX



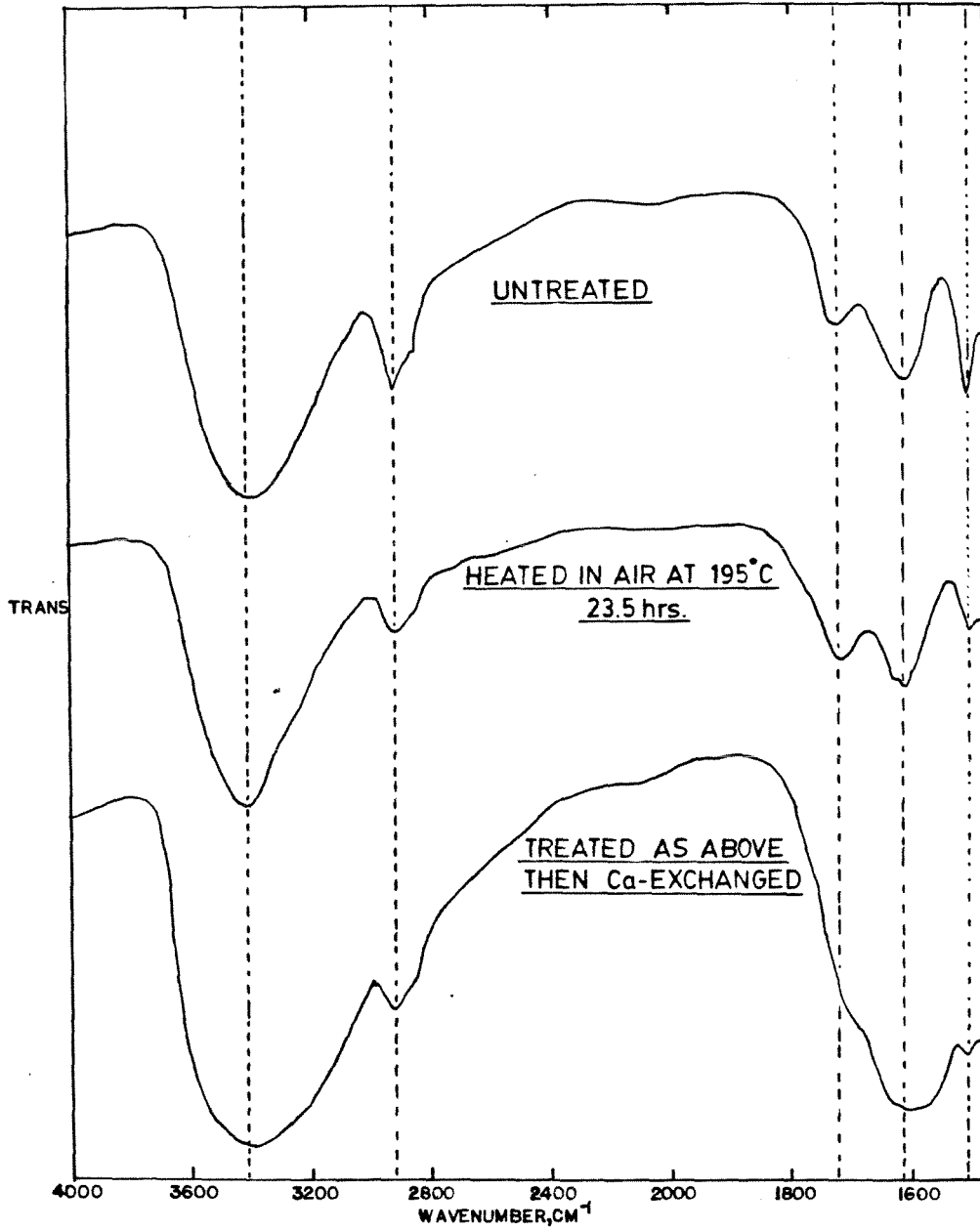


FIGURE 2-7 I-R SPECTRA OF OXIDIZED WOOD EX

FIGURE 2-8
EFFECT OF AIR-OXIDATION ON
ABSORBANCE OF WOODOX AT 1725 CM⁻¹

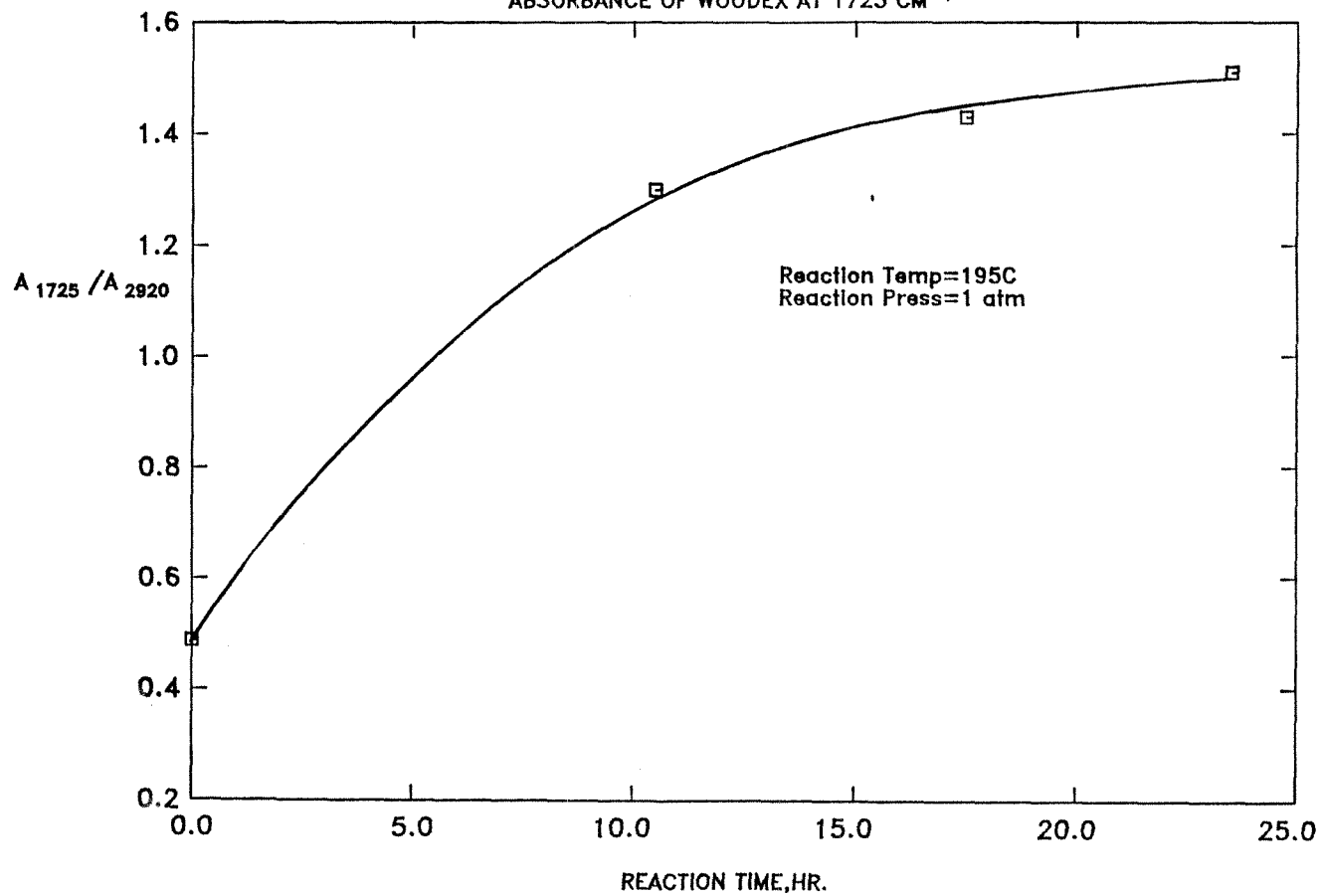
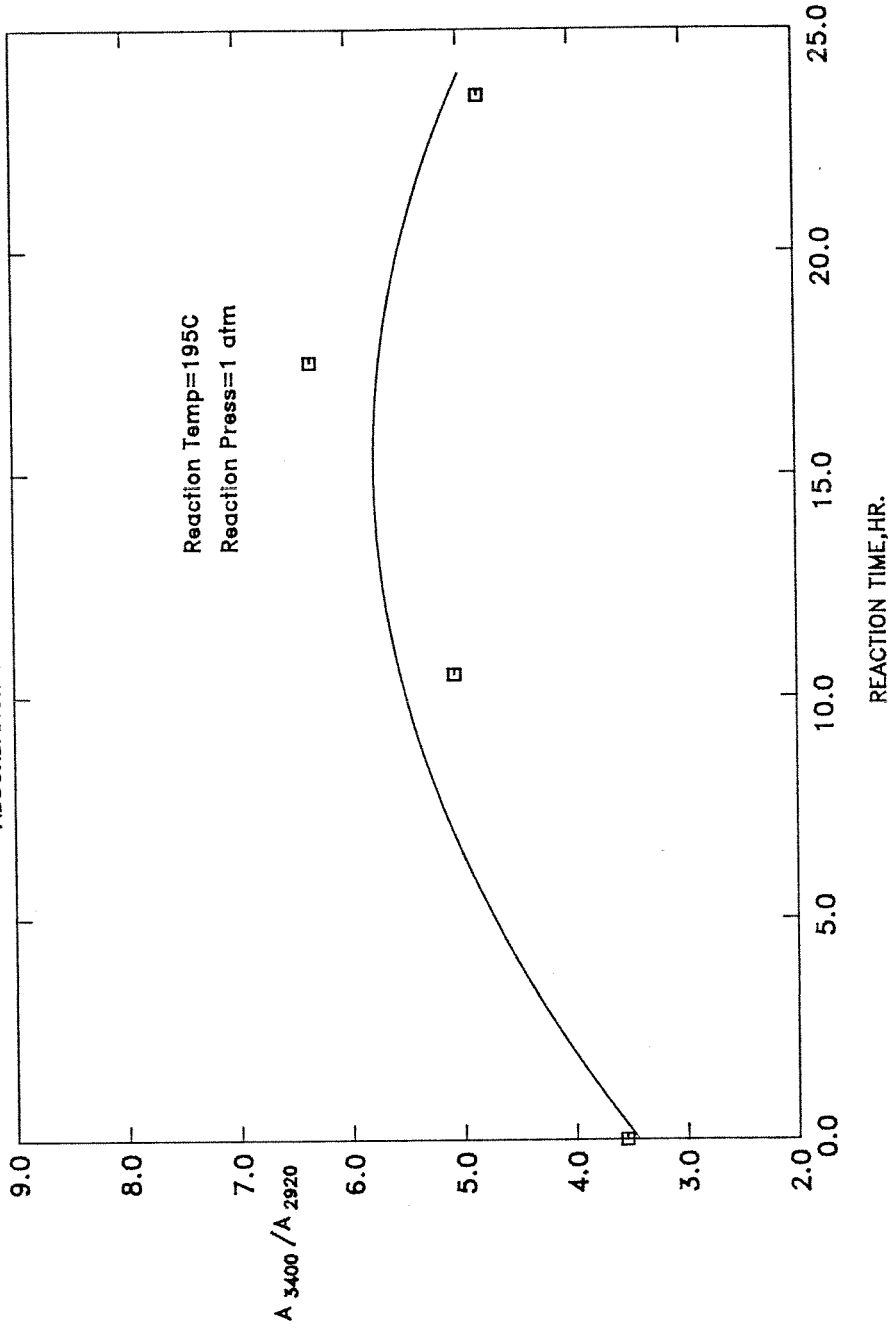
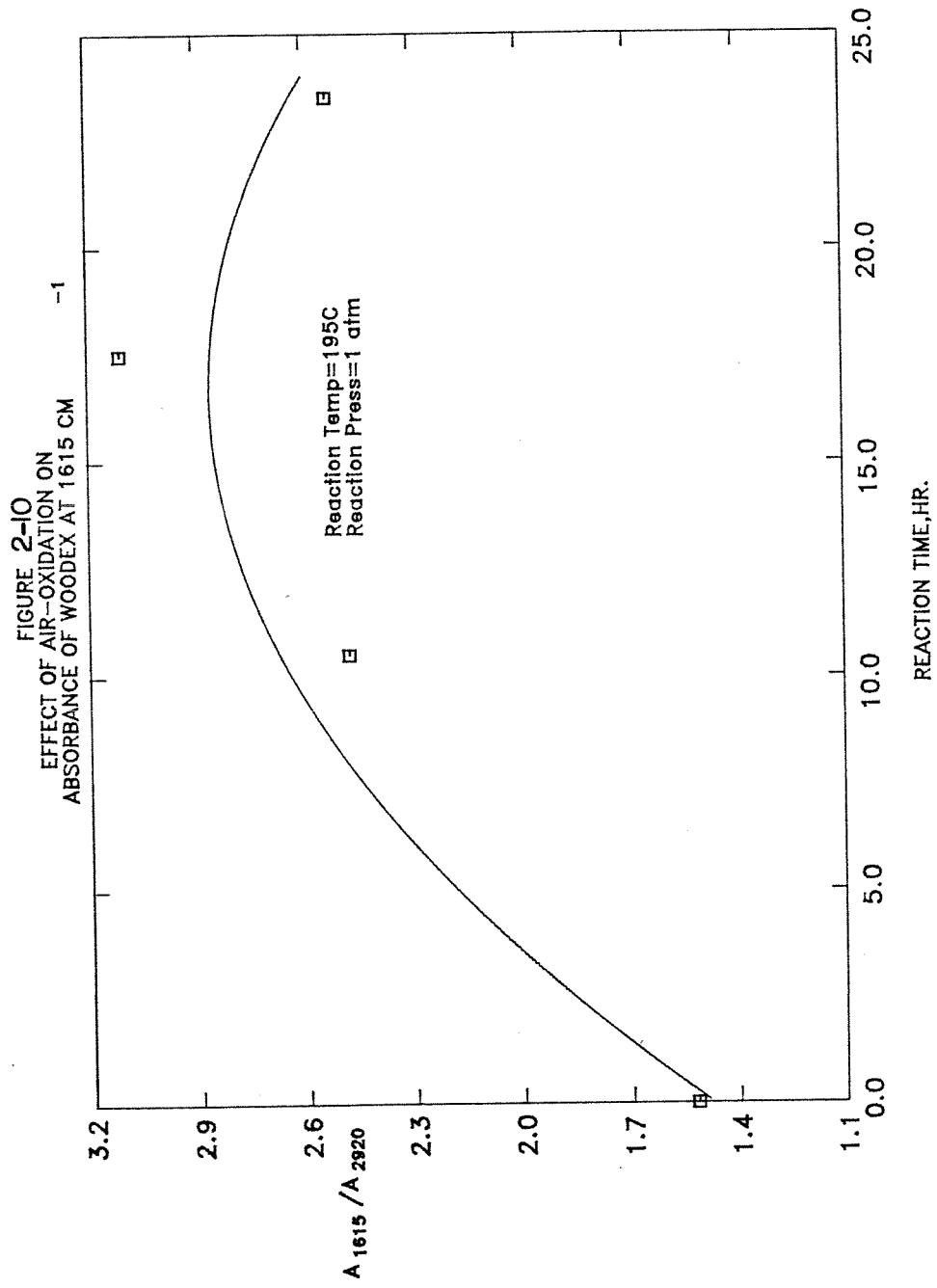


FIGURE 2-9
EFFECT OF AIR-OXIDATION ON
ABSORBANCE OF WOODEX AT 3400 CM⁻¹





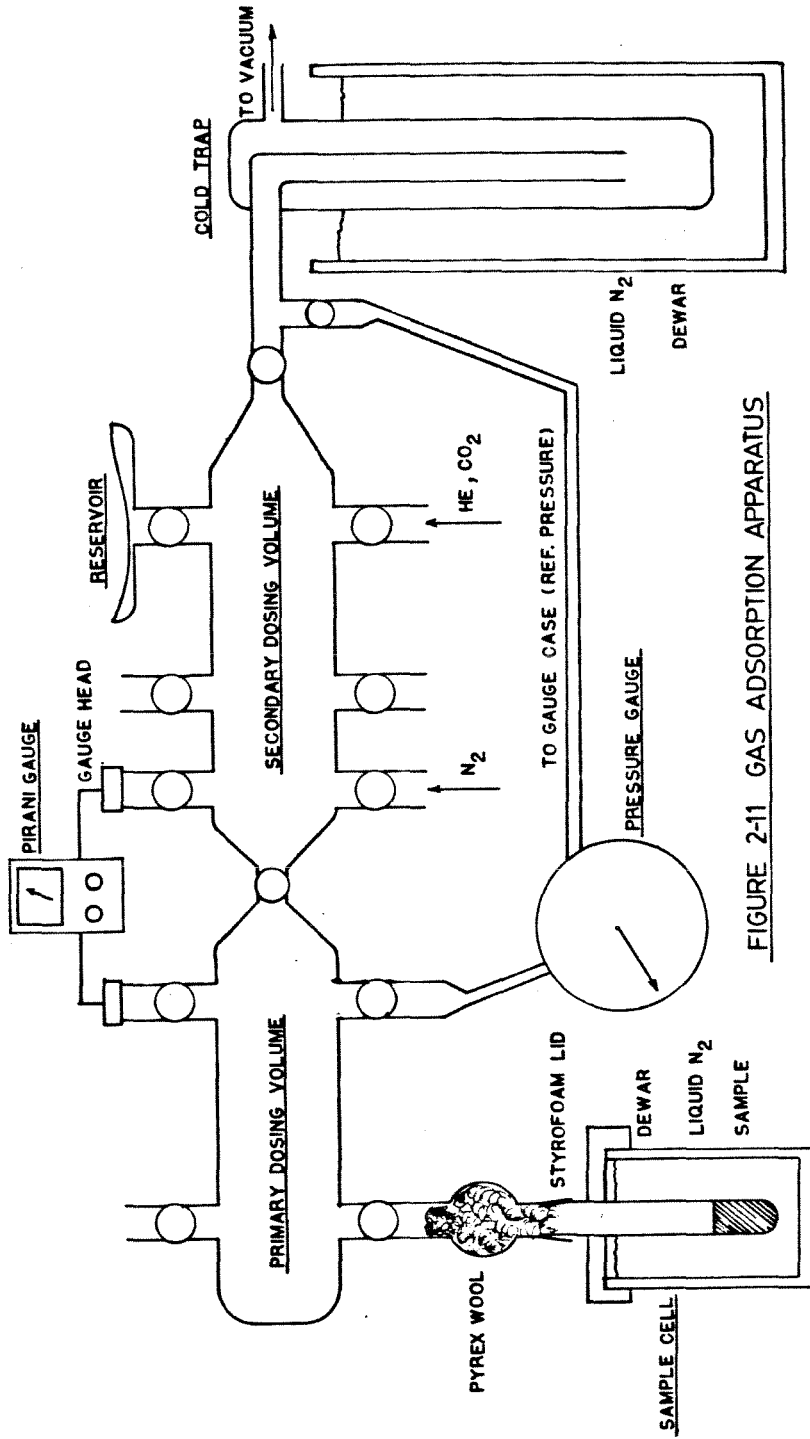


FIGURE 2-11 GAS ADSORPTION APPARATUS

3. PYROLYSIS OF WOOD AND RELATED MATERIALS

Wood pyrolysis can be approximated as the combined pyrolysis of lignin and hemicellulose. Hemicellulose is the most reactive polymer in wood, followed by cellulose. Lignin is the most refractory polymer, partly because it is prone to condensation reactions (Allan and Matilla, 1971). Pyrolysis reactions in wood are due to the thermal cleavage of carbon-oxygen bonds. The cleavage of carbon-carbon bonds is much less facile at wood-pyrolysis temperatures (below 650 ° C). The breakage of C-O bonds during pyrolysis gives rise to two competing processes, depolymerization of the chains and scission reactions within carbohydrate molecules. The monomer units released by depolymerization undergo cracking or condensation reactions as they diffuse out of the particles or on the hot char surface. Condensation reactions yield char while scission reactions produce gases such as CO, CO₂, H₂, CH₄, and water along with heavier molecular fragments. Slow heating, on the order of 10 ° C/min., favors orderly depolymerization and maximizes the yield of char. Extremely rapid heating, on the order of 1000 ° C/sec., yields gas, volatiles, and ash, with essentially no char being formed (Milne, 1979). Pyrolysis reactions in industrial systems usually fall between these two extremes.

The pyrolysis of cellulose has been investigated more than any other wood component. The two competing reactions in the thermal decomposition of cellulose are cleavage of the glucose-glucose bonds, which gives levoglucosan, a condensed form of glucose, and scission of the bonds within the glucose molecules, giving carbon oxides, volatile organics, and water as products. The levoglucosan released by the former reaction may undergo further gas-phase reactions or react with the surface of the char in cracking or condensation reactions (Shafizadeh, 1968; Milne, 1979). Shafizadeh et al. (1979) found that the

yield of levoglucosan was lower in nitrogen than in vacuum, which demonstrated the importance of secondary gas-phase and gas-solid reactions. In vacuum the concentration of tar would be lower within the particles and in the gas phase.

3.1 Mechanisms of Pyrolysis

Klein and Virk (1981) pyrolyzed model compounds which contained the reactive entities present in lignin. The activation energies for reactions which gave gas or volatiles were in the range of 22.0 kcal/gmol. to 18.4 kcal/gmol. A concerted pericyclic reaction mechanism was inferred for the more facile pyrolytic reactions. Free-radical reaction mechanisms failed to account for the behavior of the compounds which decomposed easily. The possibility that competing reaction mechanisms could operate on less easily pyrolyzed groups was not discussed.

Studies of free-radical formation in wood and related materials by electron-spin resonance (ESR) revealed that stable free radicals were formed during pyrolysis reactions. Consequently, reactions initiated by free radicals were likely significant in the pyrolysis of solid systems.

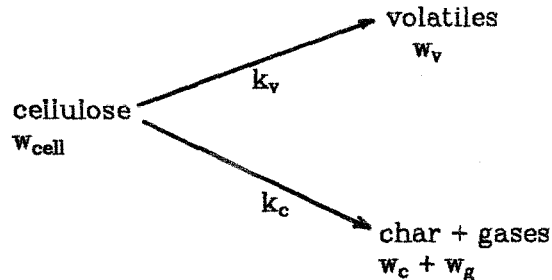
When cellulose was heated above 225° C, the concentration of free radicals in the solid residue grew very rapidly (Arthur, 1971). The radicals were unusually stable and were unaffected by exposure to oxygen at room conditions. At temperatures above 250 ° C the concentration of radicals increased exponentially, which would indicate an autocatalytic or chain-branching process (Kilzer, 1971). The above ESR studies clearly indicate that free-radical mechanisms are significant in the thermal degradation of solid materials related to wood. The effect of temperature on the radical content of cellulose described by Kilzer (1971) indicates that more than one free-radical mechanism may be operative, depending on the reaction temperature. The pericyclic

mechanisms observed by Klein and Virk (1981) represent another type of mechanism for certain reactive species in the solid matrix.

Any comprehensive model of pyrolysis must include the formation and reactions of free radicals, as well as concerted mechanisms. In addition to the primary decomposition reactions, secondary reactions which involve molecular fragments must be included.

3.2 Kinetics of Pyrolysis Reactions

Due to the complexity of the reacting system, past studies of the pyrolysis of wood and wood polymers have relied on kinetic models which used lumped or global reactions to characterize the overall process. For example, Bradbury et al. (1979) found that the pyrolysis of cellulose at 1.5 torr and 312- 364 ° C could be described by the following global model:



w_{cell} = weight of cellulose

w_v = weight of volatiles

w_c = weight of char

w_g = weight of gas

k_v = rate constant for reactions giving volatiles

k_c = rate constant for reactions giving char and gas

The reactions were first-order with respect to the weight of cellulose, w_{cell} .

$$-\frac{dw_{\text{cell}}}{dt} = (k_v + k_c) w_{\text{cell}} \quad (3.1)$$

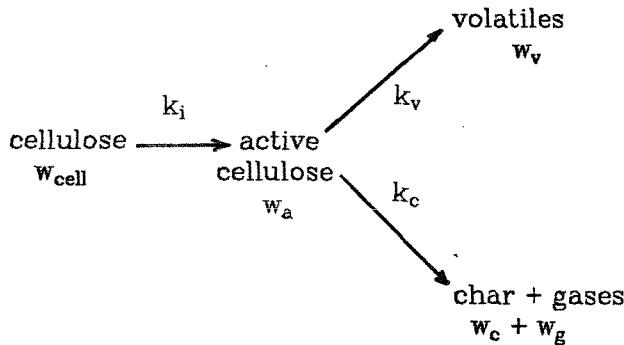
$$\frac{dw_c}{dt} = 0.35 k_c (w_{\text{cell}})$$

where $\frac{w_c}{w_c + w_g} = 0.35$ at $t = \infty$ and

$$k_v = 1.9 \times 10^{16} e^{-47,300/RT}, \text{ min}^{-1} \quad (3.2)$$

$$k_c = 7.9 \times 10^{11} e^{-58,800/RT}, \text{ min}^{-1}$$

At temperatures in the range of 259 to 312 ° C, an activation reaction was added to improve the agreement between the model and the experimental data.



w_a = weight of active cellulose

k_i = rate constant for the reaction giving active cellulose

The rate constant, k_i , was given by:

$$k_i = 1.7 \times 10^{21} e^{-58,000/RT}, \text{ min}^{-1} \quad (3.3)$$

The experiments were carried out in a batch reactor, and the effect of the initial heating of the sample on the rate of reaction was accounted for by using the following expression for the temperature:

$$T = T_0 + (T_r - T_0) (1 - e^{-\tau/t}) \quad (3.4)$$

T_0 was the initial sample temperature, and T_r was the reactor temperature. T

was the temperature of the wood at a given time and was used in the calculation of the rates of reactions by use of equations (2.2) and (2.3). The time constant, τ , was determined experimentally.

Bradbury et al. fitted only the solid residue to the model. No attempt was made to fit the yields of tar or gas to the model. The gas effluent was not collected or analyzed. Although the weight of residue from pyrolysis can be correlated with a simple two-reaction model, we cannot assume that such a model will yield even approximate predictions for the weights of gas or tar. Any reactions that form volatile products involve mass transfer which can affect the apparent kinetic parameters. In Appendix A data on lignin pyrolysis is fitted to several simple models to evaluate the ability of lumped kinetics to describe the formation of char, tar, and gases. Models such as Bradbury et al. (1979), which are adequate when applied to the weight of char, are inadequate when fitted to gas and tar simultaneously.

Klein and Virk (1981) pyrolyzed model compounds to define the kinetic parameters for the reactive groups in lignin. They then used a statistical model of the lignin polymer to combine the kinetic parameters for the reactive groups to predict the behavior of whole lignin. Their predicted yields and compositions of gas were in qualitative agreement with the observed results, but the quantitative prediction of methanol and tar compounds was not as satisfactory. The under-prediction of the yield of methanol was attributed to the existence of some reaction pathway not included in the model. The low predicted yields of tar were due to the exclusion of polymerization reactions from the model. The kinetic model of lignin pyrolysis developed by Klein and Virk predicts the primary decomposition products, but further work is required to model the secondary reactions of the tar and organic compounds, which are significant in

industrial reactors. Typically, the yield of gas from lignin pyrolysis is about 12%. The yields of tar and aqueous condensate are about 15 and 20% respectively, and the remainder is left as char (Allan and Matilla,1971). Iatridis and Gavalas (1979) found that the tar from the pyrolysis of precipitated-Kraft lignin contained as much as 3 % by weight of the original lignin as monoaromatic phenols.

The data on the pyrolysis of wood reported by previous investigators concentrated on the composition and yield of gas. In many cases the yields of tar and aqueous condensate were not reported. To some extent wood pyrolysis may be viewed as the pyrolysis of its constituent polymers. Hileman et al.(1976) found that some of the pyrolysis products of wood could not be explained by a simple addition of the products of polysaccharide and lignin pyrolysis. Several compounds present in significant quantities in the wood products were absent from the products of the component polymers. Hileman et al inferred that there was interaction between the polymers during pyrolysis, particularly in the reactions of char formation. They also pointed out the lack of certainty that the wood polymers were unchanged in the course of their extraction.

Hileman et al. and Shafizadeh and Chin (1976) identified the organic materials which formed when cellulose, xylan, and wood were pyrolyzed. Their data and the results of Gavalas and Iatridis (1979) and Klein and Virk (1981) were combined to give Table 3.1. The table lists the organic compounds which could be formed when wood was pyrolyzed and the possible sources of each compound in the wood structure. Every compound listed would not necessarily be observed in a given experiment.

Experimental pyrolysis techniques can be classified according to the contact time between the volatile products and the solid. Rapid quenching

experiments are designed so that the volatile products are removed from the solid and cooled quickly, to observe the primary decomposition reactions (Gavalas,1982). In entrained-flow reactors a dilute suspension of finely divided particles is passed through a heated pipe or tubular furnace. Secondary gas is added to maintain laminar flow and to prevent contact between particles and the wall of the reactor. A water cooled sample port is used to collect solid and gas samples within the reactor. The residence time is controlled by the secondary gas and the position of the sampler within the reactor. The short residence time of the gases in the reactor, the dilute suspension, and the rapid quench at the sample collector all contribute to reduce the contact between products and the solid char. In captive-sample systems the solid reactant is held by a metal mesh, which in turn is encased in a larger reactor vessel, filled with gas or maintained under vacuum. An electric current passing through the mesh heats the sample. The reactor vessel and the bulk of the gas stay at a low temperature of less than 50 ° C. The volatile products leave the sample and are quenched by the surrounding gas (Gavalas, 1982; Gavalas and Iatridis, 1979). The contact time is controlled by the size of the sample and the gas pressure.

In fixed or fluid-bed reactors the volatile products are allowed to remain in contact with the solid material for some period of time, as in industrial systems. Yeboah et al.(1980) demonstrated that when coal is pyrolyzed, the rapid-quench technique gives higher tar yields than measurements from fluidized-beds. The fluid bed gives contact between the tar and the hot solids to allow cracking and higher yields of gas.

The kinetics of pyrolysis have generally been based on the weight of sample remaining at a given time, excepting the work of Klein and Virk (1981). The kinetic data which have been published do not include all of the products of

pyrolysis of wood to allow a material balance. The overall reaction has generally been correlated as being first-order with respect to the weight of sample at a given time. Iatridis and Gavalas (1979) found that the evolution of individual gas species such as methane could not be treated in this fashion, and suggested that more complex kinetic models incorporating pathways of competing reactions would be required. A model similar to the one of Bradbury et al. would have this feature and could work well over a limited temperature range for one or more products of pyrolysis.

REFERENCES

- [1] Allan, T. and Matilla, T. in, *Lignins*, eds. Sarkanen, K.V., and Ludwig, C.H., Wiley, New York, 1971.
- [2] Arthur, J.C., Jr., *High Polym.* **5(pt 5)**, 977-90, 1971.
- [3] Bradbury, A.W.G., Sakai, Y., Shafizadeh, F., *J. Appl. Polym. Sci.* **23**, 3271-3280, 1979.
- [4] Gavalas, G. R., *Coal Pyrolysis*, Elsevier, Amsterdam, 1982.
- [5] Hileman, F.D., et al., in *Thermal Uses and Properties of Carbohydrates, Lignins*, ed. F. Shafizadeh, ACS, 49-71, 1976.
- [6] Iatridis, B.A. and Gavalas, G.R., *Ind. Eng. Chem. Proc. Des. Dev.* **18(2)**, 127 - 130, 1979.
- [7] Kilzer, F.J., *High Polym.* **5(pt 5)**, 1015-46, 1971.
- [8] Klein, M.T. and Virk, P.S. *Model Pathways in Lignin Thermolysis*, Massachusetts Institute of Tech. Energy Lab. Rep. MIT-EL 81-0015, 1981.
- [9] Milne, T., in *A Survey of Biomass Gasification, Vol II Principles of Gasification*, SERI, July, 1979.
- [10] Shafizadeh, F., *Advances in Carbohydrate Chemistry* **23**, 419 - 465, 1968.
- [11] Shafizadeh, F., and Chin, P.P.S., in *Wood Technology: Chemical Aspects*, I.S. Goldstein ed., ACS Symp. Ser. No. 43, 57-81, 1976.
- [12] Shafizadeh, F., et al., *J. Appl. Polym. Sci.* **23**, 3525 - 3539, 1979.
- [13] Yeboah, Y. D., Longwell, J. P., Howard, J. B., and Peters, W. A., *Ind. Eng. Chem. Proc. Des. Dev.* **19**, 646 - 653, 1980.

Table 3.1 Aqueous Products From Pyrolysis of Wood		
Compound	Other Names	Sources
methanol		c,x,l
formaldehyde	methanal	
formic acid	methanoic acid	
acetaldehyde	ethanal	c,x
acetic acid	ethanoic acid	c,x,l
ethandial	glyoxal	c,x,l
2-propanone	acetone	c,x,l
1-propanal		x
propenal	acrolein	c
propanoic acid		
1-hydroxy-2-propanone	acetol	c,x
2-oxopropanal	pyruvaldehyde	
2,3-butanedione	diacetyl	c,x
2,3-pentanedione		
furan		c
5-methylfuran		c
2-fufurol		c
2-fufural	fufuraldehyde	c,x
5-methyl-2-fufural		c
phenol		l
cresol		l
o-methoxyphenol	guaiacol	l
2-methoxy-4-methylphenol		l
c=cellulose		
x=xylan		
l=lignin		

4. EFFECT OF MOISTURE ON THE PYROLYSIS OF WOOD EX

4.1 Introduction and Background

Wood waste is produced in large quantities as a byproduct of pulp and paper and lumber production. This waste is usually burned as "hog fuel" to generate steam, but its heating value is low due to a high moisture content. This waste is a potential feedstock for processes to produce gas and liquid fuels and chemicals. Pyrolysis is a rapid and efficient means of converting the waste into more valuable products. Although the chemistry of pyrolysis has been studied intensively, the effects of water have been largely ignored. Moisture in a solid feedstock has the obvious effect of reducing the thermal value of the material due to the latent heat of the water. The reaction of steam with char to form CO and H₂ is well understood, but occurs after pyrolysis is complete.

Moisture in a solid can behave very differently from steam in the gas phase, depending on the relative rates of pyrolysis and mass transfer within particles. In an entrained or fluidized reactor the rate of pyrolysis is faster than the rate of transport of steam from the surrounding gas into the particles. During pyrolysis a convective flux of volatile compounds and gases leaves the particle and retards the diffusion of the surrounding gas into the solid. Steam would only interact with the char after the pyrolysis reactions were complete. Moisture present in the solid would have an effect during the initial phase of pyrolysis before diffusing out of the particles with the volatile and gaseous products. Thus moisture would interact with the solid during the degradation reactions, while steam would only influence char gasification and gas-phase reactions of the volatile compounds.

In the pyrolysis of moist wood the rate of heating and size of the wood particles will determine whether water is present when thermal reactions occur.

Under rapid heating, water will evolve by pressure driven flow and bubble formation in the fluid Woodex particles until the vapor pressure of water drops below the ambient pressure. Wood is hydrophilic and some water is very strongly adsorbed (Skaar, 1972), so even at high temperatures water would remain to diffuse out of the wood in response to concentration or vapor pressure gradients. As water is removed the wood structure becomes less permeable to water vapor. Permeability can decrease by as much as two orders of magnitude when the moisture content drops from 5% to 10% (Van Arsdel, 1947). This reduction in permeability would prolong the time required for water to diffuse out of the solid. Although the amount of moisture present during pyrolysis could be small, it would exert a significant vapor pressure and have high thermodynamic activity.

4.1.1 Physical Effects of Moisture The moisture content of polymers affects their structure by swelling the matrix. Both wood polymers and low-rank coals exhibit such swelling when moist (Browning, 1963; Gorbaty, 1978). The swelling of cellulose in particular has a major effect on its surface area and pore structure. During pyrolysis such an expanded structure would facilitate transport of tars and volatile products out of the solid. An expanded solid structure would also reduce the pressure of tar and other compounds within the solid particles. The yields of tars such as levoglucosan from the pyrolysis of cellulose are very sensitive to the total gas pressure.

The material used in this study, Woodex[®], was rich in lignins, hemicellulose and bark components. These polymers are thermoplastic and melt well below the temperatures required for pyrolysis. Hence under pyrolysis this material behaves like viscous fluid rather than a solid structure with definite configuration. Moisture affects the melting characteristics of amorphous

thermoplastic polymers. For example, the moisture content of lignin affects its glass transition temperature; the addition of 27 % by weight of moisture to a sample of lignin lowered the glass transition temperature from 195 ° C to 90 ° C. The decrease in the transition temperature was proportional to the moisture content (Goring, 1971). Since pyrolysis occurs at much higher temperatures, the thermoplastic polymers in wood are fluids, independent of the moisture content. Just as moisture lowers the glass transition temperature, however, it could also lower the viscosity of the polymer melt. Such a reduction in viscosity would facilitate bubble formation and evolution from the wood particles. The pressure inside the bubbles would remain lower resulting in reduced residence time and increased yield of tar. Moisture would also enhance the formation of bubbles by increasing the volume of volatile material evolved during pyrolysis. Thus in the absence of other effects, moisture would increase the yield of tar from pyrolysis of wood.

4.1.2 Chemical Effects of Moisture Direct chemical interaction between water and hydrocarbons has been documented by several investigators. Aliev et al. (1964) found that steam and paraffins reacted directly to form small amounts of carboxylic acids, ketones, and aldehydes. When wet cellulose was held at 200 ° C in a closed system, decomposition was much more rapid than when dry cellulose was subjected to the same conditions (Shafizadeh, 1968). Mikulich and Mikulich (1975) found that when sprucewood was pyrolyzed in steam the ESR (Electron Spin Resonance) response was greatest at 350 ° C, as compared to 500 ° C when the same material was pyrolyzed in a dry atmosphere. Such observations indicate that moisture has a direct effect on the reactions that occur during pyrolysis.

Other compounds are known to affect free-radical reactions. Niclause et al.

(1976) pyrolyzed light alkanes in the presence of HCl, HBr, and H₂S at 500 ° C. When isobutane was pyrolyzed in the presence of HCl or HBr, cracking reactions which yielded propylene and methane were accelerated. Competing reactions which led to dehydrogenation were unaffected. When n-butane was pyrolyzed in the presence of H₂S, the formation of propylene, methane, ethane, and ethylene was accelerated and the dehydrogenation reactions were inhibited. The authors attributed these results to the creation of new reaction pathways, wherein radicals abstracted hydrogen from the additives to form new radicals, which in turn abstracted hydrogen from unreacted hydrocarbon. The ease of formation of a radical from the additive, relative to the other possible reactions, determined the overall effect of the additive on the chain reactions. The additives would only be consumed in termination reactions.

Water could act as a hydrogen-containing additive in a similar manner to HCl or HBr. The enthalpy of formation of radicals from water is higher than from HCl by 16.3 kcal/mol, and higher than H₂S by 28.4 kcal./mol. Such an enthalpy difference indicates that water should be less active than HCl as an accelerator of free radical reactions. Nevertheless the difference is not so large as to rule out the possible significance of water in pyrolysis as a chemical agent. The small amounts of oxygenated compounds found by Aliev et al. (1964) from the steam cracking of hydrocarbons could be due to the termination of the free radical reactions. The OH• radicals would react to form ketones, aldehydes, and carboxylic acids, either directly or via a peroxide intermediate.

The purpose of the present work was to determine the impact of water on pyrolysis reactions by measuring the product distribution from the pyrolysis of moist and dry Woodex over a range of temperatures. The samples were demineralized prior to reaction to eliminate the catalytic effects of the ash

constituents. Using a fluid-bed reactor it was possible to react well-mixed samples at uniform temperatures, and achieve an overall material balance of better than 95% on average. In the absence of active catalysts, free-radical reactions would dominate the thermal reactions. A speculative mechanism for free-radical behavior was compared with the observed effects of moisture and temperature.

4.2 Experimental

4.2.1 Material Bio-Solar Research of Eugene, OR, supplied Woodex[®] pellets for use in this study. The pellets were manufactured by compressing wood and extruding it, without using any binders. Woodex is rich in bark constituents and has a composition typical of wood wastes. The pellets were ground to -60 +100 U.S. mesh size and treated with dilute acid to remove the active minerals from the solid. The ground Woodex was stirred with 0.5 N HCl in a ratio of 50 ml./g. for 7 hours at 25 ° C. The acid treatment was sufficient for the removal of the finely distributed mineral content, yet mild enough to prevent cellulose hydrolysis. The samples did contain residual ash, due to discrete particles of sand mixed with the sample which are thought to be inert from the standpoint of reactivity. After the acid wash the slurry was filtered and rinsed with demineralized water to neutral pH. The powder was then vacuum dried at 105 ° C for 12 hours.

Moist Woodex samples were prepared by mixing ground wood, prepared as above, with distilled water. The mixture was allowed to stand for a week to ensure that the water had been fully absorbed.

4.2.2 Apparatus and Procedure The experimental apparatus is shown as a block diagram in Figure 4-1. Helium was used to fluidize the samples in the reactor and to purge the feed hopper. The helium stream was heated and then

passed into the base of the reactor. The reactor was heated in two zones, a lower zone which was controlled at the desired pyrolysis temperature, and an upper zone which was held at 300 ° C. Figure 4-2 shows the reactor in detail. The draft tube was used to inject the samples from the feed hopper into the empty reactor. The packings of steel wool and glass wool at the top of the reactor served to trap the tar as it was formed. Gases and volatile vapors passed out of the top of the reactor. Vapors were removed by a water condenser, followed by a cold trap in an ice bath, followed by a dessicant tube filled with magnesium perchlorate. When gas analyses were not required, the water condenser and cold trap were replaced by a trap immersed in liquid nitrogen. Replicate runs showed that the composition of a sample from the liquid nitrogen trap was similar to a sample collected from the water condenser, under the same reaction conditions. The main difference was a higher yield of methanol and 2-oxopropanal from a liquid nitrogen trap. Less volatile compounds were unaffected. Both trapping methods gave self consistent, repeatable results.

The non-condensable gases were passed through sampling valves for chromatographic analysis. A multi-loop sample valve was used to take nine gas samples at 15-30 sec intervals at the start of an experiment. An automatic sample valve was then used to take samples for the remainder of the experiment at 2-3 minute intervals. A gas chromatograph, equipped with a Porapak Q/R column and a thermal-conductivity detector, was used to measure the concentrations of CO, CH₄, and CO₂ in the gas samples. These discrete measurements of gas concentration were integrated to give the overall yield of each gas. The concentration of gases was not measured for every sample because tests had shown that in the range 300 ° C to 500 ° C moisture had no effect on the yields of gases, within experimental error.

To start the reaction, the helium line to the draft tube was opened and the full flow of fluidizing gas was directed through the hopper. When the wood was agitated it flowed down the draft tube into the base of the reactor. When the hopper was empty, the fluidizing gas was switched back to the base of the reactor and the hopper was shut off. The hopper was made of glass so that the feeding of the Woodex sample could be observed. All experiments used about 5g. of wood. The samples were fed into the reactor within two minutes. When the sample was introduced in the reactor, the temperature dropped by about 30 ° C, or less, and then gradually recovered to its final value within six minutes.

Each experiment was allowed to proceed until the chromatographic analysis of the effluent showed no gaseous products from pyrolysis. The reactor was allowed to cool while the condenser, condensate samples, cold trap, and dessicant were weighed to determine the weight of aqueous product. The reactor was opened after it had cooled to less than 100 ° C and packings, liner, and char were weighed to determine the weights of tar and char. The gas samples were analyzed and an integral yield of gas was calculated using the trapezoidal rule. Overall material balances were normally closed to within 5%.

Table 4.1 lists the mean variation between replicate experiments that were within 10 C °. Also given are the standard deviation and maximum variation for each pyrolysis product. The variations in Table 4.1 are due to random experimental error and differences in temperature between experiments, so the variations given in the table overestimate the random variation between samples. From the mean variations, relative to the yield of each product, and experimental considerations, the relative reliabilities of the data were:

Char > Tar = Gas > Aqueous

The recovery of aqueous product varied by 4 yield points on average because of

differences in the effectiveness of the dessicant column from run to run. The lightest and heaviest components within the aqueous product were most subject to random variation. The light components, such as methanol, were only partially trapped in the condenser, and the guaiacols were partitioned between the tar and the aqueous product. As a result of this variability we consider change of less than a factor of two in the yield of an organic component to be insignificant.

4.3 Results

Figure 4-3 shows the yield of tar from dry and moist samples of Woodex. At temperatures above 420 ° C the moist samples gave less tar than dry samples. This difference in the yields increased with temperature. The yield of char from moist samples was about 5 yield % higher above 396 ° C than from the dry samples. (See Figure 4-4 and Tables 4.2 and 4.3.) Clearly the reduction in the tar yield from the moist samples at 460 ° C was accompanied by an increase in the yield of char.

Table 4.4 lists the yields of organic compounds in the aqueous product. At 460 ° C moisture did not affect the yield of these compounds or the overall yield of aqueous product ,within experimental error. At 396 ° C moisture in the sample reduced the yield of organics.

Table 4.5 shows the effect of increasing moisture content at 396° C. The main trend in the data was the increase in the yield of char with moisture content. The yield of char rose from 41.9 % to 48.7 % when the moisture content was raised from 0 % to 28 %. The increase in char was balanced by a decrease in the formation of total volatiles (tar + aqueous products).

Table 4.6 lists the surface areas of chars from dry and moist Woodex, as measured by nitrogen adsorption. The chars from pyrolysis at low temperatures

had small surface areas of less than 5 m²/g.. Moisture in the wood decreased the surface area of the resulting char by a factor of two at 460° C, from 57 to 23 m²/g..

4.4 Discussion

The decrease in the yield of tar from moist samples of Woodex above 400 ° C and the increase in the yield of char were the opposite trends to what the physical effects of water would lead us to expect. Moisture in the molten Woodex would enhance bubble formation and help to remove tar from the melt before further reactions could occur. If moisture reduced the viscosity of the melt, bubble formation would be aided even more. Consequently the action of moisture on the yield of tar must be via a chemical mechanism.

The acid wash removed any basic catalyst sites from the wood matrix by dissolving metal cations. Some acid sites would be associated with mineral or clay surfaces, but would be poorly distributed and ineffectual in promoting reactions such as the hydrolysis of ethers. Consequently free-radicals would dominate the thermal reactions. The most plausible explanation for the observed trends in char and tar yield is an interaction between moisture and free-radical species during pyrolysis. Therefore we propose a speculative mechanism to explain the effects of moisture and temperature on the yield of tar.

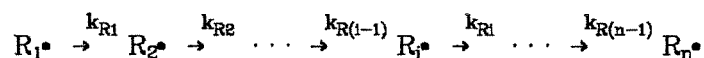
4.4.1 A Mechanism for the Effect of Moisture on Free Radicals in Wood

Free radicals form when wood is pyrolyzed, and play a significant role in the thermal degradation reactions. Ether linkages are thermally unstable at pyrolysis temperatures and can cleave to give two radical species (Shafizadeh, 1968). Figure 4-5 shows the cleavage of a cellulose inter-unit linkage as an example of a typical reaction of this type. The product radicals from this reaction are highly

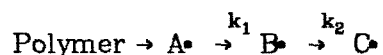
reactive and would rearrange and combine with neighboring groups. Various concerted reactions compete with the free-radical reactions.

Given that the free radicals form in pairs when carbon-oxygen bonds dissociate, how do free radicals react further? Nanassy and Fung (1975) found that the concentration of spins (or radicals) increased rapidly and then stayed relatively constant, when Douglas fir wood was pyrolyzed at 300 ° C to 600 ° C. The samples lost weight, due to the evolution of volatiles, only when the concentration of radicals was rising rapidly. The activity of the radicals was high initially, and then dropped off with time as condensation, addition, cyclization, and rearrangement reactions developed structures in which the delocalized electron was immobilized by steric hindrance, stabilized by resonance, and prevented from reacting even with oxygen. Arthur (1971) observed similar behavior when cellulose was pyrolyzed.

We can view the reactions of a free radical in the solid phase as a series of steps, going from a highly active species to an inactive, stabilized radical.

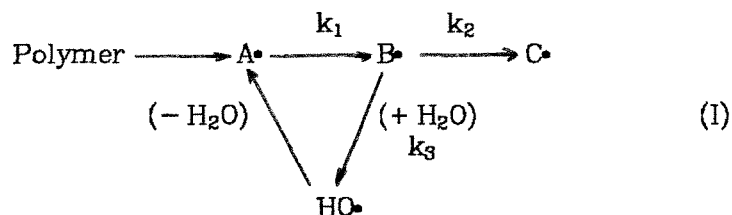


Such a scheme includes n steps going from the most active species, R_1^\bullet to the least active, R_n^\bullet . Each successive step would be slower than the previous one, because of the increasing stabilization of the free radical, so that $k_{Ri} > k_{R(i+1)}$. We can lump the species together according to their reactivity to obtain a simpler scheme:



Radicals of type A^\bullet would be highly reactive with tar and would be present at small concentrations. They would quickly rearrange to form more stable

structures of type B^\bullet , which would only react with small molecules. Since the more stable radicals react more slowly, $k_1 \gg k_2$ and after a short reaction time $[A^\bullet] \ll [B^\bullet]$. At long reaction times the stabilized, unreactive radicals of type C^\bullet would predominate. In the presence of small molecules that could donate hydrogen, such as water, the following reaction scheme would result:



Water would react with B^\bullet to form highly reactive HO^\bullet radicals which would abstract a hydrogen from another site to form A^\bullet . Under these conditions the rate of formation of hydroxyl is equal to the rate at which radicals hop from one site to another. The ratio of the rates of hopping and stabilization of radicals would be a measure of the effect of moisture on the concentrations of radicals A^\bullet , B^\bullet , and C^\bullet . If the rate of hopping is greater than the rate of stabilization, then the concentration of active sites, $[A^\bullet]$, would increase.

After tar molecules form they must diffuse out of the solid particles in order to appear as a product. As the molecules diffuse they can recombine with active free-radical sites on the solid phase or lose a hydrogen and be converted into radical molecules. Consequently, with the increase in the concentration of active sites, $[A^\bullet]$, due to the presence of water, the probability increases that a tar molecule will be trapped in the solid phase. Any such trapping, or recombination, would decrease the tar yield, and increase the yield of char. In the absence of other processes, trapping of tar molecules due to free-radical reactions would control the overall yield of tar.

In the following section we shall estimate the rate at which the radicals

free radicals. We can view the formation of char as being driven by the tendency of free radicals to react in the solid phase until they are stabilized. Consequently, the rate of char formation is related to the rate of stabilization, and k_c can be used to obtain a crude estimate of k_2 in scheme I.

Considering all reactions as first order gives the following expression for the weight of solid at any time:

$$w_{\text{solid}} = w_p + w_c = e^{-(k_m + k_c)t} + \frac{k_c}{(k_m + k_c)} \left[1 - e^{-(k_m + k_c)t} \right] \quad (4.1)$$

From equation (4.1), the rate of weight loss is:

$$-\frac{dw_{\text{solid}}}{dt} = -k_m e^{-(k_m + k_c)t} \quad (4.2)$$

A plot of $\ln \left(\frac{dw_{\text{solid}}}{dt} \right)$ versus time at a given temperature gives the slope $-(k_m + k_c)$ and the intercept $\ln k_m$. The rate constants listed in Table 4.12 were calculated from the data of Nanassy and Fung and gave an activation energy of 13.3 kcal./gmol. for the monomer-formation reaction and 8.74 kcal./gmol. for the char-formation reaction.

The number of interunit-ether linkages in a wood polymer would be approximately equal to the number of monomer units. An approximate mean-monomer weight was used to convert the rate constants from a mass basis to a molar basis. A molecular weight of 160 is a reasonable estimate, given the fractions of glucose, xylose, and p-propyl-o-methoxy-phenol in the wood polymers. This weight gave a monomer concentration of about 4.9 gmol./l.

4.4.1.b Definition of Hop Ratio for Free Radicals The estimates for the rate of stabilization, the rate of reaction between water and radicals (leading to new sites) and the monomer concentration were combined to calculate the 'hop

ratio" (R_h). This ratio is a measure of the extent of the effect of moisture on the concentration of active radicals, $[A^\bullet]$.

$$\begin{aligned}
 R_h &= \frac{\text{Rate of Relocation}}{\text{Rate of Stabilization}} & (4.3) \\
 &= \frac{k_3 [B^\bullet] [H_2O]}{k_2 [B^\bullet]} \\
 &\approx \frac{k_3 [B^\bullet] [H_2O]}{k_c w_p / 4.9 \text{ mol/l.}}
 \end{aligned}$$

$R_h \ll 1$ -stabilization dominates

$R_h \approx 1$ -rates of same order

$R_h \gg 1$ - formation of A^\bullet by water dominant

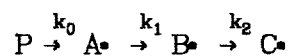
Table 4.8 gives the calculated hop ratios for Douglas-fir wood. The hop ratio becomes greater than one at about 350 ° C so that moisture would begin to have an appreciable effect on the number of type A^\bullet radical sites at between 350 and 400 ° C. Above this temperature type B^\bullet sites would relocate via reaction with water molecules faster than they would stabilize to form type C^\bullet sites. This crossover in rates between relocation and stabilization was due to the relative magnitude of the activation energies of the two reactions. The number of active sites would increase until the concentration of water molecules began to drop off due to transport out of the wood particles. These considerations could not be made quantitative without an estimate of the concentration of A^\bullet .

Moisture increased the yield of char by 5 points at 396 and 460° C, in qualitative agreement with the prediction from the mechanism that water would increase trapping of tar in the solid phase beginning at 350-400° C. A further

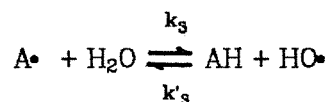
increase in moisture content from 16 to 28% at 396° C resulted in additional char formation, possibly due to the higher concentration of water in the particles during pyrolysis.

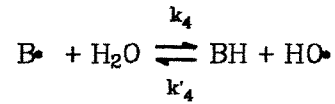
At 460° C moisture reduced the yield of tar by 7-8 points, in accord with trapping by active sites and a large hop ratio. The effect of moisture at 396° C on the yield of tar was close to the magnitude of the experimental error. The addition of 16% moisture to dry wood gave an increase in the yield of tar of 1.5 yield %, which was not significant given the error in the tar measurements (Table 4.1). A further increase in moisture to 28% reduced the yield of tar by 2.6 points to 24.8 %. Thus the effects of moisture on the yield of tar were much smaller at 396° C than at 460° C. The total concentration of radicals at 460° C would be more than twice as great as at 396° C, as would the hop ratio, and so $[A^\bullet]$ would also be greater (Tables 4.12 and 4.13). Consequently we would expect the extent of the trapping of tar to increase with temperature. Any changes in the yield of aqueous product due to moisture were within the range of uncertainty of the data.

4.4.1.c Concentration of Radical Species The mechanism for the behavior of radicals can be used to determine how the addition of water affects the concentration of the radical species. Given the reaction sequence:



The reactions of the radicals with water are as follows:





We define the following variables:

$$a_3 = k_3 [H_2O]$$

$$a'_3 = k'_3 [AH]$$

$$a_4 = k_4 [H_2O]$$

$$a'_4 = k'_4 [BH]$$

The following balance equations result:

$$\frac{d[A^\bullet]}{dt} = k_0[P] - k_1[A^\bullet] - a_3[A^\bullet] + a'_3[HO^\bullet] \quad (4.4)$$

$$\frac{d[B^\bullet]}{dt} = k_1[A^\bullet] - k_2[B^\bullet] - a_4[B^\bullet] + a'_4[HO^\bullet] \quad (4.5)$$

$$\frac{d[HO^\bullet]}{dt} = a_3[A^\bullet] + a_4[B^\bullet] - (a'_3 + a'_4)[HO^\bullet] \quad (4.6)$$

If we assume that the concentration of HO^\bullet is in steady state with respect to the other reactants then:

$$[HO^\bullet] = \frac{a_3[A^\bullet] + a_4[B^\bullet]}{a'_3 + a'_4} \quad (4.7)$$

Substituting the equation for $[HO^\bullet]$ into equations (4.4) and (4.5) and combining, we obtain an equation for the change in $[A^\bullet]$ with $[B^\bullet]$:

$$\frac{d[B^\bullet]}{d[A^\bullet]} = \frac{\left[k_1 + \frac{a_3 a'_4}{a'_3 + a'_4} \right] [A^\bullet] - \left[k_2 + \frac{a'_3 a_4}{a'_3 + a'_4} \right] [B^\bullet]}{k_0 P - \left[k_1 + \frac{a_3 a'_4}{a'_3 + a'_4} \right] [A^\bullet] + \frac{a'_3 a_4}{a'_3 + a'_4} [B^\bullet]} \quad (4.8)$$

Equation (4.8) can be simplified by recognizing which terms are small. Any

accessible C-H or O-H bond can give up a hydrogen to a hydroxy radical. The number of easily accessible sites will be much larger than the number of sites that are sterically hindered due to free-radical enhanced rearrangements. Since [AH] represents accessible sites, and [BH] represents hindered sites, we can say that [AH] >> [BH]. Hence $a'_3 >> a'_4$, because the rate constants k'_3 and k'_4 are of the same order of magnitude. The concentration of active radicals is always small so that [AH] >>> [A•]. From this we know that $a_3/a'_3 <<< 1$ and so the following simplification applies:

$$k_1 + \frac{a_3 a'_4}{a'_3 + a'_4} \approx k_1 + \frac{a_3 a'_4}{a'_3} \approx k_1$$

Using the hop ratio, $R_h = a_4/k_2$, equation (4.8) reduces to a much simpler form.

$$\frac{d[B\bullet]}{d[A\bullet]} = \frac{k_1[A\bullet] - k_2(1 - R_h)[B\bullet]}{\frac{k_0}{k_2}P + k_2 R_h [B\bullet] - k_1[A\bullet]} \quad (4.9)$$

Equation (4.9) can be used to investigate the effects of the parameters on the relative rates of change of concentration.

Case 1: $R_h << 1$

$$\frac{d[B\bullet]}{d[A\bullet]} = \frac{k_1[A\bullet] - k_2[B\bullet]}{k_0P - k_1[A\bullet]}$$

This is the expression that we would get in the absence of water. At short reaction times $\frac{d[B\bullet]}{d[A\bullet]}$ will be positive as active radicals form.

$$\text{Short time: } k_1[A\bullet] > k_2[B\bullet] \quad \frac{d[B\bullet]}{d[A\bullet]} = \frac{k_1[A\bullet]}{k_0P - k_1[A\bullet]}$$

The relative rate will then become negative as active radicals decay more rapidly than they form, and the denominator of the above equation becomes negative.

At long reaction times $\frac{d[B^{\bullet}]}{d[A^{\bullet}]}$ will again be positive as the slower decay of B^{\bullet} comes to dominate.

$$\text{Long time: } P \text{ small, } [A^{\bullet}] \text{ small} \quad \frac{d[B^{\bullet}]}{d[A^{\bullet}]} = \frac{k_2[B^{\bullet}]}{k_1[A^{\bullet}]}$$

Case 2: $R_h \gg 1$

$$\text{Short time: } k_0P > k_1[A^{\bullet}] \quad \frac{d[B^{\bullet}]}{d[A^{\bullet}]} = \frac{k_1[A^{\bullet}] - k_2R_h[B^{\bullet}]}{k_0P + k_2R_h[B^{\bullet}]}$$

The relative rate will be $O(0)$ because the two terms in the numerator are of similar magnitude.

$$\text{Long time: } k_0P < k_1[A^{\bullet}] \quad \frac{d[B^{\bullet}]}{d[A^{\bullet}]} = \frac{k_1[A^{\bullet}] - k_2R_h[B^{\bullet}]}{k_2R_h[B^{\bullet}] - k_1[A^{\bullet}]} = -1$$

The presence of water increases the concentration of A^{\bullet} at the expense of B^{\bullet} at longer reaction times, just as we would expect. This is the opposite result from the case where R_h was small, and sites of type B^{\bullet} were favored.

Two conclusions are evident from the above equations. First, there are no reaction conditions where water causes a net transfer of sites from type B^{\bullet} to type A^{\bullet} . The rate $\frac{d[B^{\bullet}]}{d[A^{\bullet}]}$ can only be positive in the presence of water at short reaction times when sites of type A^{\bullet} are forming rapidly. The second result is that the addition of water would serve to maintain a concentration of active radicals, even after the radical forming reactions were complete.

4.4.2 Surface Area of Chars The char surface areas listed in Table 4.6 indicate that Woodex is a thermoplastic material for pyrolysis below 390 ° C. Areas of less than 5 m²/g. are consistent with a solid having little internal surface. The chars at 460 ° C had much higher surface areas, possibly due to the relative rates of

solidification and formation of volatiles. If the melt began to crosslink at higher temperatures and become more viscous, then bubble formation and shrinkage would lead to some internal surface. Under an optical microscope these higher temperature chars did not appear different from their low-temperature counterparts. All exhibited a glossy appearance which was consistent with melt formation.

The char from 16% moist Woodex had only half the surface area of the char from dry Woodex at 460 ° C, 22.6 m²/g. versus 56.7 m²/g.. The moist sample also produced 5 yield % more char than did the dry sample. The lower surface area is consistent with trapping of the tar in the solid. Accretion of tar onto the char structure would reduce the diameter of pores within the solid and limit the surface area that would be accessible to nitrogen molecules. The change in surface area could also be due to physical effects of water. If moisture reduced the viscosity of the molten Woodex, then bubble formation would be facilitated. In a less viscous melt the evolution of bubbles would form less internal surface.

4.4.3 Simultaneous Drying and Pyrolysis of Wood The results presented earlier in this paper show that moisture does indeed affect pyrolysis under appropriate conditions, which leads us to assume that water was present during the decomposition reactions. We shall test this assumption by examining the yields of aqueous condensate and gas with time, and the rate of heating of the powdered samples within the reactor.

Aqueous fluid from the water-cooled condenser was collected, in up to four flasks, over the course of a reactor run. The weight of fluid in each flask gave an indication of the rate of formation of water and light organics, and of the rate of drying of the sample. The major component of the condensate samples was water. Dry Woodex produced residual water that had been adsorbed strongly in

the polymer matrix and water formed by dehydration reactions. Moist samples gave additional water due to drying of the wood. Table 4.9 lists the yield of aqueous condensate with time from moist and dry samples, each containing 5 grams of Woodex on a dry basis. A comparison of the yields from dry and moist samples shows that the moist samples produced more condensate than the dry samples in every time interval. Even after 3 minutes of reaction, the moist samples produced more condensate, due to continued drying.

The composition of the effluent gas from the reactor was measured during each reactor run, as described earlier. The amount of pyrolysis gas produced during a given time interval indicates the change in the extent of overall reaction. Table 4.10 lists the yields of condensate and gas (as a percentage of total product) for the same samples and time intervals as in Table 4.9. All samples produced the greatest amounts of gas and condensate during the same time intervals. Drying did not precede the pyrolysis reactions.

The times given in the tables have not been corrected for the time lag between reaction inside the reactor and the collection of a sample. Tracer experiments with CO₂ showed that there was a lag time of about 15 seconds from the reaction zone to the chromatograph sampling valve. A similar lag time would occur with the condenser samples. Since the results are given over relatively long intervals of time, this lag is not significant.

The temperature of reaction was monitored from a thermocouple inserted into the fluid bed. The resulting values of temperature were an average of the gas and solid temperatures. After a sample was loaded into the reactor the temperature-time curve could be described by the following equation:

$$T \approx T_i \left[1 - a_1 e^{-\alpha t} - a_2 e^{-\beta t} \right] \quad (4.10)$$

T = mean temperature in reactor

T_i = initial and final temperature

t = time

α, β = time constants, $\alpha > \beta$

The temperature difference was approximated by a sum of exponentials because the wood was heating, drying, and reacting simultaneously. As the temperature approached the final temperature, $\ln(T - T_i)$ varied linearly with time. We can use the slope, β , from a plot of $\ln(T - T_i)$ versus time to see the effect of drying on the rate of heating. The greater the slope the greater the rate of temperature rise and the smaller the effect of drying. Moisture content affected only the last 5-6 C° of temperature rise. Table 4.11 lists the values of β for moist and dry samples. These values are averages from a number of experiments at 390° C. The samples with a higher initial moisture content heated more slowly during the last 5 C° of temperature rise, due to continued drying. Although the moisture content influenced the temperature of the particles as they were reacting, the effect was within the variation in heating rates between replicate experiments. Furthermore earlier pyrolysis tests showed that the final reaction temperature was more significant than the rate of heating in determining the distribution of products (see Appendix C).

The production of condensate and the heating rate curves both indicated that drying continued even when the measured temperature inside the reactor was over 300 ° C. Drying data for wood, although at much lower temperatures, shows that the rate of drying falls rapidly with decreasing moisture content, below 20% moisture by weight. Although the effects of pyrolysis on adsorption

isotherms and permeability are not known, our observations on drying are consistent with data on wood at lower temperatures.

4.5 Summary

1. Moisture increased the yield of char from the pyrolysis of Woodex by 5 yield % at 390 and 460° C. The presence of moisture reduced the yield of tar from pyrolysis above 400 ° C. Physical effects such as swelling by moisture, melting, and enhanced intraparticle transport cannot account for these results.
2. A mechanism for the interaction between free radicals and water during pyrolysis gave qualitative predictions that agreed with the observed effects of temperature on the yield of products from moist and dry Woodex.
3. The surface area of char from moist Woodex at 460° C was less than half the area from a dry sample. This reduction in the surface could be due to trapping of tar within the solid, or to the effect of water on the viscosity of molten Woodex.
4. The yields of aqueous product and gas with time showed that drying continued throughout the course of pyrolysis.

REFERENCES

- [1] Alfassi, Z. B., and Benson, S. W., *Int. J. Chem. Kin.*, **5(5)** , 879-892, 1973.
- [2] Aliev, D.A. et al., *Khim. i Technol. Topliv. i Masel* **9(4)** , 30-32, 1964. From *Chem. Abstr.* **61** ,abstract no. 1677h, 1964.
- [3] Arthur, J.C., Jr., *High Polym.* **5(pt 5)** , 977-90, 1971.
- [4] Benson, S. W., *Thermochemical Kinetics* , 2nd Ed., Wiley, New York, 1976.
- [5] Bradbury, A.W.G., Sakai, Y., Shafizadeh, F., *J. Appl. Polym. Sci.* **23** , 3271-3280, 1979.
- [6] Browning, B.L., in *The Chemistry of Wood* ,ed. B.L. Browning, Wiley, New York, 1963.
- [7] Gorbaty, D. A. I., *Fuel* **57** , 796-797, 1978.
- [8] Goring, D. A. I., in *Lignins* , eds. Sarkanen, K. V., and Ludwig, C. H., Wiley, New York, 1971.
- [9] Mikulich, S. M., and Mikulich, A. S., *Svoista Strukt. Gazov, Zhik. Tverd. Tel.*, ed. by M. S. Tsedrik, Minsk Gos. Pedagog. Inst., Minsk, U.S.S.R., , 48-52, 1975. From *Chem. Abstr.* **87** , Abstract # 203269, 1977.
- [10] Nanassy, A.J., and Fung, D.P.C., *Wood Sci.* **7(3)** , 232-9, 1975.
- [11] Niclause, M., et al., in *Ind. and Lab. Pyrolysis* , ed. by L. F. Albright and B. L. Crynes, ACS, 1976.
- [12] Shafizadeh, F., *Advances in Carbohydrate Chemistry* **23** , 419-465, 1968.
- [13] Skaar, Christen, *Water in Wood* , Syracuse University Press, Syracuse, 1972.
- [14] Van Arsdel, W. B., *Trans. Am. Inst. Chem. Eng.* **43(1)** , 13-24, 1947.
- [15] Zavitsas, A. A., and Melikian, A. A., *J. Am. Chem. Soc.*, **97** , 2757-2763, 1975.

Appendix - Rate of Reaction of Water with Radicals

Figure 4-6 shows how water would react with radicals from the cleavage of an ether linkage. In this case the initial radicals were derived from cellulose, but reactive groups derived from hemicellulose or lignin would react similarly. Although the glucose radicals in Figure 4-6 would be unstable, and subject to rearrangement and addition reactions, the free radical sites would remain associated with a carbon or oxygen atom. Ether linkages, radicals, and water would be distributed at random through the matrix of the wood. We can view the active species as being in a solid solution, and work in terms of concentrations with units of moles/liter of wood polymer.

The changes in enthalpy and entropy for the two types of reactions were estimated by assuming that the reactions could be reduced to the interactions of appropriate molecular groups as shown in Figure 4-7. The radicals that formed from the original cleavage of the ether linkage (type A•) would rearrange to form new structures (type B• and C•). The reaction of water with radicals A• or B• would be equivalent to that shown in Figure 4-7. Using the group additivity methods of Benson (1976) and assuming that gas phase data could be used to describe reactions in the molten Woodex, we calculated the following parameters:

Reaction	ΔH^0_R	ΔS^0_R	$\Delta C_{p,R}^{300}$	$\Delta C_{p,R}^{400}$	$\Delta C_{p,R}^{500}$	$\Delta C_{p,R}^{600}$
1	26.35	-2.71	-0.27	0.0	0.33	-0.17
2	14.52	2.17	0.63	0.54	1.02	0.31

The reverse reactions are exothermic, but involve the same transition states. The Arrhenius parameters for the reverse reactions were estimated from

data for similar reactions. Reactions 1 and 2 were both metathesis reactions, involving the transfer of a hydrogen atom from one species to another. Alfassi and Benson (1973) found that metathesis reactions depend on the electron affinities of the reactive end groups more than on the identity of the transferred atom. The Arrhenius constants were based on data for reactions with the same end groups. Zavitsas and Melikian (1975) listed Arrhenius constants for a number of reactions involving hydroxy radicals. The following table gives the data for the analogous reverse reactions:

Reaction	Similar Reverse Rxn.	E*	log ₁₀ A
1	(CH ₃) ₂ CH ₂ + HO•	4.2	8.5
2	(CH ₃) ₃ COH + (CH ₃) ₃ CO•	1.4	6.5

The first reaction analog gave a good estimate of the parameters for the reverse of reaction 1. Both reactions involve similar transition states whose rate of formation is determined by the approach of the small hydroxy radical to a much larger molecule. The second reaction analog would give an overestimate of the activation energy for reaction 2 because the smaller hydroxy radical would be less hindered in forming the transition state than the large t-butoxy radical. Since the value of E_a was small, the possible error would be small. The value 10^{6.5} for A is smaller than the normal range of 10⁸ - 10¹⁰ which is normally observed in hydrogen-metathesis reactions. Zavitsas and Melikian (1975) attributed the low value of A to the formation of a tight transition state. The energy and entropy of the transition state would be determined by the bonding between oxygen and hydrogen as well as the end groups, in this case two oxygens. The contribution of the O-O bond to the transition state would be

much smaller than in carbon-centered systems where the C-C or C-O bonds were involved.

Given the above data for the reverse reactions, we obtained the following constants for the forward reactions:

Reaction	ΔH^0_R	E^*	$\log_{10}A$
1	26.35	30.55	8.5
2	14.52	15.92	6.5

The data of Nanassy and Fung (1975) on spin concentrations were used to estimate the rate of reaction between water and radicals in wood. The spin concentrations were extrapolated back to time $t=1$ minute, and each spin was assumed to correspond to a radical of type B. All these estimates apply to short reaction times, before depletion of wood and moisture by volatilization become significant.

The radicals are assumed to derive from the dissociation of C-O bonds, so that half are of the alkoxy type and the other half carbon centered. Given the particle density of wood the initial concentration of each radical was calculated. A constant moisture content of 16% by weight was used. Table 4.12 shows the rate constants and concentrations at each temperature, and Table 4.13 gives the rate of each reaction and the total rate of reaction of water with radicals.

Table 4.1 Variation Between Replicate Samples (Temperature within 10 C°)				
Variable	Mean	Std. Deviation	Maximum	# of Pairs
	$\overline{ x_1 - x_2 }$	$\sigma_{\overline{ x_1 - x_2 }}$	Variation	
Yield of Char, %	2.1	1.3	4.1	9
Yield of Tar, %	1.5	1.7	5.4	9
Yield of Gas, %	0.74	0.5	1.1	5
Yield of Aqueous, %	4.0	2.8	9.3	9

Table 4.2 Yields of Products from Dry Ash-free Woodex Yields as % of Initial Weight				
Pyrolysis Temp. ° C	335	398	456	464
Char	49.3	41.9	33.0	31.2
Tar	23.6	25.9	34.2	36.5
Gas	2.7	4.1	5.4*	5.4
Aqueous	20.8	23.7	27.8	23.1
Total	96.4	95.6	100.5	96.2

Table 4.3 Yields of Products from 16%-Moist Ash-free Woodex				
Yields as % of Initial Dry Weight				
Pyrolysis Temp. ° C	337	396	450	465
Char	50.1	46.5	39.9	35.4
Tar	26.1	27.4	27.2	28.9
Gas	2.7*	4.1*	5.4*	6.4
Aqueous	20.3	23.3	22.9	26.4
Total	99.2	101.4	95.4	96.9

* - Estimated from other Woodex samples

Table 4.4 Yield of Liquid Products From Ash-free Woodex (Samples collected in liquid nitrogen trap)		
Pyrolysis at 396 ° C, % of Initial Dry Weight		
Compound	Dry Woodex	16% Moisture
Methanol	0.98	0.58
2-oxopropanal	1.23	0.62
Acetic Acid	2.54	1.94
1-hydroxy-2-propanone	1.38	0.66
Furfuraldehydes	0.96	0.71
Guaiaicols	1.08	1.20
Total	8.16	5.71
Pyrolysis at 460 ° C, % of Initial Dry Weight		
Compound	Dry Woodex	16% Moisture
Methanol	0.87	0.89
2-oxopropanal	0.96	1.34
Acetic Acid	2.70	2.79
1-hydroxy-2-propanone	1.56	1.08
Furfuraldehydes	0.71	0.94
Guaiaicols	1.82	1.36
Total	8.62	8.40

Table 4.5 Yields of Products from Moist Ash-free Woodex at 396° C			
Yields as % of Initial Dry Weight			
Weight % Moisture	0	16	28
Char	41.9	46.5	48.7
Tar	25.9	27.4	24.8
Gas	4.1*	4.1*	4.1*
Aqueous	23.7	23.3	20.4
Total	95.6	101.4	98.0

* - Estimated from other Woodex samples

Table 4.6 Nitrogen Surface Areas of Chars		
Temperature, ° C	Dry	16% Moist
330	< 0.8	0.9
390	2.8	4.6
460	56.7	22.8

Table 4.7 Rate Constants for Pyrolysis		
Temperature, ° C	$k_m \text{ sec}^{-1}$	$k_c \text{ sec}^{-1}$
300	1.38E-4	1.62E-4
350	9.59E-4	4.71E-4
400	9.49E-4	7.31E-4
500	3.69E-3	1.25E-3
600	1.11E-2	2.83E-3

Table 4.8 Hop Ratio for Douglas Fir Wood				
Temp., ° C	k_c , sec. ⁻¹	Immobilization	Relocation	R_h
		Rate, $\frac{\text{gmol.}}{\text{l.-sec.}}$	Rate, $\frac{\text{gmol.}}{\text{l.-sec.}}$	
300	1.62E-4	7.95E-4	4.93E-5	6.20E-2
350	4.71E-4	2.31E-3	3.68E-3	1.59
400	7.31E-4	3.58E-3	9.53E-2	26.6
500	1.25E-3	6.13E-3	1.854	302.0
600	2.83E-3	1.39E-2	14.91	1.07E3

Table 4.9 Aqueous Condensate from Woodex Pyrolysis at 390 ° C					
Dry		16% Moist		28% Moist	
Time Interval	Weight	Time Interval	Weight	Time Interval	Weight
sec.	grams	sec.	grams	sec.	grams
0-180	0.2597	0-107	0.9216	0-115	0.8908
180-end	0.0643	107-240	0.3502	115-216	0.6358
-	-	240-end	0.0333	216-end	0.3997

Table 4.10 Gas and Condensate from Woodex at 390 ° C		
Dry Woodex		
Time sec.	Gas %	Condensate %
0-180	73	80
180-end	27	20
16% Moist Woodex		
Time sec.	Gas %	Condensate %
0-107	67	71
107-240	24	27
240-end	9	2.6
28% Moist Woodex		
Time sec.	Gas %	Condensate %
0-115	50	46
115-216	33	33
216-end	17	21

Table 4.11 Time Constants for Heating of Woodex	
Sample	Time Constant, β , sec. ⁻¹
Dry Woodex	0.0155
16% Moist	0.0079
28% Moist	0.0046

Table 4.12 Rate Constants for Reaction of Water with Free Radicals				
Temp. ° C	Reaction 1 k, l./mol.-sec.	Reaction 2 k, l./mol.-sec.	[Total Radicals] mol./l.	[Water] mol./l.
300	7.04E-4	2.68	5.3E-6	6.94
350	6.05E-3	8.22	1.3E-4	6.94
400	3.77E-2	21.25	1.29E-3	6.94
500	0.728	100.1	5.30E-3	6.94
600	7.18	325.9	1.29E-2	6.94

Table 4.13 Rate of Reaction of Water with Free Radicals			
Temp. ° C	Reaction 1 rate, mol./l.-sec.	Reaction 2 rate, mol./l.-sec.	Total Reaction rate, mol./l.-sec.
300	1.29E-8	4.93E-5	4.93E-5
350	2.71E-6	3.68E-3	3.68E-3
400	1.69E-4	9.51E-2	9.53E-2
500	1.33E-2	1.841	1.854
600	3.21E-1	14.59	14.91

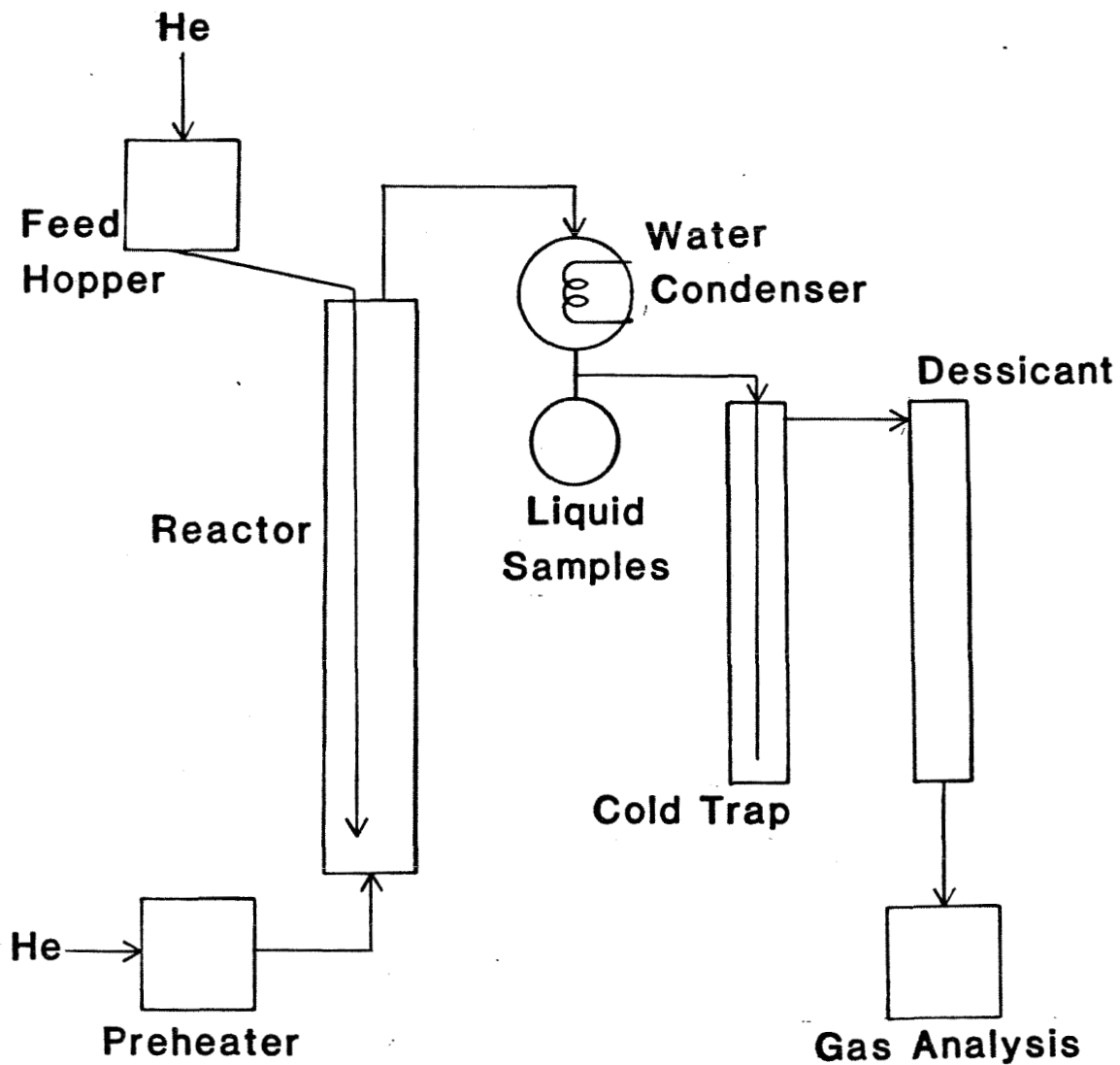


FIGURE 4-1
PYROLYSIS REACTION APPARATUS

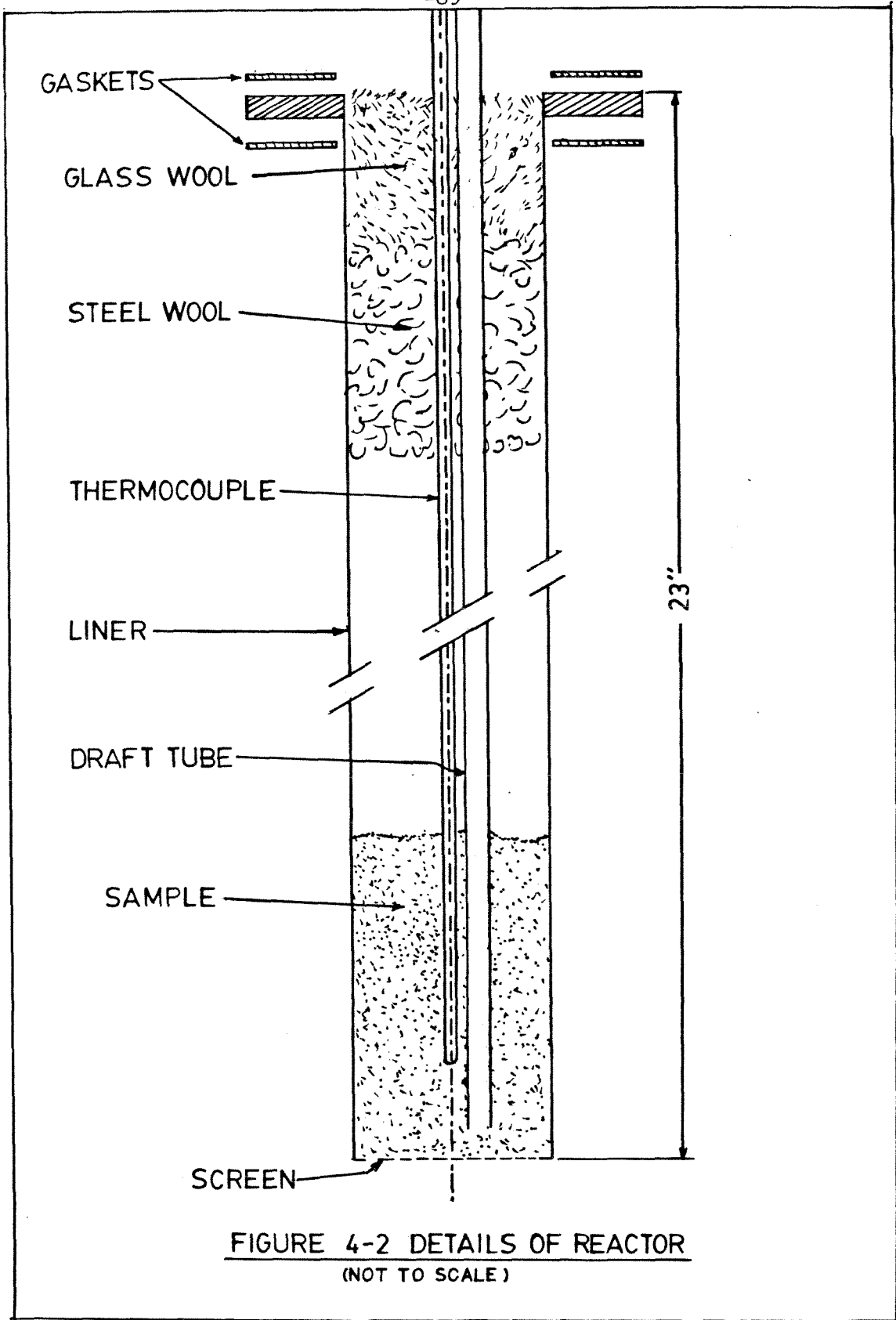


FIGURE 4-2 DETAILS OF REACTOR
(NOT TO SCALE)

FIGURE 4-3
EFFECT OF MOISTURE ON YIELD
OF TAR FROM ASH-FREE WOODDEX

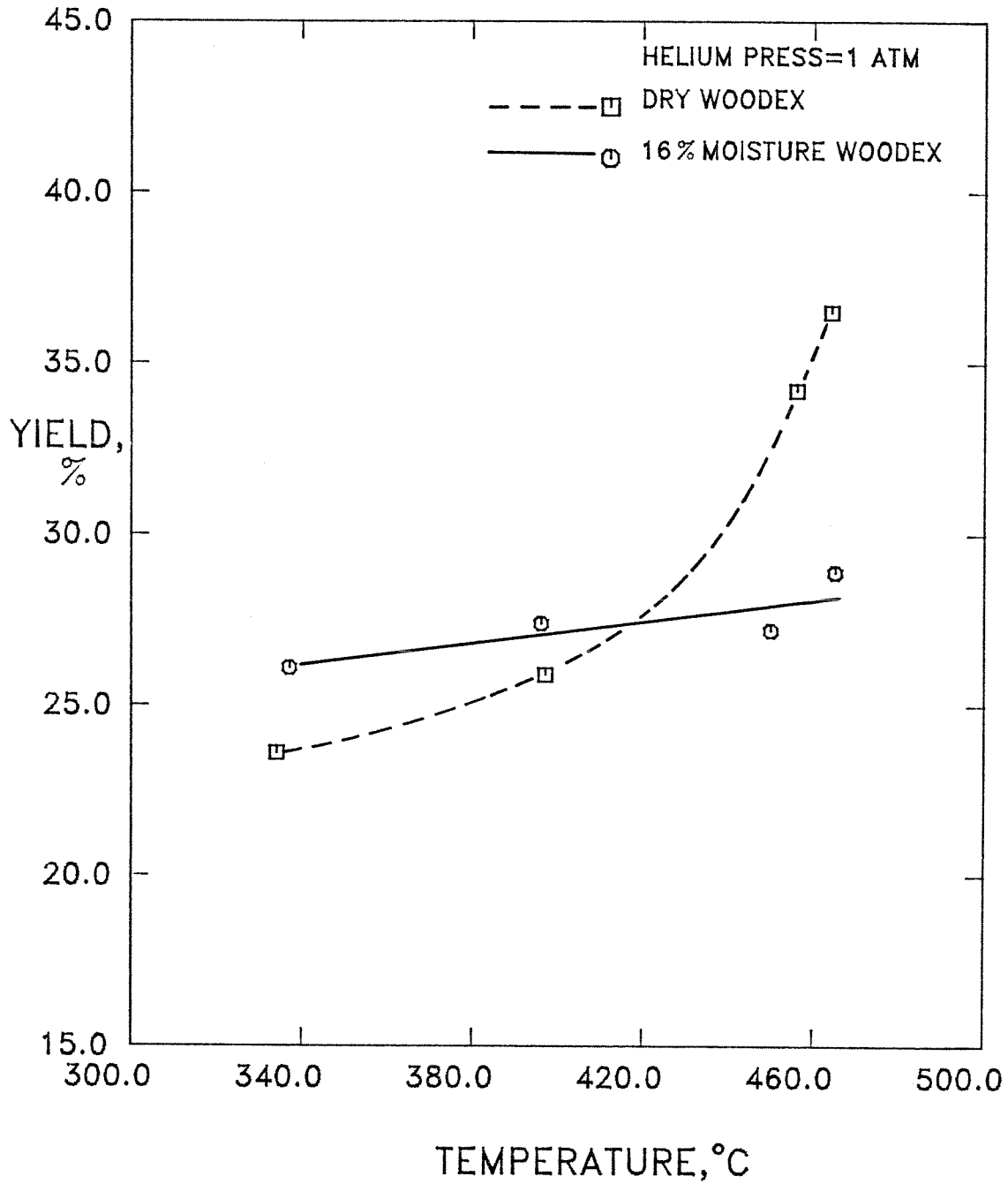


FIGURE 4-4
EFFECT OF MOISTURE ON YIELD
OF CHAR FROM ASH-FREE WOODDEX

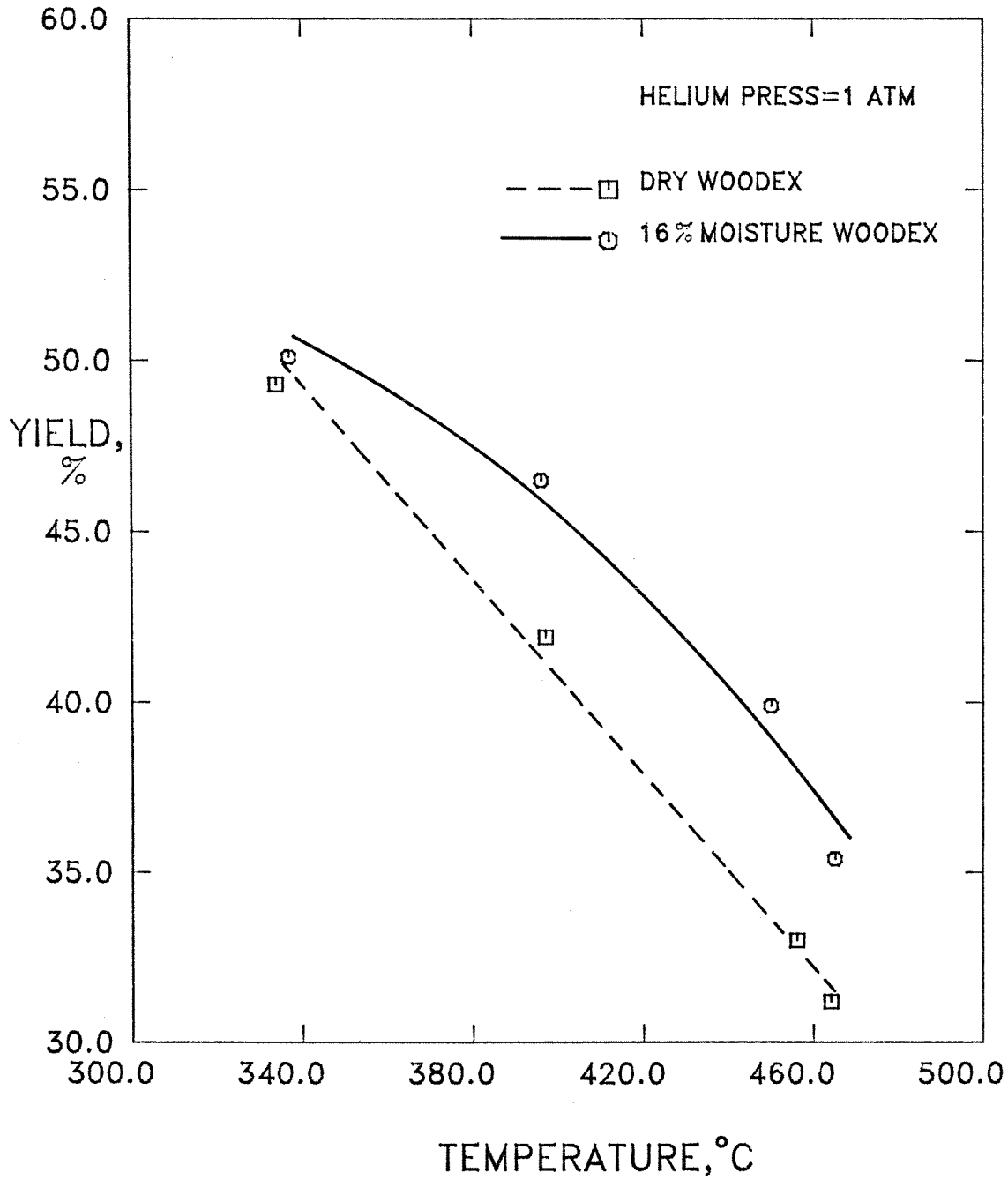


Figure 4-5 Cleavage of Cellulose Linkage

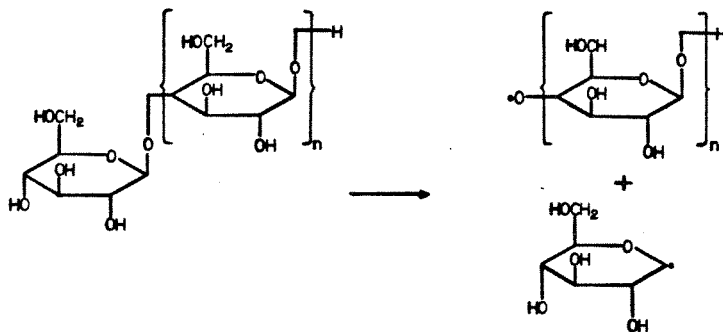


Figure 4-6 Reaction of Water with Radicals

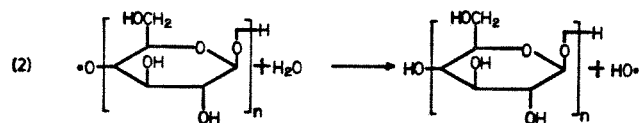
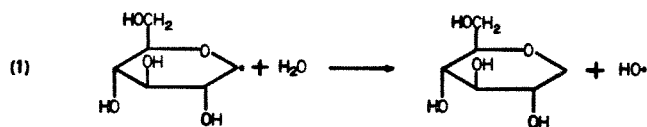
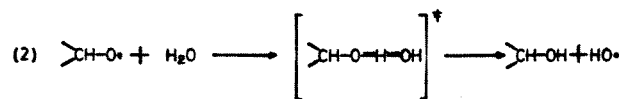
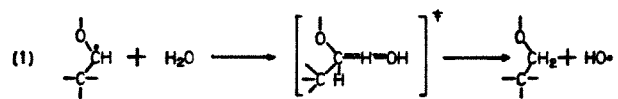


Figure 4-7 Reaction of Water with Molecular Groups



5. EFFECT OF INORGANIC COMPONENTS ON THE PYROLYSIS OF WOOD EX

5.1 Introduction and Background

The inorganic or mineral content of solids such as wood or coal occurs in two forms. The first is discrete mineral particles which form a distinct and separate domain from the surrounding organic phase. In wood these particles consist of silicate and aluminate minerals which were incorporated into the structure, especially in the bark during tree growth. Mineral grains in coal are often pyrites or clays.

The second form of inorganic matter is cations associated with anions in the organic phase. These cations are distributed throughout the solid at an atomic scale and are much more active than the discrete particles in catalyzing the reactions of pyrolysis. Likewise the effect of added metal ions depends on how intimately they are brought into contact with the solid structure of the wood.

The mineral content of wood or coal is sometimes referred to as the ash content, which is the material left behind after burning the the organic matter. The ash from wood contains Ca, Fe, Al, Na, Mg, and K.

Among coals, lignite has a high inorganic content in the form of metal ions and provides considerable ion-exchange capacity. Schafer (1970) utilized infra-red spectrophotometry to demonstrate that the ion-exchange capability of lignite was due to the presence of carboxyl groups. When the lignite was washed with acid, the characteristic absorption peak for carboxyl groups appeared in the IR spectrum. When the lignite was ion exchanged with a metal salt the absorption peak almost disappeared, indicating that the carboxylate salt of the metal formed. Metals added to this ion-exchange structure would be evenly distributed through the solid.

5.1.1 Observed Effects of Inorganic Compounds on Pyrolysis of Solids Several investigators have reported the effects of very small amounts of minerals on pyrolysis. Broido (1966) compared the pyrolysis of cellulose with an ash content of less than 0.01% to cellulose with an ash content of 0.15%, and found that the latter gave a higher char residue. The composition of the ash was not given. Shafizadeh et al.(1979) found that washing wood and wood components in 1% H_2SO_4 for two hours increased the yield of tar from vacuum pyrolysis at 400 ° C by about 5 yield points, and the yield of levoglucosan in the tar by as much as seven fold. A dilute HCl wash was even more effective in promoting the formation of tar from newsprint, giving an increase of 17 yield points. The composition and yield of gas and aqueous products was not reported. The action of the acid wash was attributed to hydrolysis or the removal of inorganic constituents.

Tyler and Schafer (1980) investigated the effect of cation content on the flash pyrolysis of lignite. The metal cations associated with the carboxylic acid groups which occurred naturally in the lignite were replaced with hydrogen ions by washing with 2N HCl at room temperature. Using ion exchange with a 1N solution of calcium acetate at controlled pH, they were able to select the cations associated with carboxylic acid groups in the lignite structure. Increased calcium content was observed to reduce tar yield by a factor of two but did not affect the yield of hydrocarbon gases. The yields of hydrogen and carbon oxides were not reported. Fang and McGinnis (1976) evaluated the influence of sodium hydroxide on the flash pyrolysis of holocellulose and found that the salt increased the yield of hydrogen, carbon dioxide, acyclic carbonyl compounds, and light hydrocarbons. The effect was most significant at temperatures above 500 ° C. The sodium hydroxide was introduced into the holocellulose as an aqueous solution. Feldmann et al.(1981) found that mixing wood ash or calcium oxide with wood increased the yield of light organic compounds.

Franklin, Peters, and Howard (1981) subjected coal-calcite and coal-lime mixtures to rapid pyrolysis. The mixtures were prepared by slurring coal and minerals in water and subsequently drying off the water. They found that both additives reduced the yield of tar and increased the yield of char, in agreement with the trend observed by Tyler and Schafer (1980) at much lower calcium levels. Franklin et al. postulated that calcium catalyzed the decomposition of phenolic groups to carbon monoxide and polymeric char, which would account for the observed evolution of carbon monoxide.

5.1.2 Effects of Moisture on Pyrolysis Wood and low-rank coals always contain some moisture, depending on composition and drying history since collection. Unless a special effort is made to dry such materials, they will always contain some moisture. Water is present as liquid in small pores, as hydrates of minerals, or attached to the polymer structure by hydrogen bonding.

In Section [4] we considered the effects of moisture on wood pyrolysis in the absence of ash. Moisture suppressed the formation of tar above 390 ° C. We speculated that water aided the relocation of free radicals within the wood matrix. Relocation would increase the concentration of radical sites which are accessible to recombination by tar molecules and would thereby result in a lower tar yield.

Jones et al. (1964) pyrolyzed moist and dry coal samples in steam and nitrogen at 800 ° C. The effects of steam alone were consistent with simple gasification of the char, after the pyrolysis was complete. Moist samples in nitrogen gave less char, less aqueous liquor, more tar and more gas than did dry samples. Moist samples in steam gave less char and tar than did moist samples in nitrogen, consistent with gasification of char and gas phase reactions of tar in the presence of steam. The magnitude of the changes in the yield of tar due to

moisture was 1 to 2 yield points.

Workers at Occidental Petroleum found that steam or CO₂ reduced the cracking of tar by recycled char in a pyrolysis reactor (Gavalas, 1982). Water and carbon dioxide apparently blocked active sites on the surface of the char between 600 and 800 ° C.

The purpose of the present work was to determine the effects of inorganic components on the pyrolysis of moist and dry wood by measuring the product distribution and the composition of the gas and aqueous condensate over a range of temperatures. Using a fluid-bed reactor it was possible to react well-mixed samples at uniform temperatures, and achieve an overall material balance of better than 95% on average. The effects of inorganic compounds were evaluated by reacting ash-free, calcium-exchanged, and untreated samples. The results are discussed qualitatively in terms of the underlying chemistry of the reactions.

Samples which contained their original ash content and 0-28% moisture were pyrolyzed between 330 and 460 ° C to observe interactions between water and catalysis of reactions by inorganic components. The results are explained in terms of hydration of active sites and the effect of water on the transport and reaction equilibria of tar.

5.2 Experimental

The apparatus and method were described in Section [4.2]. All tests used about 5g. of wood. Woodex[®] pellets, supplied by Bio-Solar Research of Eugene, OR, were ground and sieved to separate the +60-100 U.S. mesh fraction. The powdered wood was vacuum dried at 105 ° C to remove essentially all of the water of hydration. Moist Woodex samples were prepared by mixing the dry powder with distilled water. The mixture was allowed to stand for a week to

ensure that the water had been fully absorbed.

Woodex powder was treated with dilute acid to remove the active minerals from the solid. The ground Woodex was stirred with 0.5 N HCl in a ratio of 50 ml./g. for 7 hours at 25 ° C. The acid treatment was mild enough that the cellulose was not hydrolyzed yet the mineral compounds in the wood structure were effectively removed. The samples did contain residual ash, due to discrete particles of sand mixed with the sample. The samples were, however, ash free from the standpoint of reactivity. After the acid wash the slurry was filtered and rinsed with demineralized water to neutral pH. The powder was then vacuum dried at 105 ° C for 12 hours. Table 5.1 lists the amounts of each ash component in the untreated and acid-washed samples, as determined by ASTM methods. The active ash content of the untreated samples was estimated from the weights of Al, Fe, Ca, Mg, Na, and K removed by the acid. The ash content of the acid-washed sample was subtracted from the untreated sample to obtain the active ash, after correcting for the weight of organic matter lost during the wash to put the weights on a common basis. Using equivalents of cations, the total active ash content of the untreated samples was about 1.30 m.equiv./gram.

Calcium-exchanged samples were prepared by slurring ground wood with 1 N calcium acetate solution at 25 ° C for 24 hours. The pH was kept at 8.3 by the dropwise addition of 0.01 N NaOH solution. The final calcium content was 0.62 m.equivalents/gram of sample, as determined by direct analysis of the ash for calcium. Table 5.1 lists the mineral contents of acid-washed, calcium-exchanged, and untreated Woodex samples.

Table 5.2 lists the mean variation between replicate experiments that were within 10 C °. Also given are the standard deviation and maximum variation for each pyrolysis product. The variations in Table 5.2 are due to random

experimental error and differences in temperature between experiments, so the variations given in the table overestimate the random variation between samples. From the mean variations, relative to the yield of each product, and experimental considerations, the relative reliabilities of the data were:

Char > Tar = Gas > Aqueous

The recovery of aqueous product varied by 4 yield % on average because of differences in the effectiveness of the dessicant column from run to run. The lightest and heaviest components within the aqueous product were most subject to random variation. The light components, such as methanol, were only partially trapped in the condenser, and the guaiacols were partitioned between the tar and the aqueous product. As a result of this variability we consider change of less than a factor of two in the yield of an organic component to be insignificant.

One pair of tests was run with carbon dioxide as the fluidizing gas, to see if water and CO₂ had similar effects on the pyrolysis reactions.

5.3 Results

5.3.1 Effects of Inorganic Components Table 5.3 lists the yields of char, on a dry ash-free basis, vs. temperature from Woodex samples of different ash contents. Char formation was influenced both by the ash content and by the acid-washing procedure. Consequently, the yields of the other products are reported in Table 5.4 as % of weight loss, to remove the effect of pretreatment, and to correct for small differences in pyrolysis temperature. Calcium and the native minerals had a very large effect on the yields of aqueous and tar products. The addition of calcium reduced the yield of tar by 13 % at 330 ° C and by 40 % at 460 ° C. The untreated samples gave from 30 to 50 % less tar than the acid-washed samples. An increase in the yields of aqueous products, char, and

gas corresponded to the reduction in yield of tar. Table 5.5 lists the composition of aqueous products from samples of Woodex pyrolyzed at 330 and 460 ° C. The yields of organic components were enhanced by the presence of calcium cations.

The change in product distribution with temperature from the pyrolysis of dry untreated Woodex is shown in Figure 5-1. The yields of gas, tar, and aqueous product increase monotonically with temperature, while the yield of char decreases. Figure 5-2 illustrates the effect of temperature on the yield of char from dry and moist Woodex. At temperatures above 340 ° C the addition of moisture to Woodex increased the yield of char by as much as 5 yield points. Pyrolysis of moist and dry demineralized Woodex gave almost the same yields of char (Figure 4-4).

Figure 5-3 shows that the yield of tar from moist Woodex went through a minimum at 390 ° C. Above and below this temperature the moist Woodex produced significantly more tar than did the dry samples. The yield of aqueous material went through a corresponding maximum at 390 ° C, as shown in Figure 5-4. The data are listed in Tables 5.6, 5.7, and 5.8. The increase in tar yield due to moisture above 396° C was opposite to the result from demineralized samples (Figure 4-3).

Table 5.9 shows that the formation of gases was unaffected by the presence of moisture. Similarly Table 5.10 shows that moisture did not have a major effect on the yield of light organic compounds. The yields of methanol and 2-oxopropanol did increase with moisture content, but the increase was similar at 330 ° C and 460 ° C. This result could be due to improved trapping of compounds in the larger volume of condensate from moist samples.

Table 5.11 shows that carbon dioxide and moisture had similar qualitative effects on the pyrolysis reactions at 460 ° C. Both CO₂ and moisture increased

the yields of tar and char.

5.4 Discussion

5.4.1 Effect of Inorganic Components The addition of calcium ions to acid-washed Woodex increased the yield of char by as much as 3 yield points (Table 5.3). Broido (1966) and Shafizadeh and Chin (1976) observed a similar increase in the formation of char due to inorganic components. Corresponding to the increase in char was a significant decrease in the yield of tar (Table 5.4). The major effect of calcium was to convert tar to aqueous product. For example, calcium reduced the recovery of tar by 12.5 yield points and increased the aqueous product by 11.4 yield points at 390 ° C. Char formation was increased by only 1.3 yield points. Similar changes were observed by Shafizadeh et al. (1979) in the vacuum pyrolysis of untreated and acid washed newsprint at 400 ° C. Clearly the calcium ions catalyzed reactions that formed light organic compounds and water with a minimum of condensation and coking.

Although the acid-wash removed active ash components, it also increased the yields of char at temperatures above 330° C, as shown in Table 5.3. The acid-washed and Ca-exchanged samples were treated with acid and both gave more char than did the untreated samples. The wash procedure removed low molecular weight compounds; polymers such as starches which would form volatiles rather than char during pyrolysis. The samples lost about 6 % by weight during the wash, which accounts for the differences in char formation.

Table 5.4 shows that both the untreated and calcium exchanged samples gave less tar and more aqueous condensate and gas than did the ash-free samples, on a % weight loss basis. The untreated samples gave less tar than did the Ca-exchanged samples because they contained twice as much active ash; 1.3 m. equiv./ g. versus 0.6 m. equiv./ g. Calcium ions introduced into the structure

by ion exchange, after an acid wash, give effects that are equivalent to the original ash compounds. This result shows unequivocally that the increase in the formation of tar from acid washed samples was due to the removal of metal cations and not the hydrolysis of cellulose. Tyler and Schafer (1979) observed that equivalent amounts of ion-exchanged calcium and native ash components gave the same reactivity in the pyrolysis of lignite.

5.4.1.a Nature of Catalyzed Reactions The inorganic components that are active during pyrolysis are metal cations associated with carboxylate anions within the structure of the wood. These metal-oxygen groups are Lewis bases that can donate electrons (or accept protons) and initiate a variety of reactions. Also present in the wood are high concentrations of hydroxyl, carbonyl, carboxylate, and ether groups. These groups stabilize the negative charge that results when a proton is donated to a base. The presence of bases which donate electrons and the presence of oxygen groups that stabilize the resulting negative charge gives reaction intermediates that have a largely anionic character. Basic metal-oxygen groups catalyze a variety of reactions which include: hydrogenation, dehydrogenation, hydrogen transfer, polymerization, aldol condensation, isomerization, cyclization, and dehydration (Pines and Stalick, 1977). These reactions proceed through anionic intermediates with primary and secondary carbanions being the most stable (Carey and Sundberg, 1977). Acids catalyze many of the same reactions, but give cationic intermediates. Unlike carbanions, tertiary carbonium ions are most stable. Consequently, although acids and bases give similar products when wood is pyrolyzed, the underlying mechanisms give different selectivities and yields of products.

During pyrolysis the basic sites are immobile and have a limited radius of action on the polymeric organic matrix. Although they may react with

neighboring polymer groups, their major effect will be via reactions with volatile species. The small influence of calcium on the yield of char (Table 5.3) indicates that inorganic compounds have little effect on the primary pyrolysis reactions.

Berkowitz-Mattuck and Noguchi (1963) proposed a reaction scheme to explain the evolution of light volatiles from the pyrolysis of cellulose. The key step was the formation of a linear polyol with aldehyde and carbonyl groups which would then break down to give smaller fragments such as 1-hydroxy-2-propanone, 2-oxopropanal, and methanol. Due to the stabilizing effect of oxygen groups, such a polyol will be very susceptible to anionic reactions in the presence of basic sites.

The yields of aqueous products shown in Table 5.5 confirm that calcium cations enhance fragmentation reactions. The yield of 1-hydroxy-2-propanone was increased by one to two orders of magnitude and the yield of acetic acid was increased by as much as 5 fold. Larger molecules were less affected by calcium; the yield of furfuraldehydes was increased by a factor of 1.5-3.9 times and guaiacols were unchanged, within the range of uncertainty of the data. Measurement error and variability during the collection and analysis of aqueous products was such that changes of less than a factor of two could not be considered significant.

Unlike base catalysts such as calcium, acid catalysts such as $ZnCl_2$ or sulfuric acid gave large increases in furfuraldehyde formation, and reduced the yields of acetic acid and 1-hydroxy-2-propanone (Shafizadeh and Chin, 1976; Morozov and Sobolev, 1974). Apparently anionic intermediates favored fragmentation, whereas the cationic intermediates in acid-catalyzed reactions favored cyclization.

Although untreated samples gave more aqueous product overall than did calcium-exchanged samples (Table 5.4), they gave a lower yield of organic compounds. The higher ash content of the untreated samples promoted dehydration reactions, giving more water and less organic components in the aqueous product.

5.4.2 Relative Yields of Products from Woodex and Wood Figure 5-1 shows the yields of the pyrolysis products with temperature. Woodex gave a similar product distribution to the pyrolysis of whole Douglas fir. Isothermal pyrolysis of fir wood in a fixed bed at 600 ° C gave 45% aqueous product and 12% gases, similar to the yields from Woodex (Shafizadeh and Chin, 1977). The whole wood gave less char (15%) and more tar (28%) than did Woodex. The differences are consistent with the higher pyrolysis temperature (600 vs. 470° C in this study), and the lower lignin content of the fir wood (37% polyphenols in Woodex vs. 15-20% in fir wood). Given the similar chemical composition of the two systems we expect that the chemical effects of parameters such as temperature, ash content, and moisture will be qualitatively the same for wood and Woodex. Physical mechanisms may differ considerably because fir wood is not as thermoplastic as Woodex.

5.4.3 Interactions Between Water and Inorganic Compounds Moisture increased the yield of char by about 5 yield points at 390 ° C and 460 ° C from both demineralized and untreated samples (see Figure 4-4, for the effect of moisture on acid-washed samples and Figure 5-2 for untreated samples). As speculated in Section [4] , moisture could assist trapping of tar molecules by free radical sites. We found that moisture reduced the yield of tar from acid-washed Woodex from 37% to 27% of initial weight at 460° C. The samples of untreated Woodex gave lower yields of tar due to the presence of ash; from 17 to

23% of initial dry weight at 460 ° C (Tables 5.6 and 5.7). The role of the catalytic material in the Woodex is to determine the degree of conversion of the available tar to aqueous product. If the catalyst is deactivated then the yield of tar will approach the levels obtained from demineralized samples.

A multiple linear regression analysis showed that the effect of moisture on the yield of tar was statistically significant (see the Appendix to this section). Hence the scatter of data points in Figure 5-3 around the curves is less than the difference between the curves.

The minimum with temperature in the yield of tar from moist Woodex (Figure 5-3) indicates the presence of at least two mechanisms of interaction between water and cation sites; one at low temperatures, below 390° C, and one at high temperatures. At low temperatures hydration of water on active sites would reduce the rate of catalytic reactions by reducing the availability of reaction sites. Hydrates would be less stable with increasing temperature. At high temperature the availability of reactants and reaction equilibria would begin to determine the yield of tar. Moisture would reduce the concentration of the tar in the vicinity of active sites and shift the equilibrium of dehydration reactions. The following sections explore these hypotheses in more detail.

5.4.3.a Water and Cations Below 390° C - Hydration of Sites The cations which are present in wood, such as aluminum, calcium, iron, and magnesium, tend to form stable hydrates at room conditions. The metals fill coordination positions by association with water. At low pyrolysis temperatures when catalytic effects on the overall reaction are dominant, availability of cation sites would control the overall reaction rate. Any hydration of cations would hinder the approach of reactive species to the metal and lower the activity of the catalyst sites. The key considerations in such a deactivation mechanism are the thermodynamic

stability and rate of decomposition of hydrates as a function of temperature and partial pressure of water. Throughout this discussion we will focus on the behavior of calcium and magnesium, as representative of the behavior of the cations which are found in wood char.

To model the hydration of disperse cations in wood at pyrolysis temperatures we use data from two analogous systems; hydration of calcium oxalate and adsorption of water onto CaO and MgO surfaces. Oxalate ($C_2O_4^{2-}$) is similar to the carboxylic acid sites that bind cations in the wood matrix but calcium oxalate is crystalline whereas the ions in wood are surrounded by amorphous polymer. For comparison we also consider the energetics of adsorption of water on metal oxide surfaces.

Dehydration of Calcium Oxalate Monohydrate Water fills a coordination position of the calcium atoms within the oxalate salt. The valency requirements of the calcium atom are filled by two oxygen atoms of the oxalate molecule. Hocart et al. (1964) investigated the dehydration of the monohydrate salt, and found that the reaction was reversible. The decomposition partial pressure of water was given by the following equation:

$$\ln p_{H_2O} = 9.2 - 3333/T \quad (5.1)$$

p_{H_2O} = pressure of water, mm Hg.

T = temperature, K

From this result they derived the following thermodynamic values for the decomposition reaction:

$$\Delta H = 15.7 \text{ kcal./mol.}$$

$$\Delta S = 28.9 \text{ cal./K-mol.}$$

The enthalpy of hydration is 5.2 kcal./ mol. greater than the latent heat of water at the same temperature due to the interaction of water with the salt.

When a crystalline hydrated solid decomposes in an open system, a pure anhydrite is formed from a pure monohydrate because the two solid phases have no mutual solubility. The two phases only coexist during the transient decomposition of the hydrate. Dave and Chopra (1966) used thermogravimetry to measure the kinetics of the dehydration reaction of calcium acetate. The reaction was found to be first order with an activation energy of 24.4 kcal./mol. and a pre-exponential factor of $4.96 \times 10^7 \text{ sec.}^{-1}$ (on a molar basis).

Adsorption of Water on Metal Oxide Surfaces The atoms of metal and oxygen on the surface of compounds such as MgO and CaO do not have fully satisfied valencies and can form chemical bonds with adsorbed molecules. MgO and CaO chemisorb a layer of water as hydroxyl and hydrogen, with binding energies as high as 60 kcal./ mol. (Anderson et al., 1965). The hydroxyl layer fills the vacant bonding valencies of the surface metal atoms, and the hydrogen fills the valencies of the surface oxygen atoms. Such bonding would not occur with cations in wood, whose valency requirements are fully satisfied by anions (Schafer, 1970). A second layer of water is adsorbed physically with an activation energy for desorption of roughly 20 kcal./ mol. (Anderson et al., 1965), similar to the activation energy for the decomposition of the oxalate hydrate. These physically adsorbed molecules are completely removed from CaO or MgO at above 250° C under vacuum (Anderson et al., 1965; Ito et al., 1976; Low et al., 1971). and are similar in stability to the hydrates of calcium oxalate, given the thermodynamic differences between a pure crystal and a surface layer. The chemisorbed hydroxyls are completely removed at 700-800 ° C under vacuum. The formation of chemisorbed species on the surface of oxides and

sulfides in coal char was likely responsible for the effect of water in the Occidental pyrolysis reactor mentioned earlier, since the addition of water and CO₂ would enhance the stability of chemisorbed layers at 800° C.

Hydration of Disperse Cations Cations in a polymer phase are in a different molecular environment from a that of a crystalline solid or an oxide surface. It is necessary to compare the properties of the crystalline, metal oxide, and the polymer-bound calcium before drawing conclusions about the possible role of hydration in pyrolysis reactions.

Solnyshkin (1957) found that the hydration numbers for calcium salts of fatty acids depended on the number of oxygen groups in the fatty acid. For example, calcium stearate (calcium octadeceneoate) had a hydration number of 3.6, while calcium ricinoleate (calcium 12-hydroxy-9-octadeceneoate) had a hydration number of 7.9. Cations in a wood polymer would be coordinated by several oxygen groups, and so would tend to form stable hydrates. As in a crystal lattice, the cations would have saturated valencies and be coordinated with nearby oxygen atoms.

Schafer (1972) measured the formation of hydrates of different cations in lignite. Samples were ion exchanged and equilibrated with air of 52% relative humidity at 20 ° C. The samples were then heated in an oven at 110 ° C (with air of the same moisture content). The extent of hydration was measured by removing the cations, and correcting the loss in weight for the cations themselves and the hydration of the lignite in the absence of metals. Schafer's results are given below:

Cation	Water, mol/equivalent of cation	
	20 ° C	110 ° C
Fe ⁺⁺	3.4	1.2
Mg ⁺⁺	3.31	0.74
Ca ⁺⁺	3.03	0.88
Al ⁺⁺⁺	2.5	0.55
Na ⁺	2.49	0.34

At room conditions, crystalline calcium oxalate would be in the monohydrate form, with 1 mole of water/ mole of calcium. An MgO surface would have 1-2 layers of physically adsorbed water (Anderson et al., 1965). Schafer's data show that under the same conditions the calcium ions in lignite would be associated with 0.88 mol. water/ equivalent of calcium, or 1.76 mol. water/mol. calcium ion. Hence cations dispersed in the polymer phase form hydrates that are of similar stability to the hydrates of crystalline calcium oxalate, and to the physically adsorbed water molecules on an oxide surface.

Kinetic Model of Hydrate Decomposition Using the data of Dave and Chopra (1966) and Hocart et al. (1964) on calcium oxalate we constructed a simple kinetic model for the dehydration of cation sites. Unlike a crystal, different cation sites can have different degrees of hydration. Above 250 ° C a cation site will have zero or one water molecules attached, so a Langmuir isotherm can apply assuming that the cation sites are uniform in binding energy. In this case the rates of adsorption and desorption are given as follows:

$$\text{Velocity of Adsorption, sec.}^{-1} = k_a(1 - \theta)p_{H_2O} \quad (5.2)$$

$$\text{Velocity of Desorption, sec.}^{-1} = k_d \Theta \quad (5.3)$$

$$k_a = A_a e^{-E_a/RT} \text{ (adsorption)}$$

$$k_d = A_d e^{-E_d/RT} \text{ (desorption)}$$

k = rate constant, sec.⁻¹

Θ = fraction of cation sites hydrated

p_{H_2O} = water pressure

E_d = 24.4 kcal. / mol. (desorption)

E_a = 8.7 kcal. / mol. (adsorption)

A_d = 4.96×10^7 sec.⁻¹ (Dave and Chopra, 1966)

A_a = 23.9 sec.⁻¹ (from A_d and ΔS)

The coverage Θ of active sites obeys the usual equation:

$$\frac{d\Theta}{dt} = k_a(1 - \Theta)p_{H_2O} - k_d\Theta \quad (5.4)$$

At equilibrium equation (5.4) gives the Langmuir isotherm:

$$\Theta = \frac{y_{H_2O}}{K + y_{H_2O}} \quad (5.5)$$

$$\text{where } K = \text{equilibrium constant} = e^{\frac{\Delta S}{R}} e^{-\frac{\Delta H}{RT}}$$

Effect of Hydration on Pyrolysis of Wood When moist wood is pyrolyzed as small particles in a fluid-bed, the temperature of the particles approaches the pyrolysis temperature very rapidly. At high heating rates the pressure of water inside the particles would be greater than ambient pressure until most of the water has been driven off the particles. Even after most of the water evaporates,

small amounts of moisture remain in the wood and exert considerable vapor pressure. Consequently, the water vapor pressure will be on the order of one atmosphere for a significant time, allowing us to use equation (5.4) to calculate the rate of decomposition of hydrate, and the final equilibrium, at different temperatures.

The effect of the hydrates on pyrolysis reactions depends on the occupancy of water molecules at active sites. At 330 ° C pyrolysis was active for about 2.5 min., while at 390 ° C reactions went on for about 1-1.5 min. The mean hydrate fraction during pyrolysis was obtained from the integral form of equation (5.4) for the appropriate reaction times. This calculation assumed that the water pressure in the particles was constant at one atmosphere throughout the pyrolysis reactions and would overestimate the mean hydrate fraction. Results are given in Table 5.12. Hydration would have a small effect at 390 ° C in a moist sample because only 10% of the sites would be hydrated during pyrolysis. At 330°C about 90% of the cationic sites would exist in the hydrate form during the pyrolysis reactions. The yields of tar were in accord with this result. At 330 ° C the tar yield from moist samples was higher than from dry samples. At 390 ° C the samples with 16 % moisture gave the same yields of tar as did dry samples while the 28% moisture sample gave a higher yield of tar, possibly due to the longer period of significant water pressure within the particle. We can conclude that the model put forward for hydrates blocking cations during pyrolysis gives predictions of the effect of temperature which are in qualitative agreement with the observed yield of tar below 390 ° C.

5.4.3.b Water and Cations at Above 390° C - Reaction Kinetics and Equilibria In considering the effect of moisture on high temperature reactions of tar, we will focus on dehydration reactions above 390° C. Wood tars are rich in hydroxyl

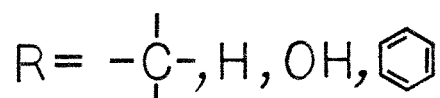
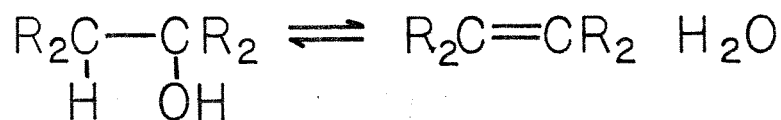
groups and base-catalyzed dehydration is a major step in forming the organic products that appear in the aqueous product.

At low temperatures the rate of dehydration is controlled by the availability and activity of catalyst sites. For example, Joly and Ollis (1979) dehydrated isopropanol over coal minerals at 350° C and observed a zero-order reaction with an activation energy of 17-22 k.cal./mol. At high temperatures the rate of dehydration would be proportional to the concentration of tar, assuming a first order reaction, as the activity of the catalyst would cease to control the reaction. The extent of dehydration would be limited by the equilibrium of the reaction, since dehydration is reversible.

Moisture would affect high-temperature dehydration in two ways. First it would lower the concentration of tar inside the wood particles by increasing the flow of volatiles out of the solid. Second a high concentration of water would shift the equilibrium of the dehydration reaction and limit the conversion of tar. Both of these mechanisms would increase the yield of tar from pyrolysis.

Reduction of Tar Concentration by Moisture Moisture in wood volatilizes along with reaction products during rapid pyrolysis, and increases outward volumetric flow of vapors taking place via the capillary system of the wood or via bubbles if the wood is molten. Thus the moisture would reduce the residence time of tars in the solid, which in turn would lower the mean concentration of tar in the vicinity of catalyst sites. At high temperature the rate of decomposition would be proportional to the tar concentration, hence moisture would increase the recovery of tar as a product. Moisture would reduce the residence time at lower reaction temperatures as well; but as the reaction is zero order under these conditions, no change in tar yield would result.

Effect of Moisture on Dehydration Equilibria The dehydration reaction can be represented in the following general form:



$$K = \text{equilibrium constant} = \frac{Y_{\text{product}} Y_{\text{H}_2\text{O}}}{Y_{\text{reactant}}}$$

All of the dehydration reactions that would occur during pyrolysis are endothermic with enthalpies of between 7 and 13 kcal./mol. and entropies of about 30 gibbs/mol. The equilibrium constants are greater than unity at pyrolysis temperatures so the addition of water would decrease the extent of tar decomposition at equilibrium. At low temperatures the reactions would be far from equilibrium, so that water could not influence yields in this way.

The overall effect of moisture on the recovery of tar was an increase of 4-6 yield % at 460 ° C. While we expect that water caused this change by both dilution and reaction equilibrium, we cannot determine the contribution of each mechanism to the yield of tar without a much more detailed knowledge of the pyrolysis reactions.

5.4.4 Pyrolysis in Carbon Dioxide Carbon dioxide would be similar to water in several ways. Like water it could be adsorbed on certain basic sites and diminish their catalytic activity. Such an effect was probably responsible for the similarity between the effects of carbon dioxide and water at 460 ° C. As shown in Table 5.11 both water and carbon dioxide enhanced tar production. Carbon dioxide would also inhibit decarboxylation reactions in much the same way that

water would inhibit dehydration. We were not able to determine if the yield of carbon dioxide from pyrolysis was affected by a decarboxylation equilibrium due to the presence of CO₂ as the fluidizing gas.

5.5 Summary

1. Addition of calcium to the wood by ion exchange increased the formation of aqueous product at the expense of tar product. The calcium was a basic catalyst and enhanced the formation of 1-hydroxy-2-propanone by as much as two orders of magnitude, and increased the formation of acetic acid and furfuraldehydes by factors of from 1.5 to 5. The basic catalyst gave the same products as have been observed with acidic catalysts such as ZnCl₂ but the product selectivity was opposite.
2. The ash constituents normally present in wood, including oxides of calcium, iron, magnesium, aluminium, sodium and potassium, exerted the same effect on yields of products as did the ion-exchanged calcium.
3. The yield of char was increased by about 5 yield % at and above 390 ° C from samples that were ash free and from samples that had the ash constituents intact. This result shows that char formation reactions are relatively unaffected by ash constituents in the temperature range of 330 to 460 ° C and suggests that ash constituents influence secondary reactions of tar species.
4. When moist Woodex, with its ash constituents intact, was pyrolyzed at temperatures between 320 and 460 ° C, the yield of tar exhibited a minimum at 390 ° C. Dry samples gave a monotonic increase in tar yield with temperature. Hence the minimum indicated the presence of at least two opposing mechanisms due to the simultaneous presence of moisture and ash.

5. Below 390 ° C the addition of moisture to Woodex containing ash increased the yield of tar. A mechanism for the hydration of catalyst sites gave qualitative predictions that agreed with the effects of temperature on the tar yield.
6. Above 390 ° C the addition of moisture to Woodex containing ash increased the tar, giving the opposite trend from samples that were ash free. This increase was consistent with the effect of added water on the transport of tar out of the solid and on the equilibrium of dehydration reactions.
7. Carbon dioxide and water had similar effects on pyrolysis. Both increased the recovery of tar, suggesting that each suppressed the catalysis of tar conversion reactions.

REFERENCES

- [1] Anderson, P. J., Horlock, R. F., and Oliver, J. F., *Trans. Faraday Soc.* **61** , 2754, 1965.
- [2] Benson, S. W., *Thermochemical Kinetics* , 2nd Ed., Wiley, New York, 1976.
- [3] Berkowitz-Mattuck, J. B. and Noguchi, T., *J. Appl. Polym. Sci.* **7** , 709, 1963.
- [4] Broido, A., *Pyrodynamics* **4** , 243-245, 1966.
- [5] Carey, F. A., and Sundberg, R. J., *Advanced Organic Chemistry, Part A: Structure and Mechanism* , Plenum, New York, 1977.
- [6] Dave, N. G., and Chopra, S. K., *Z. Physik. Chem.* **48(5-6)** , 257-66, 1966.
- [7] Feldmann, H. F. et al., in *Biomass as a Nonfossil Fuel Source* , ACS Symposium Series # , 1981.
- [8] Franklin, H. D., Peters, W. A., Cariello, F. and Howard, J. B., *Ind. Eng. Chem. Proc. Des. Dev.* **20(4)** , 670-674, 1981.
- [9] Gavalas, G. R., *Coal Pyrolysis* , Elsevier, Amsterdam, 1982.
- [10] Hocart, R., et al., *Compt. Rendus* **258(14)** , 3709-12, 1964.
- [11] Ito, T., Kanehori, K., and Tokuda, T., *Z. Phys. Chem., Neue Folge* **103** , 203-206, 1976.
- [12] Joly, J.-P., and Ollis, D., *J. Catal.* **60** , 216-227, 1979.
- [13] Jones, J. F., Schmid, M. R., and Eddinger, R. T., *Chem. Eng. Progr.* **60(6)** , 69-73, 1964.
- [14] Kirkpatrick, E. G., *Introductory Statistics and Probability for Engineering, Science and Technology* , Prentice-Hall, New Jersey, 1974.
- [15] Low, M. J. D., Takezawa, N., and Goodsel, A. J., *J. Colloid Interfac. Sci.* **37** ,

- 422, 1971.
- [16] Morozov, E. F., and Sobolev, V. I., *Obsch. Prikl. Khim.* **6**, 97-100, 1974.
- [17] Pines, H. and Stalick, W. M., *Base Catalyzed Reactions of Hydrocarbons and Related Compounds*, Academic Press, New York, 1977.
- [18] Schafer, H.N.S., *Fuel* **49**, 8-13, 1970.
- [19] Schafer, H. N. S., *Fuel* **51**, 4-9, 1972.
- [20] Shafizadeh, F., *Advances in Carbohydrate Chemistry* **23**, 419-465, 1968.
- [21] Shafizadeh, F., and Chin, P.P.S., in *Wood Technology: Chemical Aspects*, I.S. Goldstein ed., ACS Symp. Ser. No. 43, 57-81, 1976.
- [22] Shafizadeh, F., et al., *J. Appl. Polym. Sci.* **23**, 3525 - 3539, 1979.
- [23] Solnyshkin, V. I., *Kolloid. Zhur.* **19**, 736-40, 1957.
- [24] Tyler, R.J., and Schafer, H.N.S., *Fuel* **59**, 95-102, 1980.

Appendix - Regression Analysis of Tar Data

A multiple linear regression model was applied to the data on tar yield to test the statistical significance of moisture as an independent variable in the system. A quadratic regression line was fitted to the data for tar yield with temperature as the independent variable, as follows:

$$y = a_0 + a_1T + a_2T^2$$

y = tar yield, %

T = temperature, ° C

a_i = regression coefficient

A least squares fit to the data from Tables 5.3, 5.7, and 5.8 gave the following results:

Source	Degrees of Freedom	Sums of Squares	Mean Squares
Regression y T	2	139.5	69.75
Residual	11	86.7	7.88
Total	13	226.2	

The same data was fitted to a regression line with independent variables temperature and moisture (m), as follows:

$$y = a_0 + a_1T + a_2m + a_3T^2 + a_4m^2 + a_5mT$$

The corresponding sums of squares were as follows:

Source	Degrees of Freedom	Sums of Squares	Mean Squares
Regression y T m	5	197.5	39.5
Residual	8	28.66	3.58
Total	13	226.2	

The following equation tests the significance of the addition of moisture as an independent variable (Kirkpatrick, 1974):

$$\frac{\text{Sum of Squares due new variable}}{\text{Mean Squares of Residual}} > F_{0.05,1,8}$$

The 5% significance level was used, for an F-value of 5.32. From the results given earlier, we find:

$$\frac{197.5 - 139.5}{3.58} = 16.2 > F_{0.05,1,8} = 5.32$$

The addition of moisture as an independent variable was significant even with a 0.5% significance level ($F_{0.005,1,8} = 14.7$). Hence we conclude that moisture is statistically significant as an independent variable affecting the yield of tar, and that the variation between the curves in Figure 5-3 is more significant than the error level of the data points.

Table 5.1 Ash Content of Samples			
Sample	Acid-Washed	Ca-Exchanged	Untreated
Active Ash, m.eq./g.	0.0	0.62	1.30
wt. %	0.0	1.72	2.79
Total Ash, wt. %	3.03	4.63	7.83
Ash Components, wt. %			
SiO ₂	1.49	1.43	3.66
Al ₂ O ₃	1.35	1.31	2.47
Fe ₂ O ₃	0.18	0.16	0.74
CaO	0.01	1.72	0.75
MgO	-	-	0.15
Na ₂ O, K ₂ O	-	-	0.07

Table 5.2 Variation Between Replicate Samples (Temperature within 10 C°)				
Variable	Mean	Std. Deviation	Maximum	Number
	$\overline{ x_1 - x_2 }$	$\sigma_{\overline{ x_1 - x_2 }}$	Variation	of Pairs
Yield of Char, %	2.1	1.3	4.1	9
Yield of Tar, %	1.5	1.7	5.4	9
Yield of Gas, %	0.74	0.5	1.1	5
Yield of Aqueous, %	4.0	2.8	9.3	9

Table 5.3 Yield of Char from Woodex at Different Ash Levels			
Yields as % of Initial Weight (daf)			
Sample	Acid-Washed	Ca-Exchanged	Untreated
Active Ash, m.eq./g.	0.0	0.62	1.30
330 ° C	49.3	48.4	49.2
390 ° C	41.9	43.2	36.9
460 ° C	32.1	35.1	30.1

Table 5.4 Yields of Products from Woodex at Different Ash Levels			
Yields as % of Weight Loss			
Sample	Acid-Washed	Ca-Exchanged	Untreated
Active Ash, m.eq./g.	0.0	0.62	1.30
330 ° C			
Tar	46.5	41.0	26.4
Gas	5.3	5.3	7.2
Aqueous	41.0	46.5	54.5
390 ° C			
Tar	44.6	32.1	29.9
Gas	5.3	8.8	11.1
Aqueous	40.8	52.2	65.2
460 ° C			
Tar	52.1	30.7	27.2
Gas	8.0	11.3	11.9
Aqueous	40.9	53.8	61.5

Table 5.5 Yield of Liquid Products From Woodex at Different Ash Levels (Samples collected from water condenser)			
Pyrolysis at 330 ° C, % of Initial Weight			
Sample	Acid-Washed	Ca-Exchanged	Untreated
Active Ash, m.eq./g.	0.0	0.62	1.63
Methanol	0.04	0.08	0.06
2-oxopropanal	0.09	0.28	0.31
Acetic Acid	1.33	5.07	2.92
1-hydroxy-2-propanone	0.12	7.32	2.7
Furfuraldehydes	0.33	0.51	0.82
Guaiacols	1.38	1.61	1.73
Total	3.29	14.87	8.54
Pyrolysis at 460 ° C, % of Initial Weight			
Sample	Acid-Washed	Ca-Exchanged	Untreated
Active Ash, m.eq./g.	0.0	0.62	1.30
Methanol	0.07	0.50	0.24
2-oxopropanal	0.13	0.66	0.24
Acetic Acid	0.96	5.35	4.18
1-hydroxy-2-propanone	0.04	5.02	4.77
Furfuraldehydes	0.16	0.62	0.4
Guaiacols	0.74	3.99	1.37
Total	2.1	16.14	11.2

Table 5.6 Yields of Products from Untreated Dry Woodex					
Yields as % of Initial Weight					
Pyrolysis Temp. ° C	323	331	391	465	469
Char	53.5	49.6	39.9	33.1	33.8
Tar	12.9	12.6	13.2	17.2	19.0
Gas	2.9	4.0	4.9	8.4	7.3
Aqueous	25.5	27.2	39.2	40.9	31.6*
Total	94.8	93.3	97.2	99.5	91.7

Table 5.7 Product Yields from								
Untreated 16%-Moist Woodex								
Yields as % of Initial Dry Weight								
Temp. ° C	319	325	332	389	396	455	465	470
Char	50.0	48.3	49.1	44.6	42.9	39.6	35.5	37.9
Tar	16.3	16.2	16.9	13.2	11.9	23.1	23.2	17.8*
Gas	-	4.2	4.1	4.8	5.1	-	8.2	7.1
Aqueous	23.3*	28.7	27.3	32.2*	39.2	29.2	27.9	29.8
Total	-	97.5	97.4	94.8	99.1	-	94.7	91.9

* - Yield low by approximately 5 yield % due to systematic error.

Table 5.8 Yields of Products from Untreated 28%-Moist Woodex			
Yields as % of Initial Dry Weight			
Pyrolysis Temp. ° C	329	396	453
Char	50.3	43.8	40.1
Tar	16.1	15.3	24.2
Gas	4.3	5.7	8.3
Aqueous	30.5	35.3	23.7
Total	101.2	100.2	96.3

Table 5.9 Yield of Gaseous Compounds					
Untreated Dry Woodex, % of Initial Weight					
Temp., ° C	323	331	391	465	469
CO	1.44	1.52	1.94	3.93	3.08
CH ₄	0.0	0.0	0.08	0.23	0.20
CO ₂	1.47	2.48	2.91	4.25	3.97
Total	2.90	4.00	4.93	8.41	7.26

16%-Moist Woodex, % of Initial Dry Weight					
Temp., ° C	325	332	396	465	470
CO	1.67	1.64	2.29	3.67	3.33
CH ₄	0.0	0.0	0.08	0.23	0.19
CO ₂	2.58	2.50	2.78	4.26	3.53
Total	4.25	4.14	5.14	8.16	7.10

Table 5.10 Yield of Liquid Products from Untreated Woodex (Samples collected in liquid nitrogen trap)			
Compound	Pyrolysis at 330 ° C, % of Initial Dry Weight		
	Dry Woodex	16% Moisture	28% Moisture
Methanol	0.058	0.187	0.553
2-oxopropanal	0.312	0.390	1.078
Acetic Acid	2.916	5.778	3.093
1-hydroxy-2-propanone	2.700	6.094	3.315
Furfuraldehydes	0.814	1.077	0.6622
Guaiacols	1.73	2.74	0.186
Total	8.53	16.266	8.887
Compound	Pyrolysis at 460 ° C, % of Initial Dry Weight		
	Dry Woodex	16% Moisture	28% Moisture
Methanol	0.241	0.469	0.828
2-oxopropanal	0.241	0.868	1.892
Acetic Acid	4.181	4.290	4.031
1-hydroxy-2-propanone	4.771	4.689	4.660
Furfuraldehydes	0.403	0.636	0.734
Guaiacols	1.367	3.135	0.774
Total	11.204	13.087	12.919

Table 5.11 Effect of Fluidizing Gas on Pyrolysis of Woodex at 460 ° C				
	% of Initial Dry Weight			
Product	Helium	Carbon Dioxide		16%-Moist
		Test 1	Test 2	Woodex in He
Char	33.5	35.9	36.2	37.7
Aqueous	40.9	34.8	33.3	29.0
Tar	18.1	21.2	20.5	23.1

Table 5.12 Hydrate Behavior in Moist Wood		
	330 ° C	390 ° C
Fraction of Sites Hydrated at Equilibrium	0.2	0.07
Mean Hydrate Fraction during Pyrolysis	0.90	0.10
Pyrolysis Time, sec.	150	75

FIGURE 5-1
EFFECT OF TEMPERATURE ON PRODUCTS
OF PYROLYSIS OF UNTREATED WOODDEX

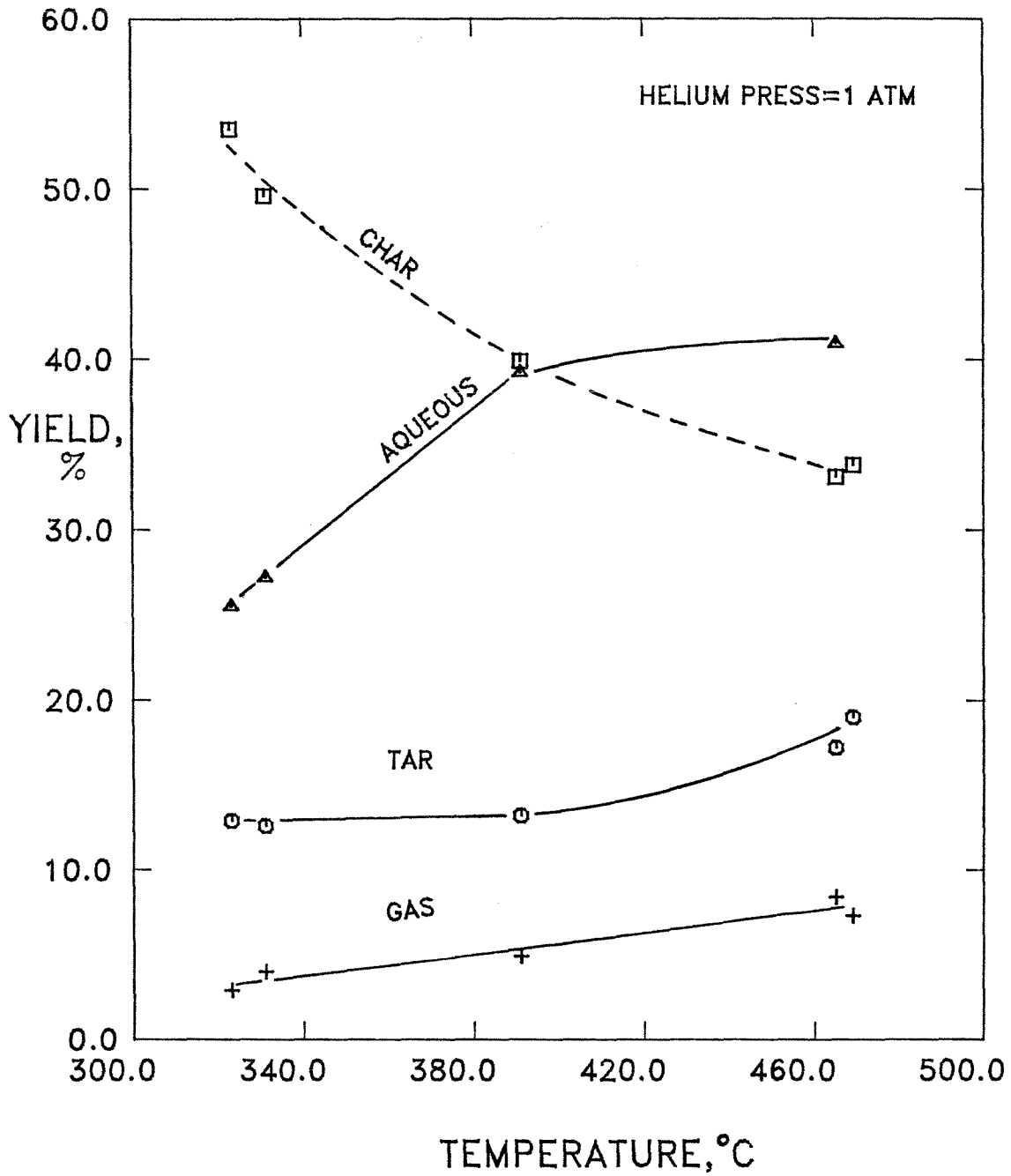


FIGURE 5-2
EFFECT OF MOISTURE ON YIELD
OF CHAR FROM UNTREATED WOODDEX

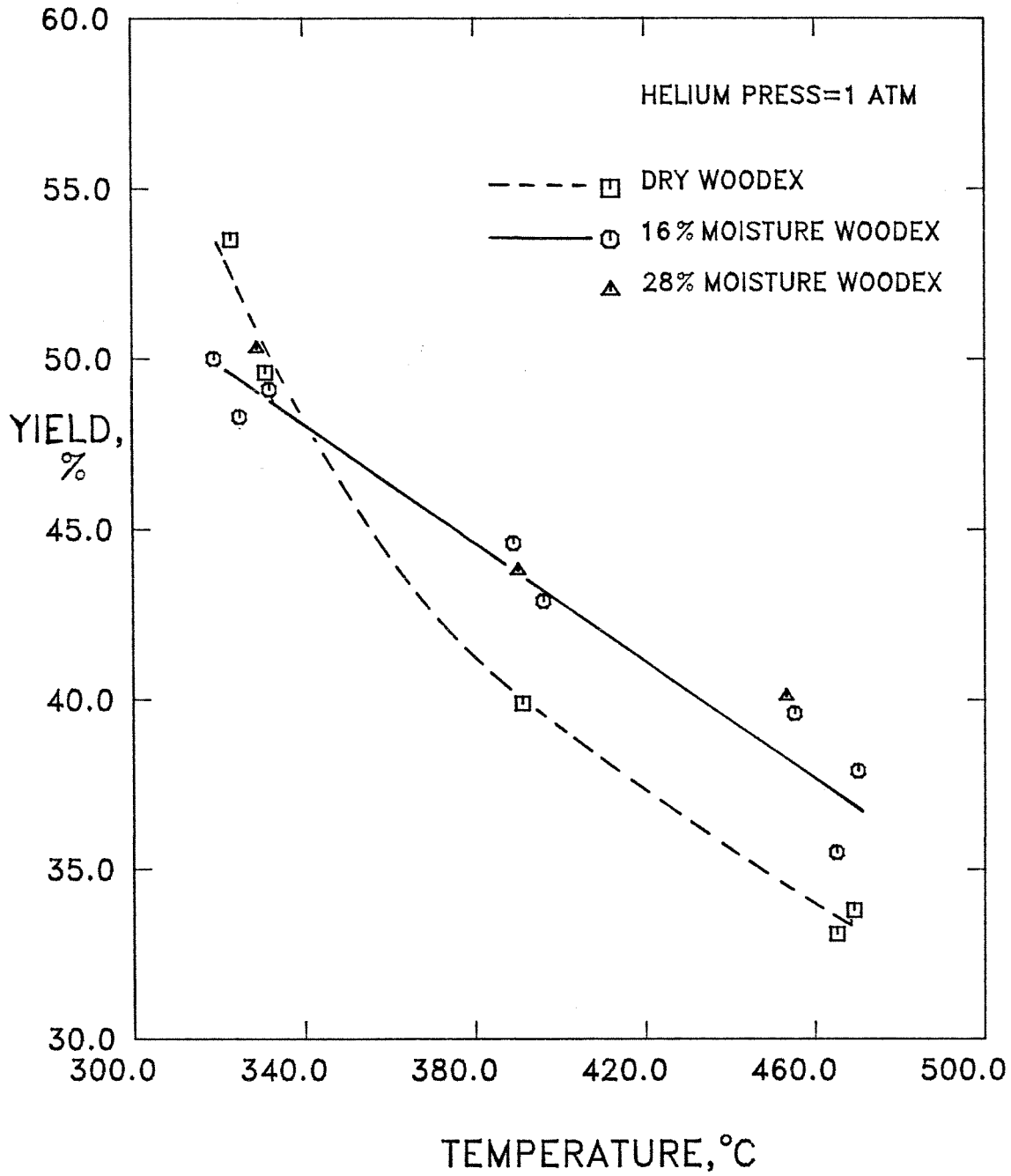


FIGURE 5-3
EFFECT OF MOISTURE ON YIELD
OF TAR FROM UNTREATED WOODDEX

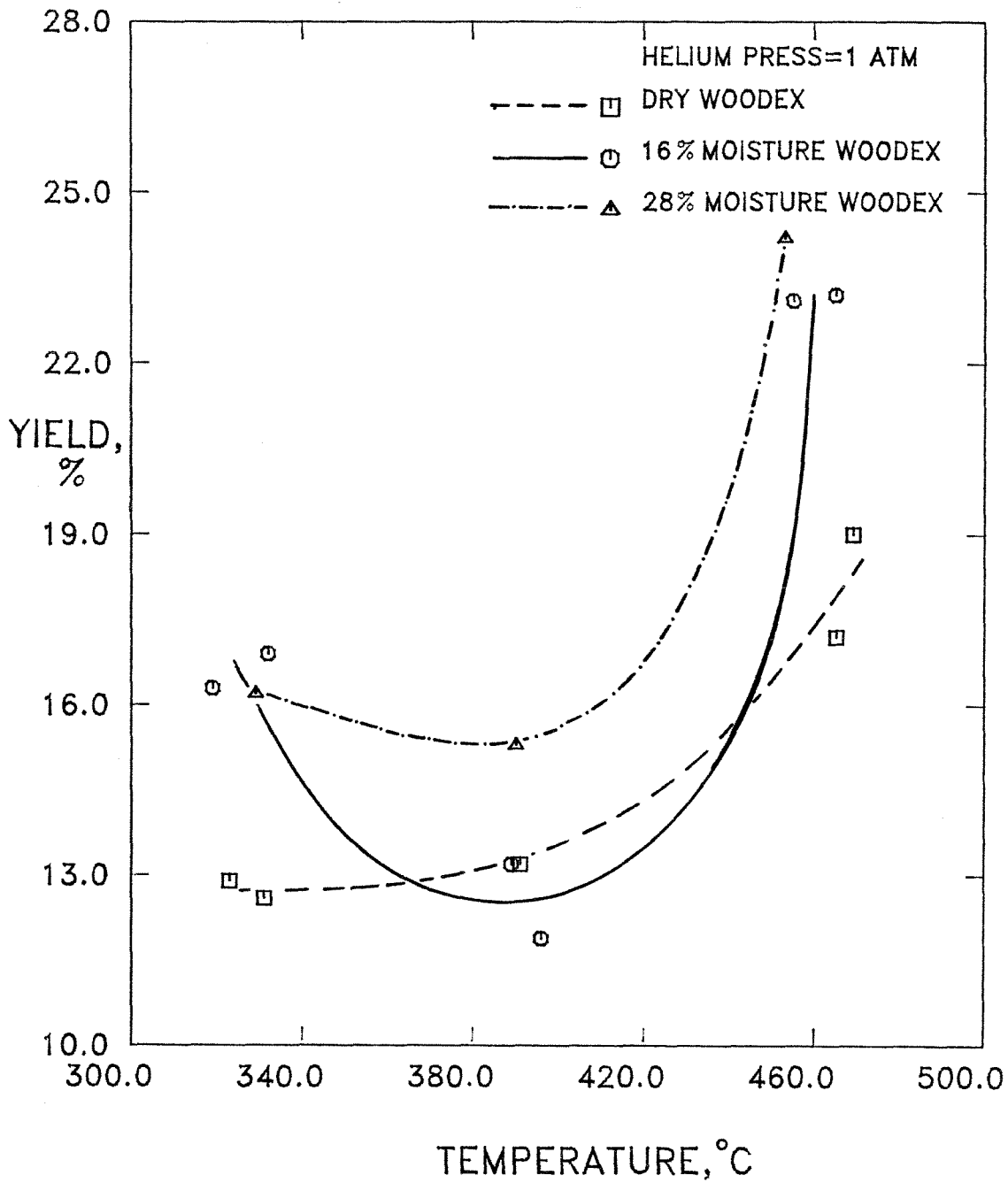
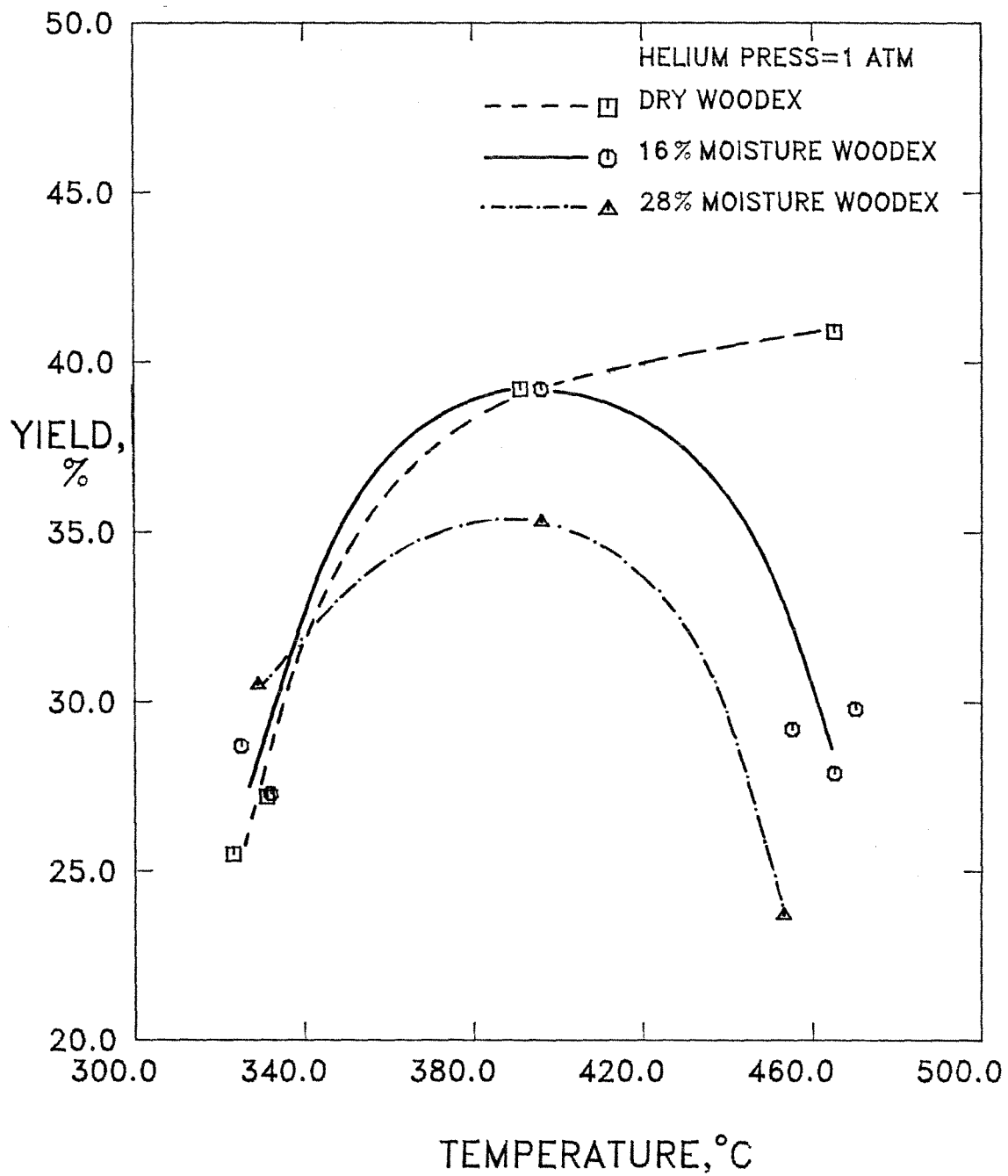


FIGURE 5-4
YIELD OF AQUEOUS PRODUCT
FROM UNTREATED MOIST WOODOX



6. CONCLUSIONS AND RECOMMENDATIONS

6.1 Conclusions

1. Moisture increased the yield of char from the pyrolysis of Woodex by 5 yield % at 390 and 460° C. The presence of moisture reduced the yield of tar from pyrolysis above 400 ° C. Physical effects such as swelling by moisture, melting, and enhanced intraparticle transport cannot account for these results.
2. A mechanism for the interaction between free radicals and water during pyrolysis gave qualitative predictions that agreed with the observed effects of temperature on the yield of products from moist and dry Woodex.
3. The surface area of char from moist Woodex at 460° C was less than half the area from a dry sample. This reduction in the surface could be due to trapping of tar within the solid, or to the effect of water on the viscosity of molten Woodex.
4. Comparison of the rate of production of gas and aqueous condensate with time, from moist and dry samples, showed that moisture was present in the wood throughout the course of the pyrolysis reactions. Analysis of temperature-time curves from a thermocouple inserted into the reactor confirmed that drying of the moist samples continued even when the thermocouple reading was close to the final reaction temperature.
5. Wood possesses significant ion-exchange capacity which can be used to introduce selected metal ions into the polymer matrix in a random distribution. The ion-exchange capability is due to the presence of carboxylate groups in the wood. The concentration of available carboxylate groups was increased by oxidation in air at 195 ° C.

6. Addition of calcium to the wood by ion exchange increased the formation of aqueous product at the expense of tar product. The calcium salts catalyze secondary reactions of tar as it is evolved, and behave as basic catalysts. The calcium enhanced the formation of 1-hydroxy-2-propanone by as much as two orders of magnitude, and increased the formation of acetic acid and furfuraldehydes by factors of from 1.5 to 5. The basic catalyst gave the same products as have been observed with acidic catalysts such as $ZnCl_2$ but the product selectivity was opposite.
7. The ash constituents normally present in wood, including oxides of calcium, iron, magnesium, aluminium, sodium and potassium, exerted the same effect on yields of products as did the ion-exchanged calcium.
8. The yield of char was increased by about 5 yield % at and above $390^\circ C$ from samples that were ash free and from samples that had the ash constituents intact. This result shows that char formation reactions are relatively unaffected by ash constituents in the temperature range of 330 to $460^\circ C$ and suggests that ash constituents influence only secondary reactions of tar species.
9. When moist Woodex, with its ash constituents intact, was pyrolyzed at temperatures between 320 and $460^\circ C$, the yield of tar exhibited a minimum at $390^\circ C$. Dry samples gave a monotonic increase in tar yield with temperature. Hence the minimum indicated the presence of at least two opposing mechanisms due to the simultaneous presence of moisture and ash.
10. Below $390^\circ C$ the addition of moisture to Woodex containing ash increased the yield of tar. This result indicated deactivation of the catalyst sites in the presence of moisture. A kinetic model for the hydration of catalyst, based on

hydration of calcium oxalate and CaO and MgO surfaces, gave predictions of hydrate occupancy of sites with time and temperature. The model was in qualitative agreement with the observed trend of the yield of tar with temperature.

11. Above 390 ° C the addition of moisture to Woodex containing ash increased the tar, giving the opposite trend from samples that were ash free. This increase was consistent with the effect of added water on the transport of tar out of the solid and on the equilibrium of dehydration reactions, which were catalyzed by the ash constituents and were significant in the formation of aqueous product from tar. Equilibrium effects would only be significant at temperatures high enough that the availability of catalyst sites did not control the extent of reaction.
12. The surface areas of Woodex chars were less than 5 m²/g. at 330 and 390 ° C, due to melting. At 460 ° C the char area increased to as much as 56 m²/g., possibly due to more rapid crosslinking reactions which would increase the viscosity of the melt and lead to more internal surface from bubble formation and evolution. Moist samples gave a char of lower surface area, which was consistent with trapping of the tar in the solid due to the presence of water.

From the Appendices:

1. When simple kinetic models were applied to yields of products from the pyrolysis of lignin, published reaction networks were found to be inadequate for correlating the data for solid residue, tar and gas. The data could be fitted to more complex 3-reaction models, but the rate constants did not fit a simple Arrhenius expression due to the effect of temperature on mass transfer processes within the solid. The data for solid residue could be fitted

with almost any two-parameter model, so that claims in the literature concerning such models should be used with caution.

2. In early experiments Woodex was heated slowly from room temperature inside the reactor to a target temperature of 330 ° C. The final technique, used in the experiments in the main portion of this report, was to inject the powdered sample into the hot, empty reactor. Despite the difference in heating rates between the two methods, the yields of products were within several yield %. This similarity shows that within the range of heating rate from about 30 ° C/min. to 300 ° C the final temperature was the most important factor in determining the distribution of products.

6.2 Recommendations

1. Any investigation of pyrolysis should be preceded by thorough chemical and physical analysis of the sample material, to aid in interpreting the experimental results.
2. The influence of moisture and ash content on the pyrolysis of wood should not be overlooked. The presence of both materials has been largely ignored in past investigations, yet both ash and moisture are ubiquitous in wood and wood wastes.
3. Lumped kinetic models should only be applied to pyrolysis within the limited contexts of fitting experimental data to a useful form or for obtaining an initial estimate of kinetic parameters. The use of such models in predicting the evolution of volatile products, based on thermogravimetric data, should be avoided. The rates of evolution of volatile materials are affected by heat and mass transfer as well as kinetic effects, and do not necessarily follow an Arrhenius expression that relates to the underlying mechanism.

6.3 Suggestions for Further Research

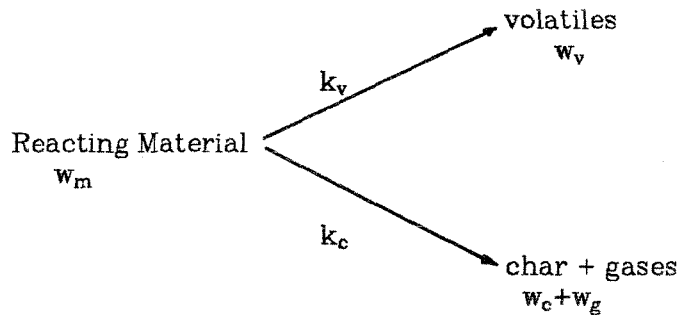
1. The present study did not analyze the tars from pyrolysis due to the difficulty in separating and identifying polyphenolic compounds. A fast method for characterizing the chemical nature of these products, based on functional groups, would be useful.
2. The concept of free-radicals "hopping" from point to point within a solid matrix due to the action of a free-radical carrier may be of general interest for pyrolysis systems. Experiments should be designed to measure and explore this suggested mechanism.
3. While the activity of ash components for dehydration and other base catalyzed reactions is well known, the behavior of such catalysts with temperature and water vapor pressure should be determined.
4. Although the kinetic modelling presented in Appendix A did not provide mechanistic insight into the pyrolysis reactions, such an approach could be more fruitful when applied to individual compounds or related groups of compounds. By appropriate choices of lumped compounds a simple model could be sufficient. In the gas phase CO, CO₂, and hydrocarbons could be considered in a model. Chemically related compounds such as aldehydes and ketones could be considered as a group.

APPENDIX A: KINETIC MODELS OF PYROLYSIS REACTIONS

The pyrolysis of Woodex gives such a large number of products, particularly in the tar, that a lumped kinetic approach is the most appropriate for empirical fitting of data. Lumped models for wood components were discussed in Section [3], and in this appendix we present the application of these models to data from the pyrolysis of lignin.

A.1 Two-Reaction Model

A simple two-reaction model of the type used by Bradbury et al.(1979) to fit cellulose pyrolysis data was selected as an initial framework in which to consider the pyrolysis reactions of Woodex. A schematic view of the model follows.



w_m = weight fraction of reacting material

w_v = weight fraction of volatiles

w_c = weight fraction of char

w_g = weight fraction of gas

k_v = rate constant for reactions giving volatiles

k_c = rate constant for reactions giving char and gas

First-order kinetics were assumed to apply so the following equations described the system variables:

$$-\frac{dw_m}{dt} = (k_v + k_c) w_m \quad (\text{A.1})$$

$$\frac{dw_v}{dt} = k_v w_m \quad (\text{A.2})$$

$$\frac{dw_g}{dt} = f_g k_c w_m \quad (\text{A.3})$$

$$\frac{dw_c}{dt} = (1 - f_g) k_c w_m \quad (\text{A.4})$$

$$f_g = \frac{w_g}{w_g + w_c} \quad \text{at } t = \infty \quad (\text{A.5})$$

$$w_m + w_v + w_g + w_c = 1 \quad (\text{A.6})$$

f_g = fraction of gas relative to char at time $t = \infty$

Thermogravimetric analysis measures a combination of w_m and w_c at any given time.

A.1.1 Isothermal Reaction Conditions When the reaction temperature is essentially constant then the differential equations which make up the model are integrated analytically to give:

$$w_g = \frac{f_g k_c}{k_v + k_c} \left[1 - e^{-(k_v + k_c) t} \right] \quad (\text{A.7})$$

$$w_v = \frac{k_v}{k_v + k_c} \left[1 - e^{-(k_v + k_c) t} \right] \quad (\text{A.8})$$

$$w_s = \frac{(1 - f_g) k_c}{k_v + k_c} \left[1 - e^{-(k_v + k_c) t} \right] + e^{-(k_v + k_c) t} \quad (\text{A.9})$$

The variable w_s is the weight of sample observed with time in thermogravimetric measurements. Equations (A.7) through (A.9) mimic the qualitative results which a variety of investigators have observed in that the final yields of gas and volatiles are a function of the reaction temperature .

A.1.2 Application of Model to the Data of Iatridis and Gavalas (1979) The data of Iatridis and Gavalas (1979) for the pyrolysis of a precipitated-Kraft lignin were used to test the Two-Reaction Model. The experiments were carried out essentially isothermally so equations (A.7) and (A.8) were appropriate. The experimental results were given as yields of individual components. For the purposes of the kinetic model the fixed gases and light hydrocarbons were lumped as gas. The remaining volatile compounds and tar were lumped as volatiles. Solid residue was classed as char. Table A.1 presents the lumped data.

The VARPRO routine (see Appendix B) was used to fit the model to the data with the minimum error by an appropriate choice of the free parameters k_c and k_v . The system of non-linear equations in matrix form is as follows:

$$\begin{bmatrix} w_g(t_1) \\ \vdots \\ w_g(t_n) \\ w_v(t_1) \\ \vdots \\ w_v(t_n) \end{bmatrix} = \begin{bmatrix} \varphi_1(t_1) & 0 \\ \vdots & \vdots \\ \varphi_1(t_n) & 0 \\ 0 & \varphi_2(t_1) \\ \vdots & \vdots \\ 0 & \varphi_2(t_n) \end{bmatrix} \cdot \begin{bmatrix} f_g \\ 1 \end{bmatrix} \quad (\text{A.10})$$

$$\varphi_1(t) = \frac{k_c}{k_c + k_v} \left(1 - e^{-(k_c + k_v)t} \right) \quad (\text{A.11})$$

$$\varphi_2(t) = \frac{k_v}{k_c} \varphi_1(t) \quad (\text{A.12})$$

The elements of the Jacobian of the above matrix were calculated with expressions derived from equations (A.11) and (A.12). The Jacobian gave the rate of change in w_g and w_v , the measured parameters, with the free parameters k_c and k_v .

The results of the least-squares fit of the system of equations (A.10) to the data are given in Table A.2. As illustrated by Figure A-1 the agreement between

the model and the data for the evolution of gas from the pyrolysis of lignin was poor. Figure A-2 depicts the curves from the model when only the data for gas were used to estimate the parameters. Clearly the Two-Reaction model was inadequate to describe the pyrolysis reactions of lignin.

Close observation of Figures A-1 and A-2 showed that the gas evolution at 600 ° C as predicted by the model was physically incorrect. Experiments have shown that $w_{g(t \rightarrow \infty)}$ increases as the temperature is raised when any carbonaceous material is pyrolyzed. The curve at 600 ° C was not bounded by the curves at 550 ° C and 650 ° C. Such behavior derived from the lack of data points at 600 ° C. Consequently the data for pyrolysis at 600 ° C were not used in further work.

One cause for disagreement between the model and the data in Figure A-1 was the lack of closure in the material balances. As indicated in Table A.1 the error in the material balance ranged from 5% to 20%. Closure of the material balance in each experiment was not achieved due to errors in measurement and the exclusion of unidentified compounds and water from the list of products. Nevertheless the reaction-model equations automatically achieved a material balance due to their formulation. In order to obtain a reasonable result from a model, some judgement on the accuracy of the data was required. Since the largest errors in the data of Iatridis and Gavalas were the exclusion of water and unidentified compounds (all of which were volatile materials) from the list of products, the data for the yield of volatiles were the most unreliable. Only the data for the yields of char and gas were used in further evaluation of kinetic models.

The data for the yields of gas were fitted to a simpler equation (A.13) to check the sensitivity of the exponential parameters to the exact form of the

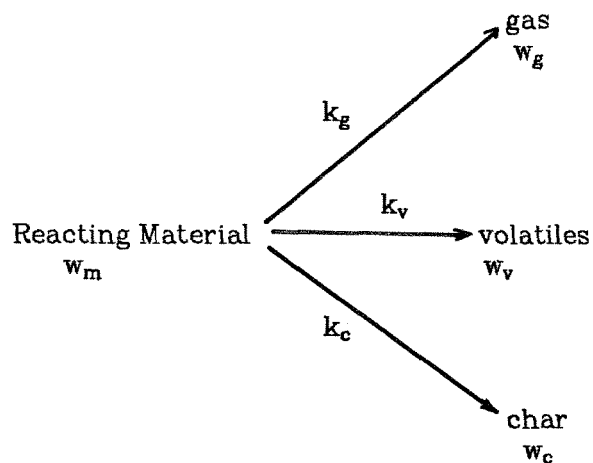
model expression.

$$w_g(t) = \beta \left[1 - e^{-\alpha t} \right] \quad (\text{A.13})$$

At all temperatures the calculated value of the exponential parameter α was very close to the corresponding value of $(k_c + k_v)$ derived from Table A.2. Thus the parameters calculated from the pyrolysis data with the VARPRO routine were dependent on the form of the exponential expression rather than the linear term β .

A.2 Three-Reaction Model

The Two-Reaction model linked gas and char formation in a single reaction step. Klein and Virk (1981) investigated the pyrolysis of compounds which were analogous to lignin and found that gas molecules were formed mainly by scission of side groups which were bound to the polyphenol nuclei. Reactions for the formation of char (condensation or polymerization) were independent of the reactions which formed gases. Consequently a model which seeks to portray the pyrolysis reactions of lignin must allow independent reactions for the formation of char and gas. The simplest model which achieves this involves three reactions as shown below:



w_m = weight fraction of reacting material

w_v = weight fraction of volatiles

w_c = weight fraction of char

w_g = weight fraction of gas

k_v = rate constant for reactions giving volatiles

k_c = rate constant for reactions giving char

k_g = rate constant for reactions giving gas

The appropriate equations for the model were similar to equations (A.1) to (A.4) and were easily integrated for isothermal conditions:

$$w_g = \frac{k_c}{k_v + k_c + k_g} \left[1 - e^{-(k_v + k_c + k_g)t} \right] \quad (\text{A.14})$$

$$w_v = \frac{k_v}{k_v + k_c + k_g} \left[1 - e^{-(k_v + k_c + k_g)t} \right] \quad (\text{A.15})$$

$$w_g = \frac{k_g}{k_v + k_c + k_g} \left[1 - e^{-(k_v + k_c + k_g)t} \right] \quad (\text{A.16})$$

$$w_s = \frac{k_c}{k_v + k_c + k_g} \left[1 - e^{-(k_v + k_c + k_g)t} \right] + e^{-(k_v + k_c + k_g)t} \quad (\text{A.17})$$

When the Three-Reaction Model was fitted only to the gas data, good agreement was achieved as depicted in Figure A-3. Figure A-4 shows the model predictions for char (based on Figure A-3) and the data points for char. Agreement was fair at long reaction times but poor when $t < 50$ sec. Rapid weight loss occurred in the early time period which was not reflected in the gas data.

Figures A-5, A-6, and A-7 depict the curves which resulted when the Three-Reaction Model was fitted to the yields of gas and char. The weight of residue at a given time was reproduced very well by the model curves. The yields of gas were not predicted well by the model at short reaction times, which was the

converse of Figure A-4 where gas data could not be used to predict the yields of char. The yields of volatiles as predicted by the model were much higher than the experimental points because the error in the material balance was lumped into the yield of volatiles.

The observation that the weight of char was predicted by a simple kinetic model was in agreement with the work of Bradbury et al. (1979) and Broido (1976). The lack of agreement between the model and the yield of gas and volatile products showed that such a simple model could not correlate all of the products of pyrolysis. This result calls into question the claims of Bradbury et al. and Broido that their models have a mechanistic significance. Neither model was checked against the data for the yields of gas or volatiles. Clearly their models are inadequate for predicting the formation of gas or volatiles from lignin.

Iatridis and Gavalas (1979) reported more data points for the yield of char than of gas. Because the model was fitted by minimizing the error between the data points and the model, it was possible that the number of data points of each type might have influenced the result. The effect of the number of data points was tested by weighting the gas data more heavily than the char data, effectively increasing the importance of the gas. The effect was negligible, which indicated that the model was the cause of the disagreement between the model curves and the experimental measurements.

Figure A-8 is an Arrhenius plot of the rate constants predicted by the Three-Reaction Model on the basis of gas data. The linear behavior of $\ln k_g$ when plotted versus $1/T$ was significant. With such a simple relationship the rate of formation of gas at different temperatures could be easily calculated. The apparent activation energy (from the slope of the curve) was much less than

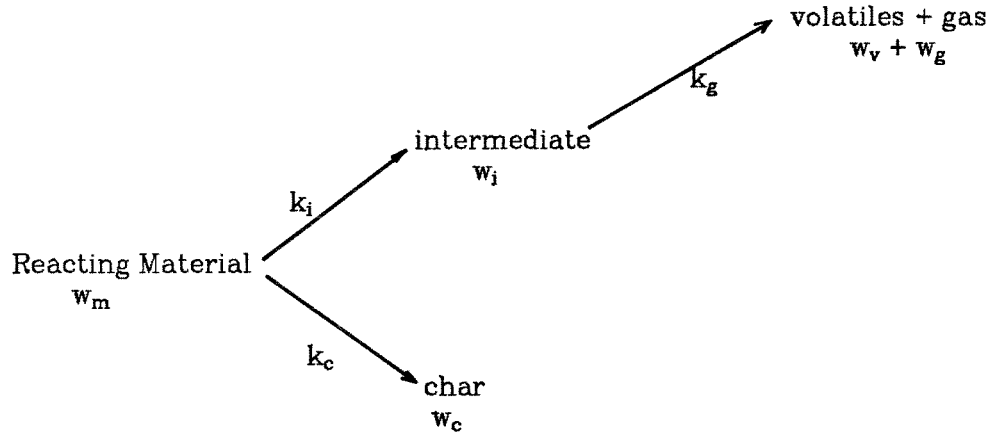
the results reported by Klein and Virk (1981) for any of their studies. Consequently while the linear behavior of $\ln k_g$ with $1/T$ is of practical utility in predicting the evolution of gas at different temperatures, the result is of limited use in exploring the mechanism of lignin pyrolysis. Figure A-9 illustrates that the rate constants derived from char and gas data using the Three-Reaction Model exhibited more random trends.

A.3 Modified-Three-Reaction Model

The low rate of formation of gas as compared to the rate of loss in weight of the solid material implied that volatiles were formed very rapidly at short reaction times and that some intermediate reaction preceded the formation of gases.

Iatridis and Gavalas (1979) determined the weight of char by weighing the solid residue of pyrolysis after the solid had been dried at 300 ° C to drive off the adsorbed volatile material. The presence of adsorbed and absorbed volatiles on the solid surface suggested that a sequence of reactions occurred whereby the lignin depolymerized to yield low molecular weight volatiles in the solid phase. The volatiles would then decompose to yield gases or desorb into the gas phase. Such a view undoubtedly represents a simplification of the actual events since gas would be produced from both unreacted material and adsorbed volatiles by scission of side chains.

The simplest way of expressing the above sequence of reactions was to use three reactions, two of which were in sequence.



w_m = weight fraction of reacting material

w_c = weight fraction of char

w_i = weight fraction of reactive intermediate

w_v = weight fraction of volatiles

w_g = weight fraction of gas

k_i = rate constant for reactions giving intermediates

k_v = rate constant for reactions giving volatiles and gas

k_c = rate constant for reactions giving char

The appropriate system of equations is given as follows:

$$-\frac{dw_m}{dt} = (k_i + k_c) w_m \quad (\text{A.18})$$

$$\frac{dw_i}{dt} = k_i w_m - k_g w_i \quad (\text{A.19})$$

$$\frac{dw_g}{dt} = f_g k_g w_i \quad (\text{A.20})$$

$$\frac{dw_c}{dt} = k_c w_m \quad (\text{A.21})$$

$$f_g = \frac{w_g}{w_g + w_v} \text{ at } t = \infty \quad (\text{A.22})$$

The equations above may be integrated for isothermal conditions to give:

$$w_g = \frac{k_i f_g}{k_g - k_c - k_i} \left[k_g - k_c - k_i + (k_c + k_i) e^{-k_g t} - k_g e^{-(k_c + k_i)t} \right] \quad (\text{A.23})$$

$$w_c = \frac{k_c}{k_i + k_c} \left[1 - e^{-(k_v + k_c)t} \right] \quad (\text{A.24})$$

The data for gas and char from Table (A.1) were fitted to equations (A.23) and (A.24) by means of the VARPRO subroutine. The results are listed in Table (A.3). Figure A-10 depicts the curves for the yield of char from equation (A.24) and the experimental points of Iatridis and Gavalas (1979). The agreement between the model and the data points was accurate to within experimental error. Figure A-11 shows the corresponding curves and data points for the yield of gas from the pyrolysis of lignin. The agreement between the model and the data points in Figure A-11 was good at 400 ° C and 650 ° C and poorer at the intermediate temperatures. The model failed to reproduce the rapid rise in the yield of gas in short times at 550 ° C and the final yield of gas at 500 ° C and 550 ° C.

Figure A-12 depicts the rate constants derived from the data with the Modified-Three-Reaction Model in an Arrhenius plot. Given the disagreement between the model and the experimental measurements of the yield of gas, the Arrhenius plot should not be given too much weight. Nevertheless the shifts in the rate constants with temperature are extremely thought-provoking and may indicate shifts in reaction mechanism. Given the observation that volatiles are trapped by the solid material during pyrolysis, mass transfer processes may contribute to the change in the rate constants with temperature. The rate constants from a global kinetic model represent the sum of the rates for the individual components in each lumped product, and in turn the rate for each component is the net rate of formation from competing and sequential reactions and mass transfer. Hence the constants indicate the net rate of

formation of a lumped product, as opposed to the rate of the underlying chemical reactions.

REFERENCES

- [1] Bradbury, A.W.G., Sakai, Y., Shafizadeh, F., *J. Appl. Polym. Sci.* **23** , 3271-3280, 1979.
- [2] Broido, A., in *Thermal Uses and Properties of Carbohydrates, Lignins* , ed. F. Shafizadeh, ACS, 19-36, 1976.
- [3] Iatridis, B.A. and Gavalas, G.R., *Ind. Eng. Chem. Proc. Des. Dev.* **18(2)** , 127-130, 1979.

Table A.1. Fractional Yields from the Pyrolysis of Lignin (From the data of Iatridis and Gavalas, 1979)					
Temp. ° C	Time, sec.	Gas	Volatiles	Char	Total
400	10	-	-	0.867	-
	20	0.0325	0.0885	0.776	0.897
	60	0.0745	0.1458	0.787	1.007
	120	0.0778	0.1528	0.718	0.9486
500	10	0.0262	0.1048	0.689	0.82
	30	0.0798	0.1512	0.542	0.773
	60	0.1026	0.1732	0.538	0.8138
550	5	-	-	0.816	-
	10	0.0486	0.1305	0.648	0.8271
	30	0.1031	0.1769	0.475	0.755
	50	0.1278	0.2039	0.475	0.8062
	120	0.1371	0.2118	0.475	0.8239
600	5	-	-	0.522	-
	10	0.0854	-	0.457	-
	30	0.1362	-	0.415	-
	40	-	-	0.412	-
650	10	0.1245	0.1801	0.440	0.7446
	30	0.1500	0.2067	0.402	0.7587
	40	-	-	0.388	-
	60	0.2151	0.2233	0.391	0.8294
	120	0.2351	0.2298	0.379	0.8439

Table A.2. Kinetic Parameters for Pyrolysis of Lignin (from Two-Reaction Model, data of Iatridis and Gavalas (1979))				
Temp. ° C	Fit to All Data		Fit to Gas Only	
	k_c	k_v	k_c	k_v
400	0.00239	0.00389	0.00274	0.00276
500	0.01415	0.03522	0.01161	0.00876
550	0.02104	0.05336	0.02026	0.01441
600	0.09207	0.12420	0.06357	0.03719
650	0.05233	0.12620	0.02366	0.03294

Table A.3 Kinetic Parameters for Pyrolysis of Lignin (from Modified-3-Reaction Model, data of Iatridis and Gavalas (1979))			
Temp. ° C	k_i	k_c	k_g
400	0.02156	0.063837	0.019238
500	0.05567	0.06131	0.02668
550	0.05742	0.04910	0.13147
650	0.15883	0.10189	0.03790

FIGURE A-1
GAS FROM PYROLYSIS OF LIGNIN
(DATA OF IATRIDIS AND GAVALAS)
CURVES FROM 2-RXN MODEL, EQUAL WTS.

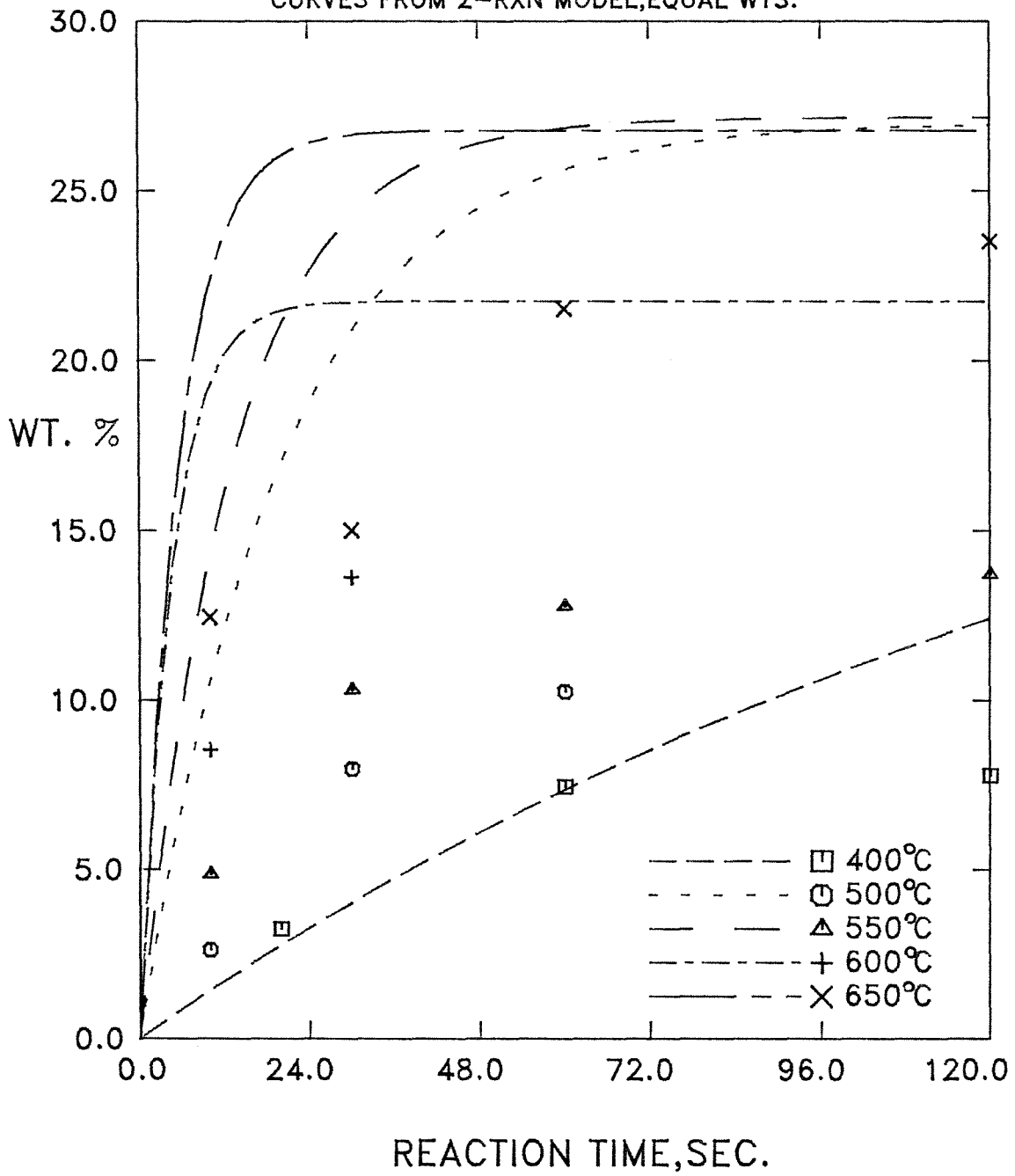


FIGURE A-2
GAS FROM PYROLYSIS OF LIGNIN
(DATA OF IATRIDIS AND GAVALAS)

CURVES FROM 2-RXN MODEL, GAS ONLY

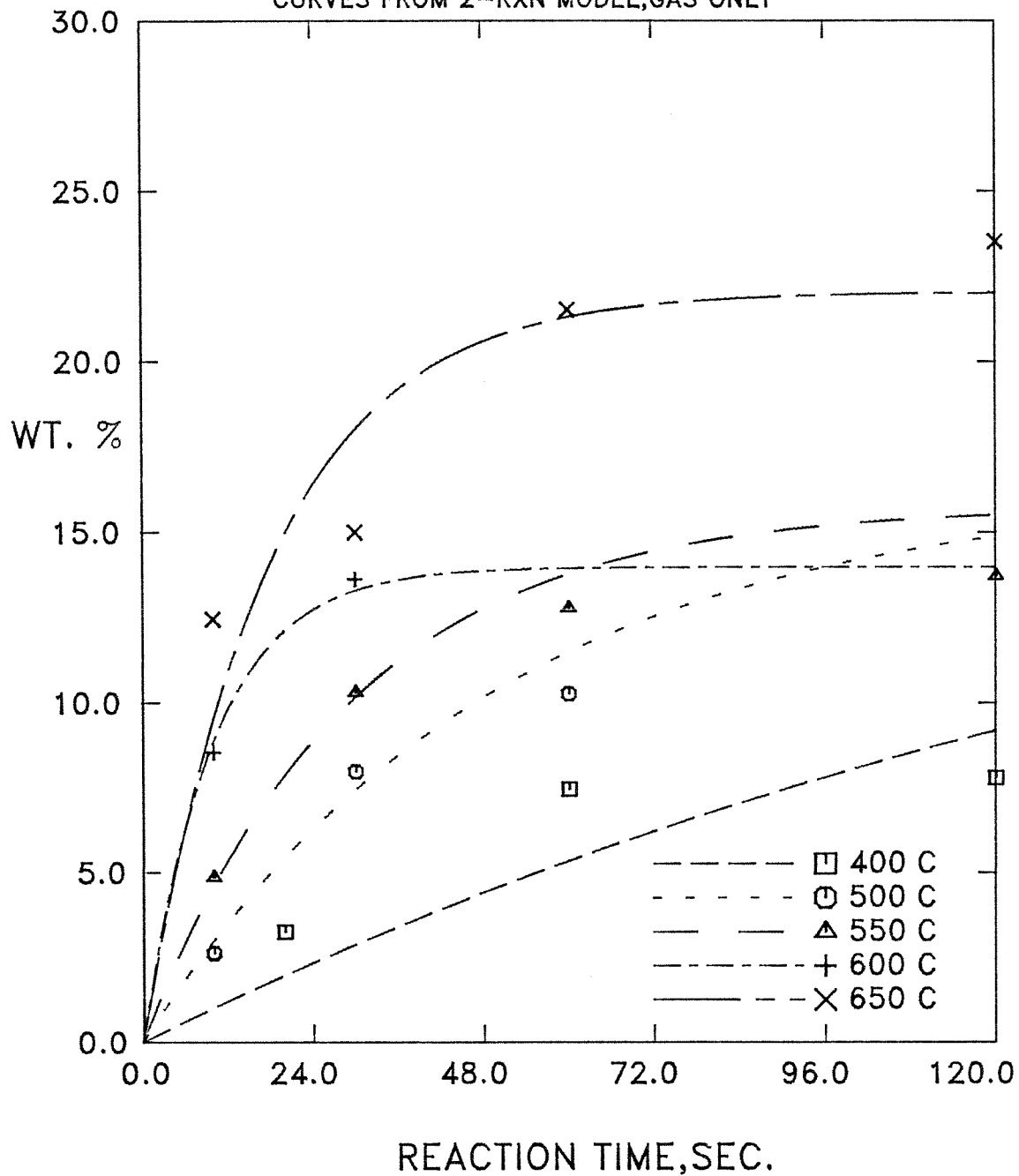


FIGURE A-3
GAS FROM PYROLYSIS OF LIGNIN
(DATA OF IATRIDIS AND GAVALAS)

CURVES FROM 3-RXN MODEL, GAS ONLY

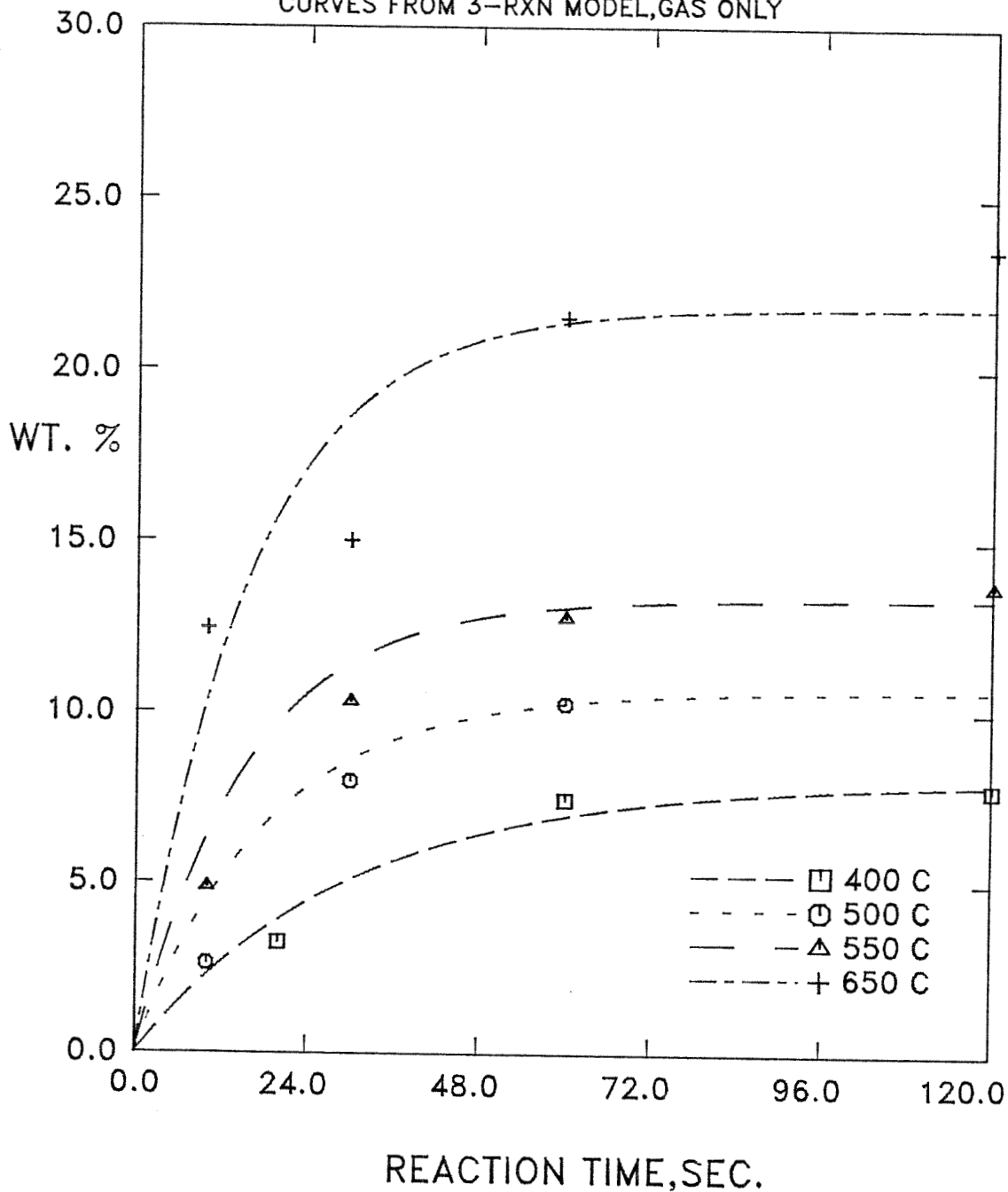


FIGURE A-4
CHAR FROM PYROLYSIS OF LIGNIN
(DATA OF IATRIDIS AND GAVALAS)
CURVES FROM 3-RXN MODEL, GAS ONLY

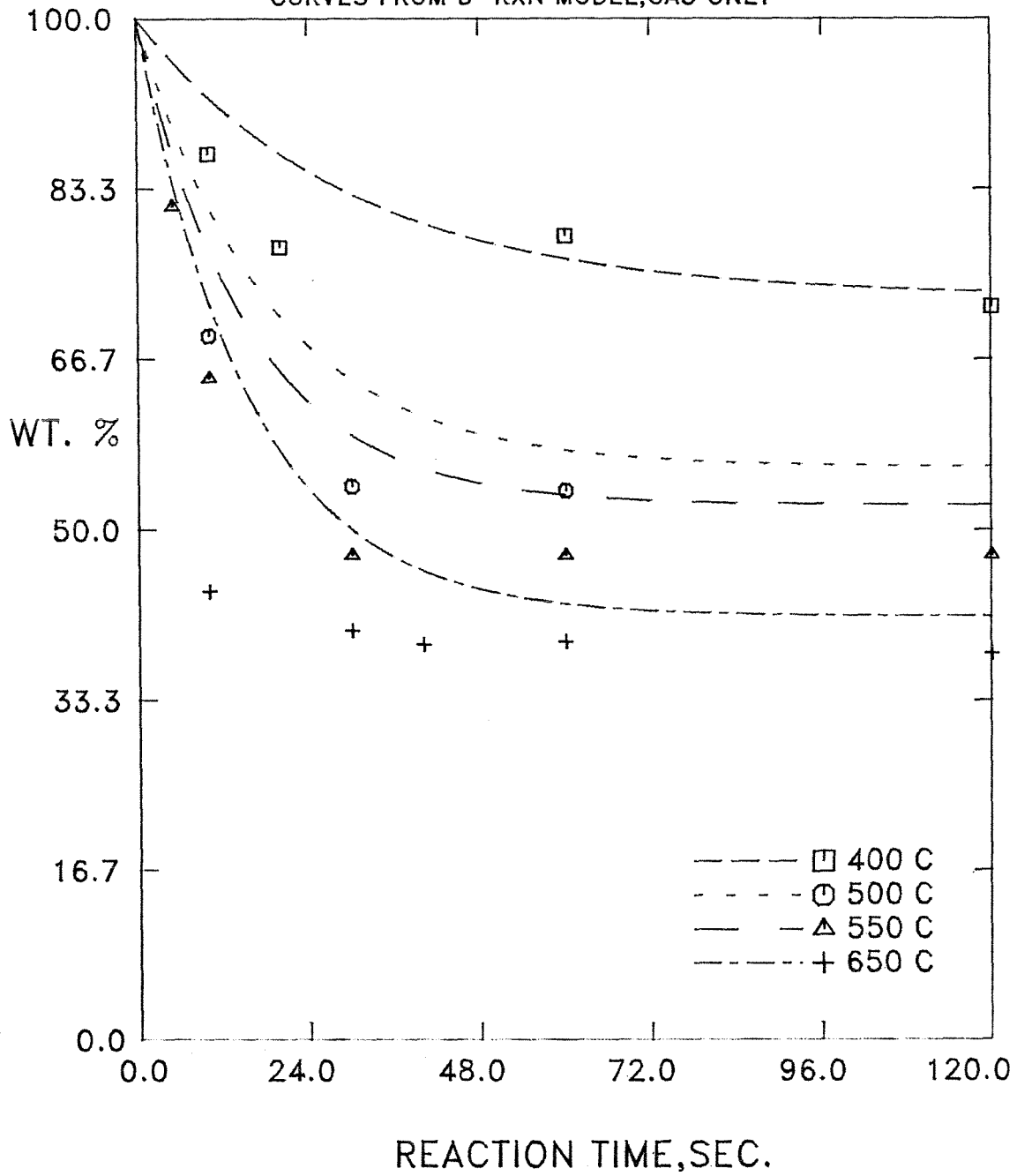


FIGURE A-5
GAS FROM PYROLYSIS OF LIGNIN
(DATA OF IATRIDIS AND GAVALAS)

CURVES FROM 3-RXN MODEL, GAS AND CHAR

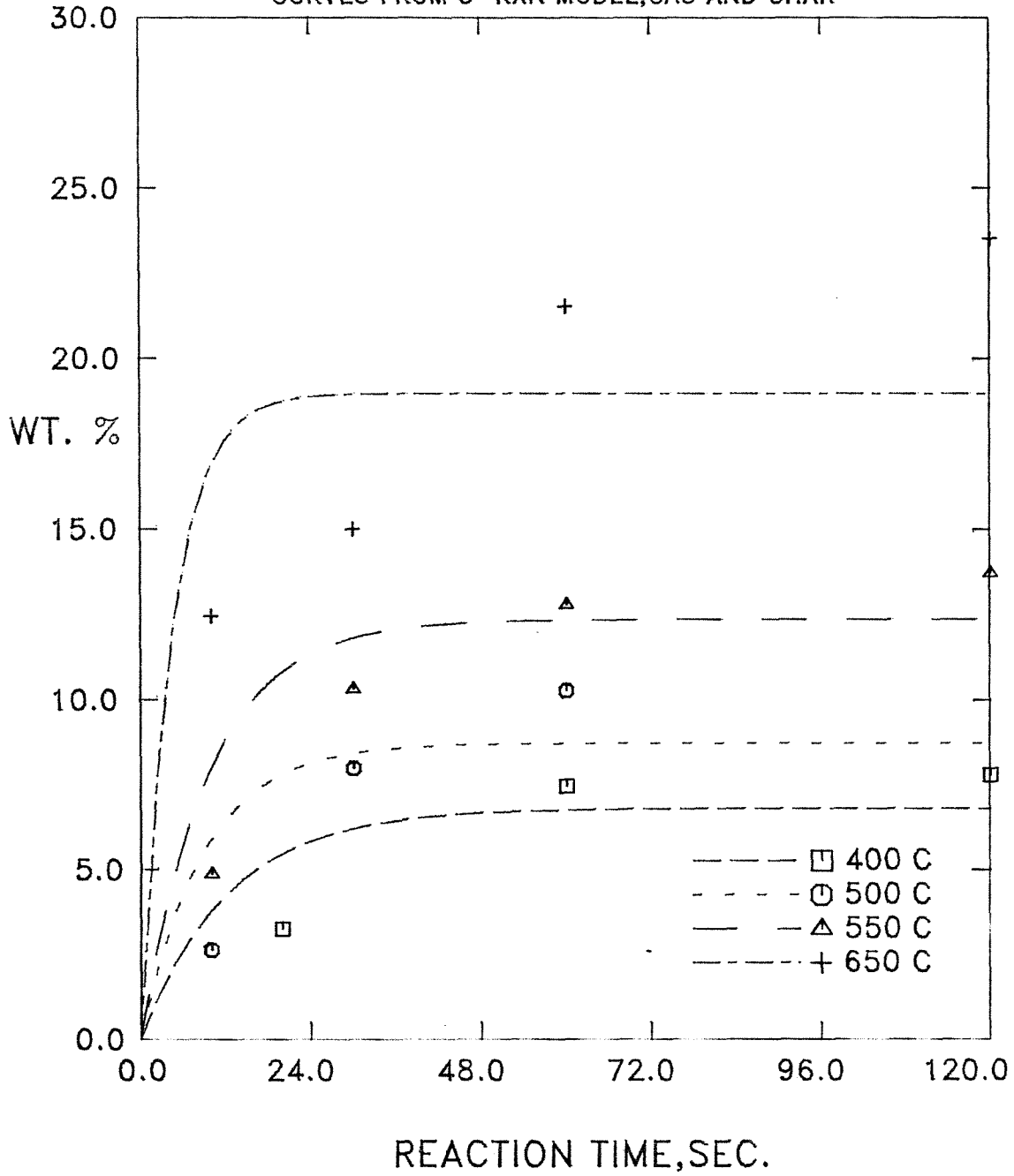


FIGURE A-6
CHAR FROM PYROLYSIS OF LIGNIN
(DATA OF IATRIDIS AND GAVALAS)

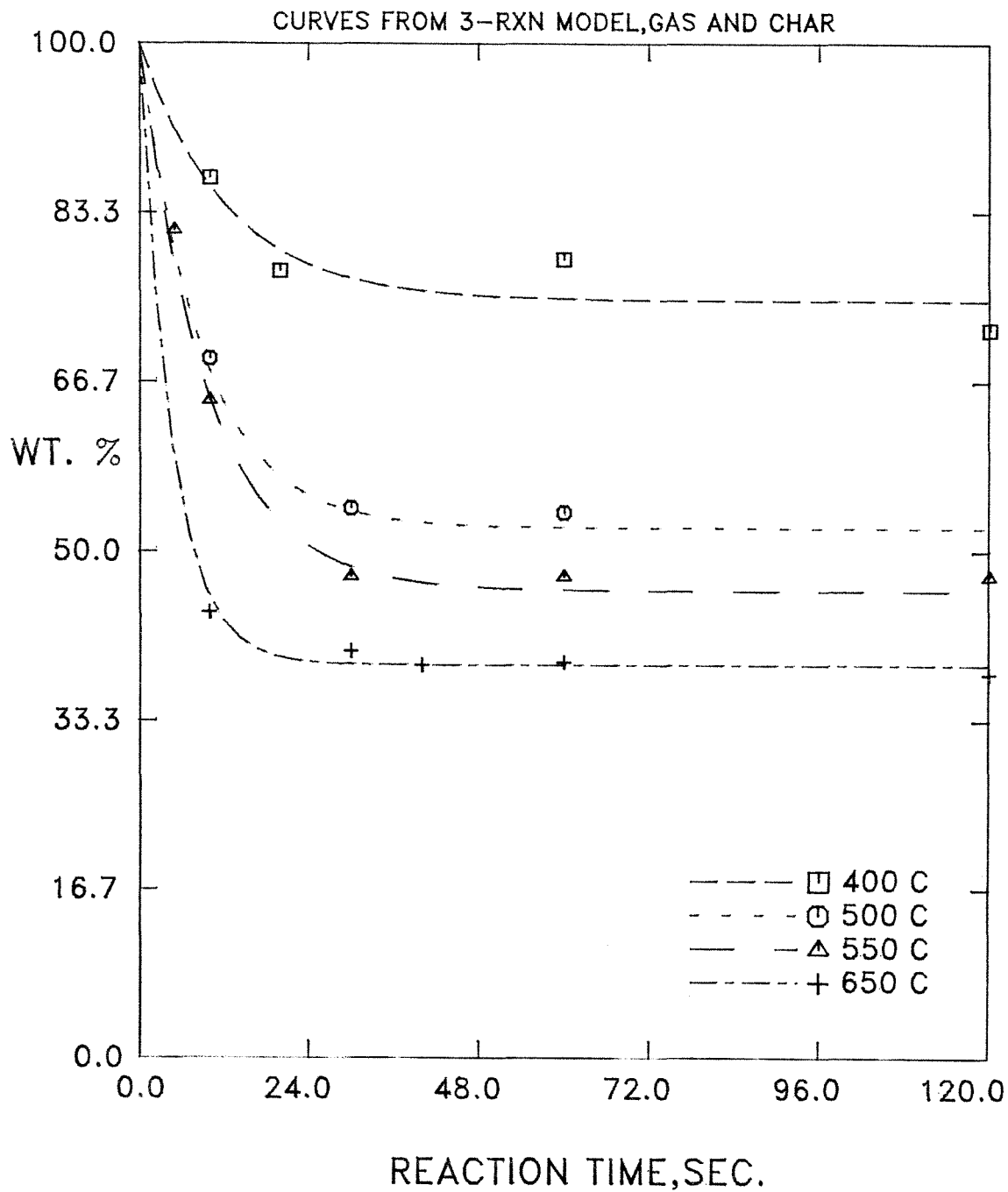


FIGURE A-7
VOLATILES FROM PYROLYSIS OF LIGNIN
(DATA OF IATRIDIS AND GAVALAS)

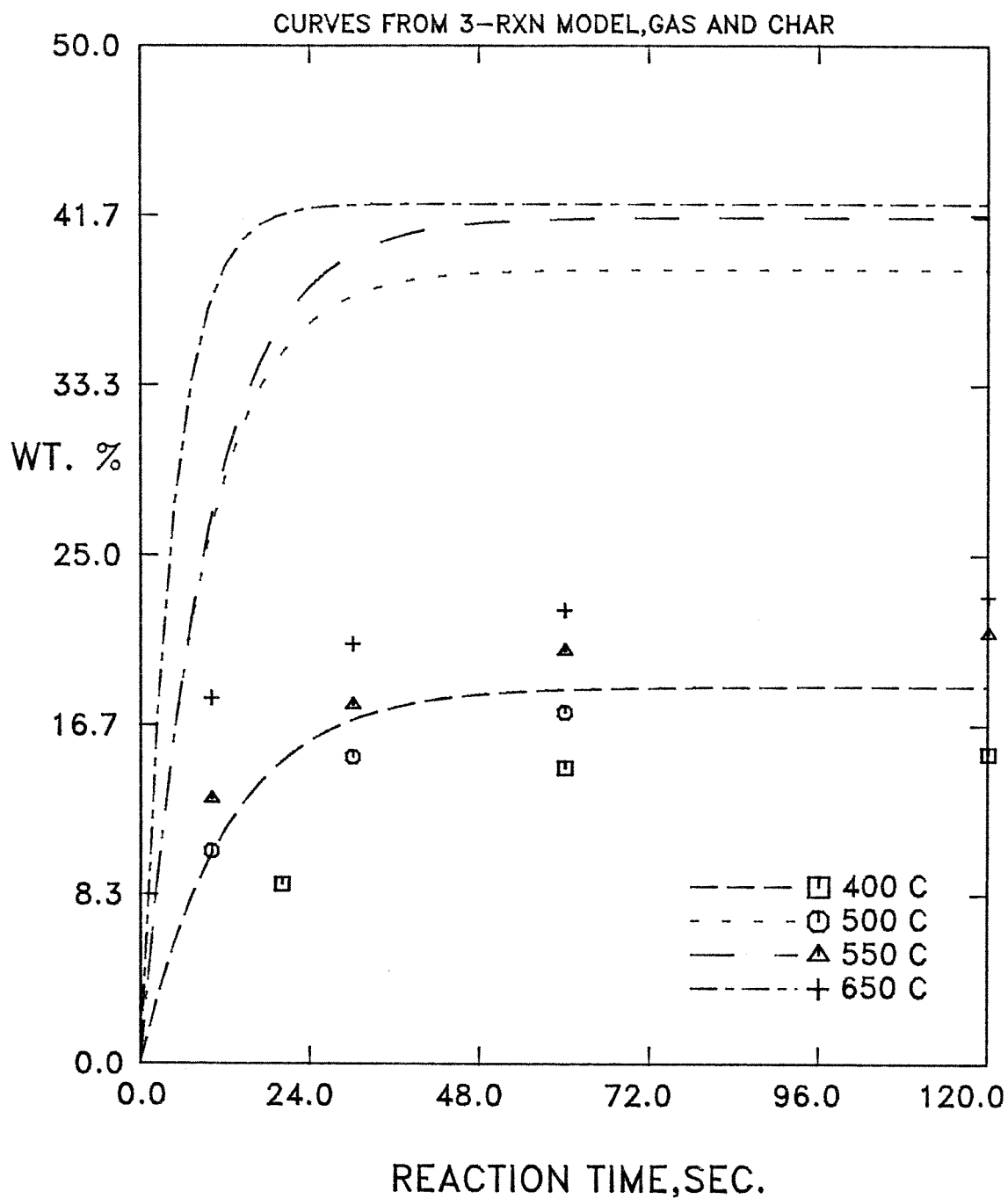


FIGURE A-8
ARRHENIUS PLOT FOR PYROLYSIS OF LIGNIN
MODEL FIT TO GAS DATA
(3-REACTION MODEL, DATA OF IATRIDIS AND GAVALAS)

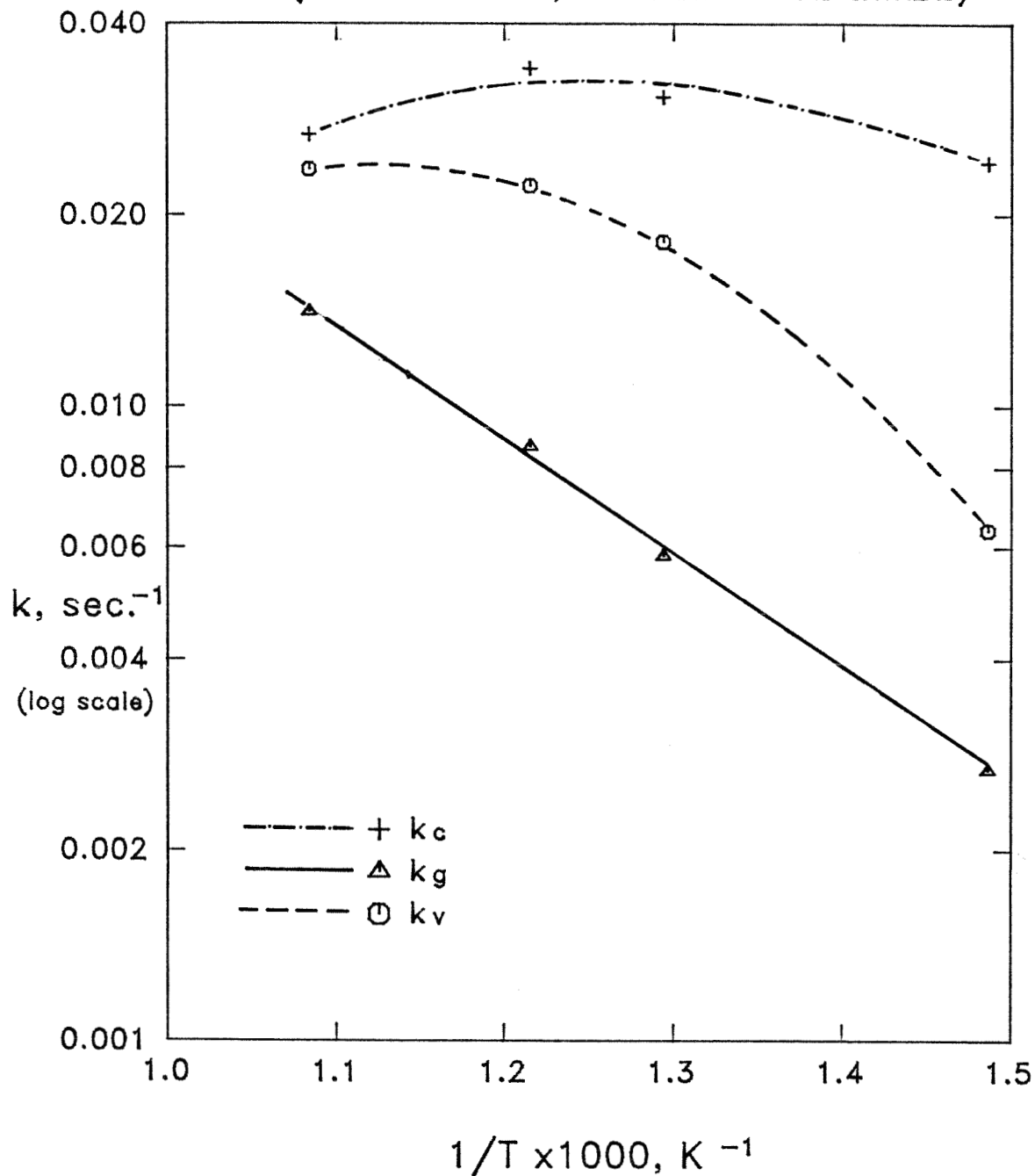


FIGURE A-9
ARRHENIUS PLOT FOR PYROLYSIS OF LIGNIN
MODEL FIT TO GAS AND CHAR DATA
(3-REACTION MODEL, DATA OF IATRIDIS AND GAVALAS)

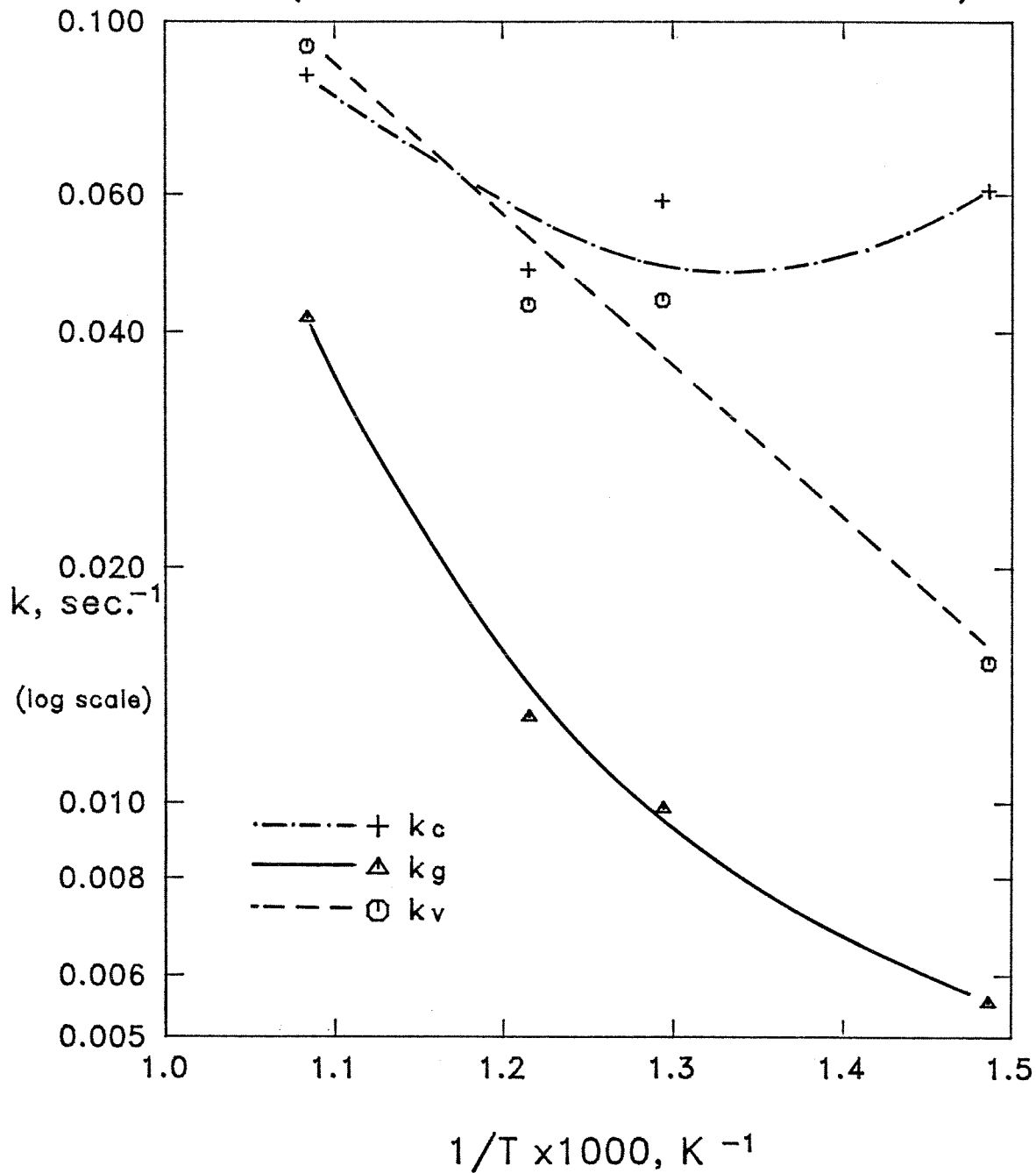


FIGURE A-10
CHAR FROM PYROLYSIS OF LIGNIN
(DATA OF IATRIDIS AND GAVALAS)

CURVES FROM MOD. 3-RXN MODEL,GAS AND CHAR

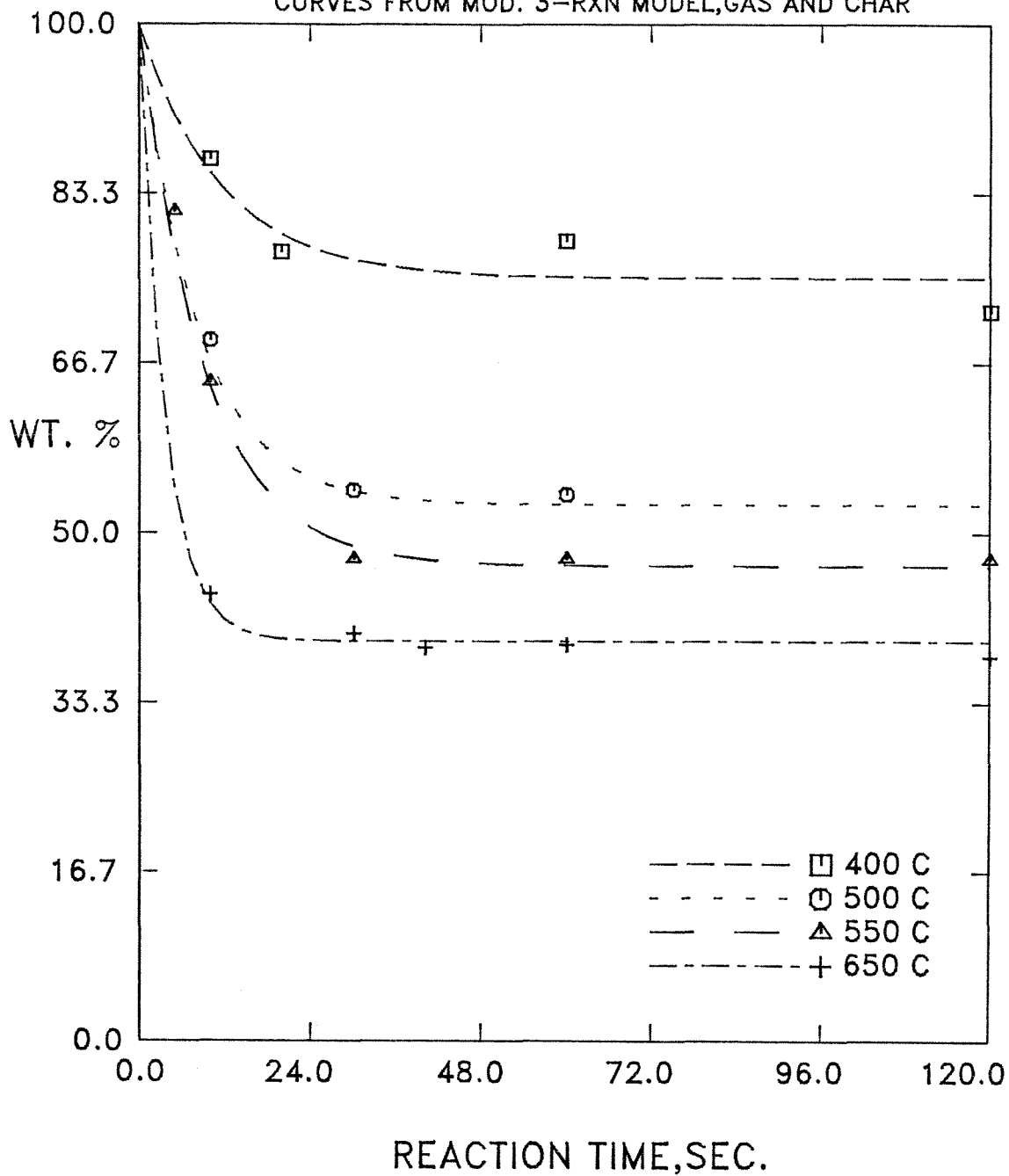


FIGURE A-11
GAS FROM PYROLYSIS OF LIGNIN
(DATA OF IATRIDIS AND GAVALAS)

CURVES FROM MOD. 3-RXN MODEL, GAS AND CHAR

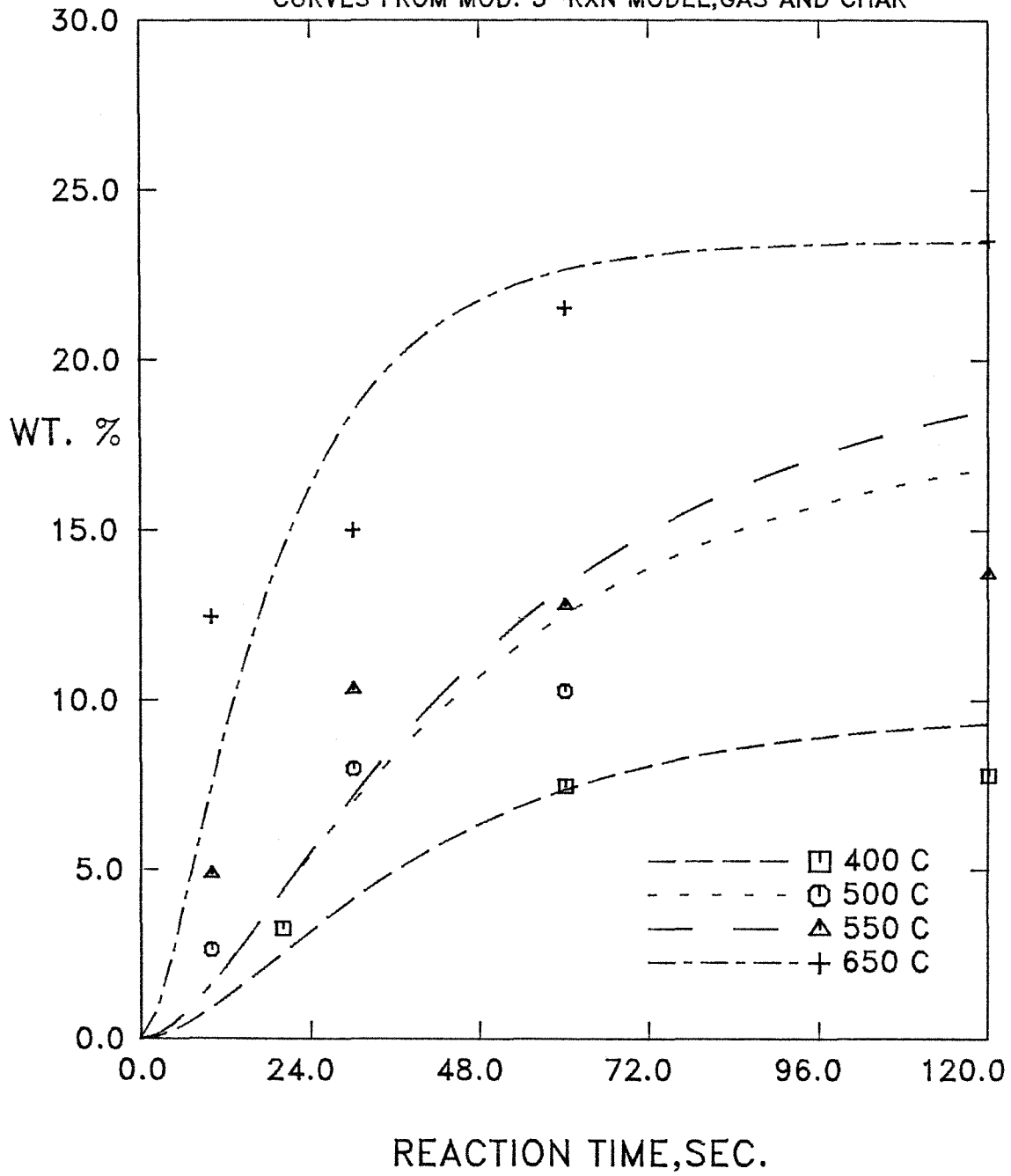
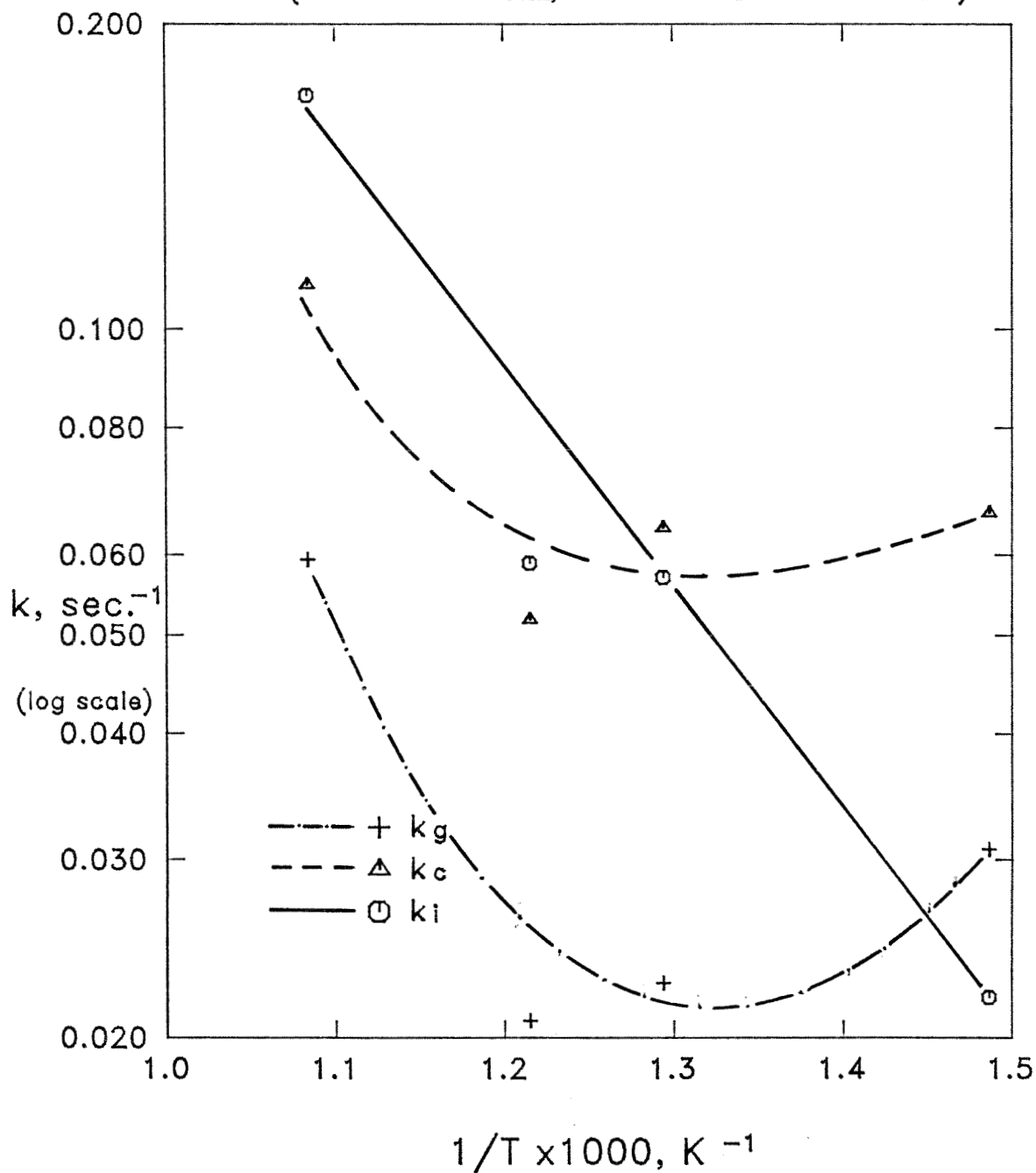


FIGURE A-12
ARRHENIUS PLOT FOR PYROLYSIS OF LIGNIN
MODEL FIT TO GAS AND CHAR DATA
(3-REACTION MODEL, DATA OF IATRIDIS AND GAVALAS)



APPENDIX B: VARPRO SUBROUTINE

The computations for fitting non-linear reaction models to experimental data in a least-squares sense were executed by the VARPRO subroutine which was developed at the Department of Computer Science, Stanford University, based on work by Golub and Pereya (1973) and Golub and LeVeque (1979). VARPRO is an acronym for Variable-Projection Algorithm, the algorithm utilized by the program.

B.1 Description of VARPRO Algorithm

The VARPRO routine was designed for problems of the separable type:

$$\eta(t) = \sum_{j=1}^n \beta_j \varphi_j(\vec{\alpha}; t) \quad (\text{B.1})$$

Expressions such as equation (B.1) are separable because the dependent variable $\eta(t)$ can be expressed as a sum of linear constants multiplied by non-linear functions φ_j of $\vec{\alpha}$, the vector of non-linear parameters, and the independent variable t . The object in a given problem is to determine the optimum set of β 's and $\vec{\alpha}$, which occur when the difference between the calculated and the measured $\eta(t)$ are minimized. If we express the problem in vector terms:

$$\vec{y} = \Phi(\vec{\alpha}) \cdot \vec{\beta} \quad (\text{B.2})$$

$$\text{where } \vec{y} = \begin{bmatrix} \eta_1 \\ \vdots \\ \eta_m \end{bmatrix}, \Phi(\vec{\alpha}) = \begin{bmatrix} \varphi_1(\vec{\alpha}; t_1) & \varphi_n(\vec{\alpha}; t_1) \\ \vdots & \vdots \\ \varphi_1(\vec{\alpha}; t_m) & \varphi_n(\vec{\alpha}; t_m) \end{bmatrix}, \text{ and } \vec{\beta} = \begin{bmatrix} \beta_1 \\ \vdots \\ \beta_n \end{bmatrix}$$

The least-squares procedure seeks to minimize the objective function,

$$r(\vec{\alpha}) = \left\| \vec{y} - \Phi(\vec{\alpha}) \vec{\beta} \right\|^2$$

is calculated by linear-least squares:

$$\vec{\beta} = \Phi^+(\vec{\alpha}) \vec{y} \quad (\text{B.4})$$

where $\Phi^+(\vec{\alpha})$ is the pseudoinverse of $\Phi(\vec{\alpha})$. Consequently the objective function becomes:

$$r(\vec{\alpha}) = \left\| \vec{y} - \Phi(\vec{\alpha}) \cdot \Phi^+(\vec{\alpha}) \cdot \vec{y} \right\|^2 \quad (\text{B.5})$$

The objective function $r(\vec{\alpha})$ is a function only of $\vec{\alpha}$ for a given set of data with functions φ_i . The vector $\vec{\beta}$ may be calculated at any time given a value for $\vec{\alpha}$ by means of equation (B.4).

The form of the objective function in equation (B.5) can be simplified by means of orthogonal transformations. For any $\vec{\alpha}$ there exists an orthogonal matrix $Q(\vec{\alpha})$:

$$Q(\vec{\alpha}) = \begin{pmatrix} Q_1(\vec{\alpha}) \\ Q_2(\vec{\alpha}) \end{pmatrix} \quad (\text{B.6})$$

which triangularizes $\Phi(\vec{\alpha})$ as follows:

$$\begin{pmatrix} Q_1(\vec{\alpha}) \\ Q_2(\vec{\alpha}) \end{pmatrix} \cdot \Phi(\vec{\alpha}) = \begin{pmatrix} U_1(\vec{\alpha}) \\ 0 \end{pmatrix} \quad (\text{B.7})$$

where $U_1(\vec{\alpha})$ is an upper triangular matrix. If $Q(\vec{\alpha})$ is multiplied into $r(\vec{\alpha})$ then,

$$\begin{aligned} r(\vec{\alpha}) &= \left\| \begin{pmatrix} Q_1(\vec{\alpha}) \vec{y} \\ Q_2(\vec{\alpha}) \vec{y} \end{pmatrix} - \begin{pmatrix} U_1(\vec{\alpha}) \\ 0 \end{pmatrix} U_1^{-1}(\vec{\alpha}) Q_1(\vec{\alpha}) \vec{y} \right\|^2 \\ &= \left\| \begin{pmatrix} Q_1(\vec{\alpha}) \vec{y} - Q_1(\vec{\alpha}) \vec{y} \\ Q_2(\vec{\alpha}) \vec{y} \end{pmatrix} \right\|^2 = \left\| Q_2(\vec{\alpha}) \vec{y} \right\|^2 \end{aligned} \quad (\text{B.8})$$

The VARPRO subroutine employed the Marquardt-Levenberg algorithm to operate on the simplified form of $r(\vec{\alpha})$ from equation (B.8) to determine the optimum value for $\vec{\alpha}$. The Marquardt-Levenberg algorithm is a modification of

operate on the simplified form of $r(\vec{\alpha})$ from equation (B.8) to determine the optimum value for $\vec{\alpha}$. The Marquardt-Levenberg algorithm is a modification of the Gauss-Newton convergence scheme in that it employs a variable parameter ν to speed convergence. The VARPRO routine accesses a subroutine written by the user to compute $\Phi(\vec{\alpha})$ and $\frac{\partial \Phi(\vec{\alpha})}{\partial \alpha_i}$, the Jacobian of $\Phi(\vec{\alpha})$, with each improved estimate for $\vec{\alpha}$. The VARPRO routine was written to encompass linear equations, separable-nonlinear equations and nonlinear equations. A normal least-squares technique is used with systems of linear equations. The Variable Projection Algorithm is not suitable for nonlinear equations which are not separable; only the convergence routine is accessed.

B.2 Test Calculation

An example from Osborn (1972) was used to test the convergence of the VARPRO routine. Table B.1 lists the data for the example problem. The data were fitted to a sum of exponentials:

$$\eta(t) = \beta_1 + \beta_2 e^{-\alpha_1 t} + \beta_3 e^{-\alpha_2 t} \quad (\text{B.9})$$

Table B.2 lists the optimum values of the linear and non-linear parameters for equation (B.9) as calculated by VARPRO from the sample data. The VARPRO program began computation by reading the values of t and $\eta(t)$ and an initial guess for α_1 and α_2 . The convergence of the algorithm was investigated by varying the initial guess for the α 's. Depending on the initial estimates VARPRO either converged to the optimum condition, diverged, or went into an oscillating cycle. The program did not converge to more than one optimum condition in the test case. Figure B-1 depicts the zone of convergence of the calculations, plotted against axes of α_1 and α_2 . Excepting points very close to the envelope of convergence, the program converged in 9 to 10 iterations. The largest number of

for α grew until the exponential terms could no longer be calculated.

Clearly two factors determined whether the computations would converge to the optimum condition. The first was the difference between the initial guess and the optimum solution. Guesses which were too much larger than the final result failed to converge. The second factor was that the ratio α_1/α_2 . No convergence was observed when the initial ratio α_1/α_2 was greater than 0.9. Consequently both the relative and absolute magnitudes of the initial estimates for α and α_2 influenced the convergence of the VARPRO routine.

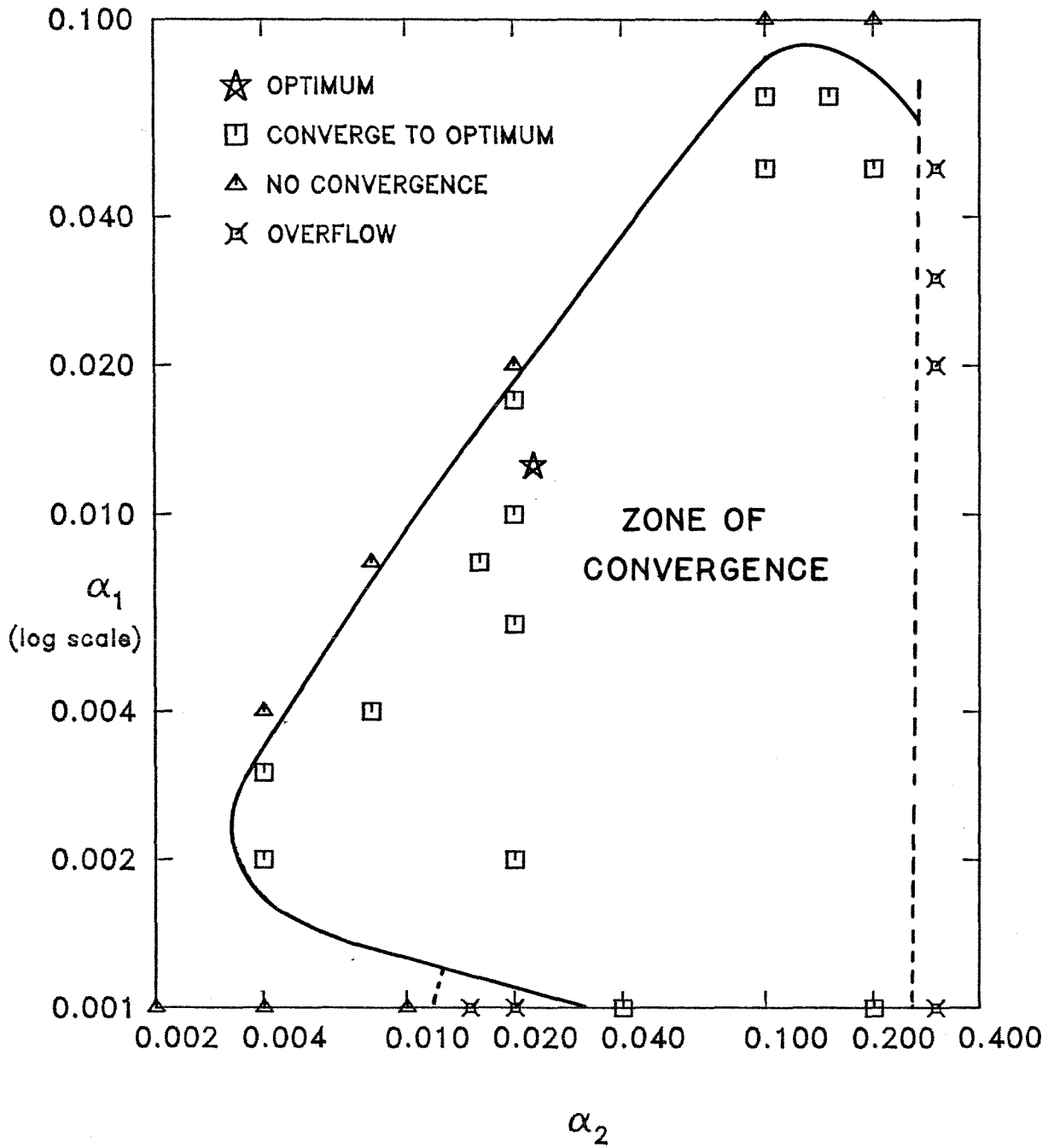
REFERENCES

- [1] Golub, G.H., and LeVeque, R.J., *Extensions and Uses of the Variable Projection Algorithm for Solving Non-linear Least Squares Problems*, , ARO Report 79-3 , Proceedings of the 1979 Army Numerical Analysis and Computers Conference, 1979.
- [2] Golub, G.H., and Pereya, V., *SIAM J. Numer. Anal.*, **10(2)** , 413-432, 1973.
- [3] Osborne, M.R.,in *Numerical Methods for Non-Linear Optimization* , ed. by C. Lootsma, Academic Press, London, 1972.

I	T(I)	Y(I)
1	0	0.844
2	100	0.908
3	200	0.932
4	300	0.936
5	400	0.925
6	500	0.908
7	600	0.881
8	700	0.850
9	800	0.818
10	900	0.784
11	1000	0.751
12	1100	0.718
13	1200	0.685
14	1300	0.658
15	1400	0.628
16	1500	0.603
17	1600	0.580
18	1700	0.558
19	1800	0.538
20	1900	0.522
21	2000	0.506
22	2100	0.490
23	2200	0.478
24	2300	0.467
25	2400	0.457
26	2500	0.448
27	2600	0.438
28	2700	0.431
29	2800	0.424
30	2900	0.420
31	3000	0.414
32	3100	0.411
33	3200	0.406

Table B.2. Optimum Parameters from VARPRO Test Case				
β_1	β_2	β_3	α_1	α_2
0.37541	1.935842	-1.464682	0.0128675	0.02212272

FIGURE B-1 CONVERGENCE OF VARPRO ROUTINE



APPENDIX C: REACTOR DESIGN AND PRELIMINARY TESTS

C.1 Reactor Design

A fluid-bed reactor was designed and assembled to allow:

- [1] complete recovery of char, tar, and aqueous products.
- [2] operation to 850 ° C at less than 135.9 kPa. to allow study of pyrolysis and gasification.
- [3] fluidization by steam, inert gas, or air
- [4] analysis of the gas stream by gas chromatography.

Figure C-1 depicts the reactor. Inert gas was supplied from a high- pressure cylinder, and steam was supplied to the reactor from a boiler where distilled, deoxygenated water was heated by high pressure steam from a steam line. The reactor was fabricated from 316-stainless-steel pipe and flanges and was designed with a removable liner to facilitate insertion and removal of samples. Figure C-2 is a detail of the reactor which illustrates the steel and glass wool employed to trap tar from the gas stream. The preheaters and reactor heaters had semi-cylindrical ceramic elements. One reactor heater was controlled proportionally while the remaining heaters were connected to on/off controllers.

The thermocouples indicated in Figure C-1 were Inconel-sheathed, type K probes referred to ice point. The electrical signals were recorded on a multipoint recorder, and one thermocouple at a time was recorded continuously and monitored on a digital meter.

The effluent gas from the reactor entered a condenser, a cold-trap, and a dessicant column in sequence, to remove condensable vapors and moisture. The condenser was equipped with a receiver which could be rotated to collect up to four liquid samples without exposing the system to the atmosphere. The effluent

from the dessicant column was sampled with either a 24-port Valco sample collection valve or a 6-port valve equipped with an automatic actuator. The gas from some runs was collected in a Teflon bag for later analysis.

Char was defined as the solid residue that remained in the liner after the run. Tar was the material which accumulated on the steel wool and the glass wool at the head of the reactor. The tar was removed by washing the wool and reactor liner with acetone. The washings were filtered to remove char and concentrated on a rotovap to remove the acetone. The filtrate was dried and weighed to correct the yield of char. A material balance on tar and aqueous material was achieved by weighing all parts before and after the run. The aqueous product was comprised of the liquid in the receiver, the fluid in the cold trap, and the weight absorbed by the dessicant.

When Woodex samples were pyrolyzed in the reactor the effluent gases and vapors passed through the steel and glass wool into a condenser at 5-10 ° C. A portion of the vapors were condensed and collected. The remaining vapors were collected downstream in a cold trap at -5 ° C and a dessicant-filled tube. The operation of the sample-collection system could be viewed as a rectification process with four stages and no reflux between stages. The highest-temperature stage was where the steel and glass wool were packed into the top of the reactor to trap tar components. The temperature of this stage was 100-150 ° C. The condenser was cooled by ice water. Downstream of the condenser was stage three, a cold trap packed with glass wool and cooled to 0 ° C to -5 ° C in a salt-ice bath. The final stage was a tube packed with dessicant. The effective dewpoint of the dessicant effluent was on the order of -20 ° C.

The analogy relating the collection system to a rectifying unit with four stages extended further than a description of the temperatures of the stages.

Like any multicomponent separation the degree of separation at each stage was limited by thermodynamic and mass transfer constraints. For example acetic acid would accumulate mainly in the condenser, with a small fraction escaping into the cold trap. The actual distribution between the two stages would depend on the temperature and efficiency of the condenser. Effectively all of the acetic acid would be trapped within the collection system. Wood can smoke during pyrolysis. Smoke is an aerosol made up of char particles, droplets of tar, and water vapor (Boyd et al., 1979; Graboski and Bain, 1979). The glass wool in the reactor and the cold trap was intended to trap smoke.

Once the production of volatile material ceased within the reactor the collected tar in the top of the liner would be selectively stripped of light components by the flowing gas. The light components would be deposited in later stages. Samples in the condenser would not be stripped because they dropped down into a receiver away from the flow of gas.

Given our understanding of the sample collection process, we can recognize several points which would affect the composition of the condensate samples.

- [1] Gas Flow - The stripping effect would increase with gas flow, and the efficiency of each stage for trapping material would decrease.
- [2] Time of Reaction - The extent of stripping would increase as the flow of gas continued.
- [3] Temperature of Reactor - The trapping and stripping of tar components would be affected by the temperature at the top of the reactor.
- [4] Residence Time - The reactor-residence time for each component in the aqueous condensate would differ with the above factors. Such effects are relevant when time, temperature, and composition data are combined into

a kinetic model.

In the first runs calcium sulphate was used as an absorbent to remove water. Moisture escaped the dessicant to interfere with the GC analysis of the effluent gas. One run used molecular sieves to trap water but the sieves were so effective that they affected the elution of CO₂. Magnesium perchlorate was found to be effective in water removal but did not affect the CO₂.

C.2 Reactor Operation - Slow Pyrolysis

The operating techniques for the reactor developed during the first series of runs. In early runs the reactor was allowed to heat up by setting the final set point on the controllers and allowing the reactor to reach operating temperature. The main operating steps in the fully developed procedure were as follows:

- [1] Purging the reactor with inert gas to remove air
- [2] Switching on preheaters and allow to come to final reaction temperature.
- [3] Beginning of flow of fluidizing gas at desired final rate. The flowrate of gas was based on the measurements described in Appendix D. An operating factor of 1.5 times the minimum gas flow was used to ensure vigorous bubbling in the fluid bed.
- [4] Setting the reactor heaters to a set point well above the final temperature. When the temperature had risen enough reset controllers to final desired temperature.
- [5] As the reactor temperature rose the gas flow was pulsed to eliminate clumping and binding of the sample.

The rate of heating of the sample was on the order of 30 °C/ min. when the reactor was started from room temperature. Recall that the injection technique

described in Sections [4] and [5] gave rates on the order of 300 °C.

C.2.1 Gas Analysis. The early reactor tests used a Hewlett- Packard 5750 gas chromatograph equipped with a thermal-conductivity detector for the gas analysis. The chromatographic columns were packed with Carbosphere, a carbon molecular sieve which separates hydrogen, oxygen, nitrogen, carbon monoxide, carbon dioxide, and light hydrocarbons.

The columns were heated to 150 ° C to give a reasonable analysis time per sample. Unfortunately the retention times for CO and N₂ were almost identical so that trace amounts of CO could not be detected. Replacement of the N₂ with argon did not eliminate the problem. Finally helium was used as the fluidizing gas. Since helium was also in use as the carrier gas in the GCs, a new procedure was developed.

With helium as the fluidizing gas, mixtures of CO, CH₄, and CO₂ could be separated on a 6' Porapak QR column at room temperature in less than three minutes. Any hydrogen in the effluent gas would appear during the transient peaks caused by switching the sample valve into the column. The yield of hydrogen was expected to be insignificant due to the relatively low reaction temperatures. Such a rapid analysis allowed the use of on-line measurements using a PE 3920 GC which was equipped with an automatic actuator. Gas samples were collected in a 0.44 ml. loop and then switched into the column for analysis. A thermal-conductivity detector was used. Prior to the start of a run the purge gas from the reactor was sampled to ensure that all of the air had been removed from the system. Only when no air was detected in the chromatogram was the sample heated. The on-line method was used for run numbers 8 and up.

C.2.2 Aqueous Condensate Analysis. The aqueous condensates collected in the receiver and cold trap were analyzed on a Perkin Elmer 3920 chromatograph equipped with dual 6' SS. Porapak QR columns and flame-ionization detectors. Porapak is a porous resin. The packing was pretreated by washing with acetone to remove residual monomers and initiators. The Porapak was vacuum dried and conditioned at 250 ° C for 24 hours in He. A sample volume of 0.8 μ l. was injected from a syringe equipped with a Chaney adaptor to ensure reproducibility.

The identities of individual peaks in each sample of condensate were checked by spiking the samples with known compounds.

C.2.3 Tar Analysis. Tar collected in the top section of the reactor where the temperature was lower. Glass and stainless-steel wool was inserted in the top of the liner to encourage condensation of the tar. When the reactor had cooled following a run, its top was disassembled, and the liner was removed. Any sections which came in contact with tar were cleaned in acetone. The weight of tar formed was determined by weighing the reactor parts before and after cleaning.

C.3 Slow Pyrolysis of Woodex in Nitrogen

The initial series of five runs were intended to develop operating methods and to observe the effects of temperature on the pyrolysis of Woodex. The relevant operating parameters are listed in Table C.1. The time of reaction and the flow of fluidizing gas were not varied significantly from run to run so that the stripping of liquid components which was described earlier was fairly constant.

C.3.1 Products of Woodex Pyrolysis Table C.2 lists the yields of the products of pyrolysis from the first sequence of runs. As operating techniques improved the mass balance rose to 95%. Figure C-3 illustrates the effect of temperature on the yields of the products. The trends of less char and more volatiles and gas with higher reaction temperatures confirmed the observations of previous investigators. The definitions of aqueous condensate and tar were based on the means of sample collection. Condensate samples accumulated in the condenser and tar samples were trapped by the glass and steel wool inside the reactor. Water removed in the ice trap and dessicant were lumped with the condensate yields.

C.3.2 IR Spectra of Char from Pyrolysis of Woodex The infra-red spectra of char samples from the pyrolysis of untreated Woodex were measured. The major peaks in each spectrum are listed in Table 2.3. The ratios of absorptions within each spectrum are listed in Table C.3. The absorptions at 1725 cm^{-1} and 1510 cm^{-1} declined with rising temperature relative to the absorption at 1610 cm^{-1} . This reduction was due to the loss of carboxylic and aromatic groups respectively. The decomposition of carboxylic acids would yield carbon dioxide as a major product. The decrease in A_{1510}/A_{1610} was much more difficult to explain as both peaks were due to aromatic groups. The absorption of lignin and polyphenols at 1510 cm^{-1} was due to vibrational coupling between ring stretching and C-H bond deformation (Hergert, 1971). The almost complete disappearance of the 1510 cm^{-1} peak with increasing temperature indicated a reduction or shifting of C-H coupled vibrations, relative to the vibrations within the aromatic rings. At least two explanations are reasonable:

- [1] Condensation of aromatic structures increased at higher temperatures which resulted in a loss of hydrogen and larger aromatic groups with fewer

vibrational modes.

- [2] Aromatic rings which contained hydrogen side groups were lost preferentially to the tar fraction. The light phenols would desorb at higher temperatures, leaving a char with less aromatic hydrogen.

What was the implication of the decreasing absorption by carboxylic acid groups? Presuming that the groups decomposed to give CO₂ and char, the mechanism by which a large portion of the measured CO₂ was generated was explained. Untreated Woodex contained 0.77 meq./gram of carboxylic acid groups. If the acids decomposed to yield CO₂ then the decomposition of all acids would yield 3.4 % of CO₂ by weight. Comparison with Table C.2 demonstrates that such a mechanism would account for half of the CO₂ measured at the highest reaction temperature.

C.3.3 Composition of Condensate Samples The procedure described in section [C.2.2] was used to analyze the samples of aqueous condensate. The color of the samples varied from clear to yellow-brown depending on the reaction conditions. Table C.4 lists the yields of the major components of the condensate for each reactor test. More of compounds such as methanol and 1-hydroxy-2-propanone were formed at higher temperatures. The yields of organic components were similar to the results from rapid pyrolysis at 330°C (see Table 5.5).

Furfural derived from saccharides in the Woodex. The dehydrated sugars would be subject to further cracking and rearrangement reactions to yield smaller species such as 1-hydroxy-2-propanone, methanol, or CO₂.

In every run the later samples were enriched in organic compounds of low volatility such as phenol. The presence of such species could be due to stripping of the tar by the flowing gas or by desorption from the surface of the char.

Quantitative comparisons between Table C.4 and the results of previous investigators were of little utility. Klein and Virk (1981) pointed out that differences in sample preparation, composition and reaction environment affect the results of pyrolysis experiments. Nevertheless the spectrum of compounds observed were qualitatively in agreement with the data of Hileman et al. (1976) from the pyrolysis of Douglas fir and the data of Shafizadeh and Chin (1976) for the pyrolysis of cottonwood.

One factor which limited the comparisons between the data of different investigators was the method of identifying the peaks from the chromatograph. Hileman et al. (1976) used mass spectrometry. Shafizadeh and Chin (1976) did not reveal their experimental method. The technique of using retention times and spiking the samples with known compounds, as in this study, was limited by the separation achieved by the chromatographic column. Use of a mass spectrometer does not necessarily give more reliable identification of compounds. A given peak from a chromatograph can give rise to a spectrum of lines from a mass spectrometer. Each line derives from a molecular fragment of a given mass. Differentiation between similar compounds such as hydroxyethanal ($C_2O_2H_4$) and acetic acid ($C_2O_2H_4$) tends to be arbitrary. Both the resolution of the GC and the interpretation of the mass spectra affect the identification of compounds.

C.4 Effect of Heating Rate on Pyrolysis of Woodex

In the early reactor experiments the wood was heated from room temperature to a target temperature of 330 ° C. Figure C-1 in Appendix C shows the product distribution from these samples with different maximum temperatures. The heating rate of these samples was on the order of 30°C/min., as compared to 300 ° C/min. for samples injected with the draft tube (Sections

[4] and [5]). In Figure C-1 the samples at 330 ° C had a simple temperature history and can be compared to draft tube results, in Figure 5-1. (See also Tables C.2 and 5.6.) The yields of the individual products are very close, within 3 yield points. We must conclude that the final reaction temperature is more significant than the heating rate, within the range tested, in determining the product distribution from pyrolysis.

Moisture in the wood lowers the temperature during the initial phase of pyrolysis, due to the latent heat of the water. Hence a moist sample has a slightly lower effective heating rate than does a dry sample, at a given reactor temperature. Any change in the heating rate due to the presence of 16 or 28 % moisture would be much less than an order of magnitude. Yet from the early tests we see that a tenfold change in the heating rate only gave a 3 yield % change in the products, so we must conclude that the effect of moisture on products, by means of the heating rate, must be small.

If heating rate were significant, then we could quantify its effect by defining a mean temperature of pyrolysis. The lower the heating rate, the lower the mean temperature, for a given final reactor temperature. Moist samples would have lower mean reaction temperatures, so a plot of yield versus temperature would give a curve that would be shifted to the right on the temperature scale, relative to dry samples. The temperatures reported in all tables and figures are the final reactor temperature. At a given final temperature the moist sample would always give more char and less volatiles. Figures 5-2 and 5-3 show that this does not occur, so we must conclude that the influence of water is not via the heating rate. Furthermore moisture only lowered the temperature in the reactor by at most 10 C° once the sample had been introduced into the heated zone, so the magnitude of the shift in temperature would be small.

C.5 Effect of Initial Composition on Pyrolysis of Woodex

A series of preliminary runs were conducted to investigate the effects of ash content, calcium content, moisture, and oxidation on the pyrolysis of Woodex. The reaction conditions are listed in Table C.5. The basic operating procedures and techniques for analysing products were as described earlier. These tests were not checked for reproducibility of results. See Section [5] for a comprehensive discussion of the effects of ash and moisture. The following sections highlight differences between the early tests and the data presented in Section [5].

C.5.1 Effects of Calcium on the Pyrolysis of Woodex Table C.6 lists the yields of products from the pyrolysis of acid-washed Woodex and Ca-exchanged Woodex. The table also shows the ash and calcium contents of each sample. The addition of the calcium ions reduced the yield of char and increased the yield of aqueous material. The yield of char dropped from 63% to 59% (1.1 g. in a 25 g. sample) and the yield of aqueous material increased by 6.3% of the initial sample weight, or 1.6 grams in a 25g. sample. The effect of the calcium on the other products was not as noticeable. By comparison, rapid pyrolysis at 330°C showed no change in the yield of char with calcium content. Although the difference in char yields could be due to the heating rate, the accuracy of the early results is likely such that the magnitude of the changes are of the same order as the experimental error. The effect of calcium on the composition of the condensate (Table C.7) was similar to the results from rapid pyrolysis.

C.5.1.a IR Analysis of Char from Ca-exchanged Woodex Table C.8 lists the ratios of the significant peaks from the infra-red spectra of char from runs 6 and 7. The spectra were in accord with the findings discussed earlier. The lower yield of aqueous material from the acid-washed Woodex should have resulted in a char

with a higher content of OH groups. Table C.8 shows that the OH groups did indeed remain in the char as evidenced by the ratios A_{3420}/A_{2910} and A_{3420}/A_{1610} , which are considerably larger than the same ratios from the char of Ca-exchanged Woodex. The ratio A_{2910}/A_{1610} indicated that the char of the acid-washed Woodex contained more aromatic units than did the char from Ca-exchanged Woodex. Two factors could be responsible for this effect:

- [1] Lower extent of pyrolysis of lignin which left more aromatic nuclei in the char.
- [2] Greater degree of condensation of polysaccharides and lignins giving rise to polymeric-aromatic structures.

C.5.2 Effect of Moisture Content on the Pyrolysis of Woodex Tables C.9 and C.10 give the data for moistened Woodex. The differences in yield due to moisture are within the range of experimental error for the slow-pyrolysis method. With the low heating rate moisture would be almost completely driven off of the sample before pyrolysis could begin.

C.5.3 Effect of Air-Oxidation on the Pyrolysis of Woodex The sample which was pyrolyzed in run 9 had been heavily oxidized. A significant portion of the weight of the sample was lost during the air-oxidation procedure. Consequently, the results of the test should be interpreted as indicating the effects of extreme oxidation.

Table C.11 compares the yields from acid-washed Woodex to the yields from the acid-washed Woodex which had been oxidized in air at over 250°C for one hour. As we would expect the yields of tar and aqueous material were lower from the oxidized sample. We can view the extreme oxidation as a removal of the volatile materials from the wood. The reduction in the char yield was more surprising. The data indicated that when the oxygen attacked the wood,

structures were created which were more likely to yield gas. One candidate would be carboxylic acids. The attack of the oxygen was not accompanied by condensation reactions. If the wood structure were more condensed then the yield of char would be higher from the oxidized sample. An important point to recall is that the yields in Table C.11 were based on the weight of the sample prior to oxidation. Otherwise we would not have a sound basis for comparison.

C.5.3.a Composition of Condensate As we would expect from the low yield of aqueous material, the organic compounds in the condensate were not produced in high yields (Table C.12). Acetic acid and 1-hydroxy-2-propanone formation were relatively unaffected by the oxidation. Other compounds such as furfural and methanol were produced in smaller amounts from the air-oxidized sample. An interesting exception was 2-furfurol. In previous samples more 2-furfural was produced than 2-furfurol. In many samples furfural was not detected. When the oxidized sample was pyrolyzed, furfural was produced in a yield of 0.731% as compared to 0.0% from the acid-washed sample. Eight times as much furfuryl alcohol as furfural was produced from the oxidized sample. The oxidation apparently affected the reactions which form the two compounds so that furfuryl alcohol was formed instead of furfural.

REFERENCES

- [1] Boyd, M. et al., *Pyrolysis and Gasification of Hybrid Poplar SPP*, paper presented at AIChE Annual Meeting, San Francisco, 1979.
- [2] Graboski, M., and Bain, R., in *A Survey of Biomass Gasification Vol II- Principles of Gasification*, Solar Energy Research Inst., July, 1979.
- [3] Hergert, H.L., in *Lignins*, eds. Sarkanen, K.V., and Ludwig, C.H., Wiley, New York, 1971.
- [4] Hileman, F.D., et al., in *Thermal Uses and Properties of Carbohydrates, Lignins*, ed. F. Shafizadeh, ACS, 49-71, 1976.
- [5] Klein, M.T. and Virk, P.S. *Model Pathways in Lignin Thermolysis*, Massachusetts Institute of Tech. Energy Lab. Rep. MIT-EL 81-0015, 1981.
- [6] Shafizadeh, F., and Chin, P.P.S., in *Wood Technology: Chemical Aspects*, I.S. Goldstein ed., ACS Symp. Ser. No. 43, 57-81, 1976.
- [7] Tyler, R.J., and Schafer, H.N.S., *Fuel* **59**, 95-102, 1980.

Table C.1 Reaction Conditions For Pyrolysis of Woodex in N ₂					
Run No.	1	2	3	4	5
Max. Temp., ° C	362	296	367	331	336
N ₂ Flow, ft ³ /sec. x 10 ³	1.69	1.69	1.58	1.58	1.58
Pulse Heating	N	Y	Y	Y	Y
Preheat to 150 ° C	Y	Y	N	N	N
Dessicant	drier	drier	dehyd	dehyd	dehyd
Pressure, inches H ₂ O	8	8	8	12	12
Gas Analysis	HP5750	HP5750	HP5750	HP5750	HP5750

Table C.2 Yields of Products from the Pyrolysis of Untreated Woodex in Nitrogen					
Maximum T, ° C	Yield of Product as a % of Initial Wt.				
	Char	Aqueous	Tar	Gas	Total
296	68.9	13.6	7.9	1.7	92.2
331	54.5	22.3	11.0	6.1	93.8
336	52.0	23.7	16.3	3.2	95.2
362	46.2	25.0	21.7	7.3	100.2
367	43.3	25.9	18.8	7.5	95.5

Table C.3 IR Absorbance Ratios of Char from Pyrolysis of Woodex		
Maximum Temp., ° C	$\frac{A_{1725}}{A_{1610}}$	$\frac{A_{1510}}{A_{1610}}$
25	0.333	0.5185
296	0.220	0.334
331	0.182	0.242
336	0.098	0.121
362	0.119	0.075
367	0.052	0.019

Table C.4 Condensate Analysis from Pyrolysis of Woodex in N ₂					
Compound	Component Yield as % of Initial Weight				
	2	4	5	1	3
Run No.	296	331	336	362	367
Max. Temp. ° C					
methanol	0.108	0.193	0.128	0.267	0.252
acetic acid	1.072	1.304	1.083	1.679	1.433
1-hydroxy-2-propanone	1.091	1.886	1.571	2.143	1.439
2-furfural	0.125	0.198	0.159	0.289	0.200
guaiacols	0.244	0.097	0.069	1.276	0.221

Table C.5 Reaction Operating Conditions - Compositional Tests				
Run No.	6	7	8	9
Sample	Ca-Exchanged	Acid-Washed	Moistened	Air-Oxidized
Max. Temp., ° C	333.5	332	338	333
Fluidizing gas	N ₂	Ar	He	He
Gas Flow, ft ³ /sec x 10 ³	1.58	1.24	3.02	1.53
Pressure, inches H ₂ O	14	14	23	10
Dessicant	dehyd	dehyd	dehyd	dehyd
Gas Analysis	HP5750	HP5750	PE3920	PE3920
Pulse Heating	Y	Y	Y	Y

Table C.6 Material Balance for Ca-exchanged Woodex		
Sample	% of Initial Weight	
	Acid washed	Ca exchanged
Char	63.44	59.00
Tar	12.52	10.98
Aqueous	16.33	22.64
(Condensate)	(9.04)	(12.00)
Gas	1.54	1.83
Total	93.84	94.46
Ash	6.57	6.66
Calcium (as CaO)	0.00	1.65

Compound	Weight % of Initial Sample	
	Acid Washed	Ca Exchanged
methanol	0.081	0.126
2-oxopropanal	0.0	0.201
acetic acid	0.221	0.826
1-hydroxy-2-propanone	0.016	1.678
2-furfural	0.175	0.207
guaiacols	0.05	0.165
Total	0.423	2.7725

Sample	Ratio of Absorbing Groups		
	$\frac{A_{3420}}{A_{2910}}$	$\frac{A_{3420}}{A_{2910}}$	$\frac{A_{2910}}{A_{1610}}$
	O-H/C-H	OH/Aromatic	C-H/Aromatic
Acid-Washed	5.181	1.893	0.365
Ca-Exchanged	1.078	1.068	0.992

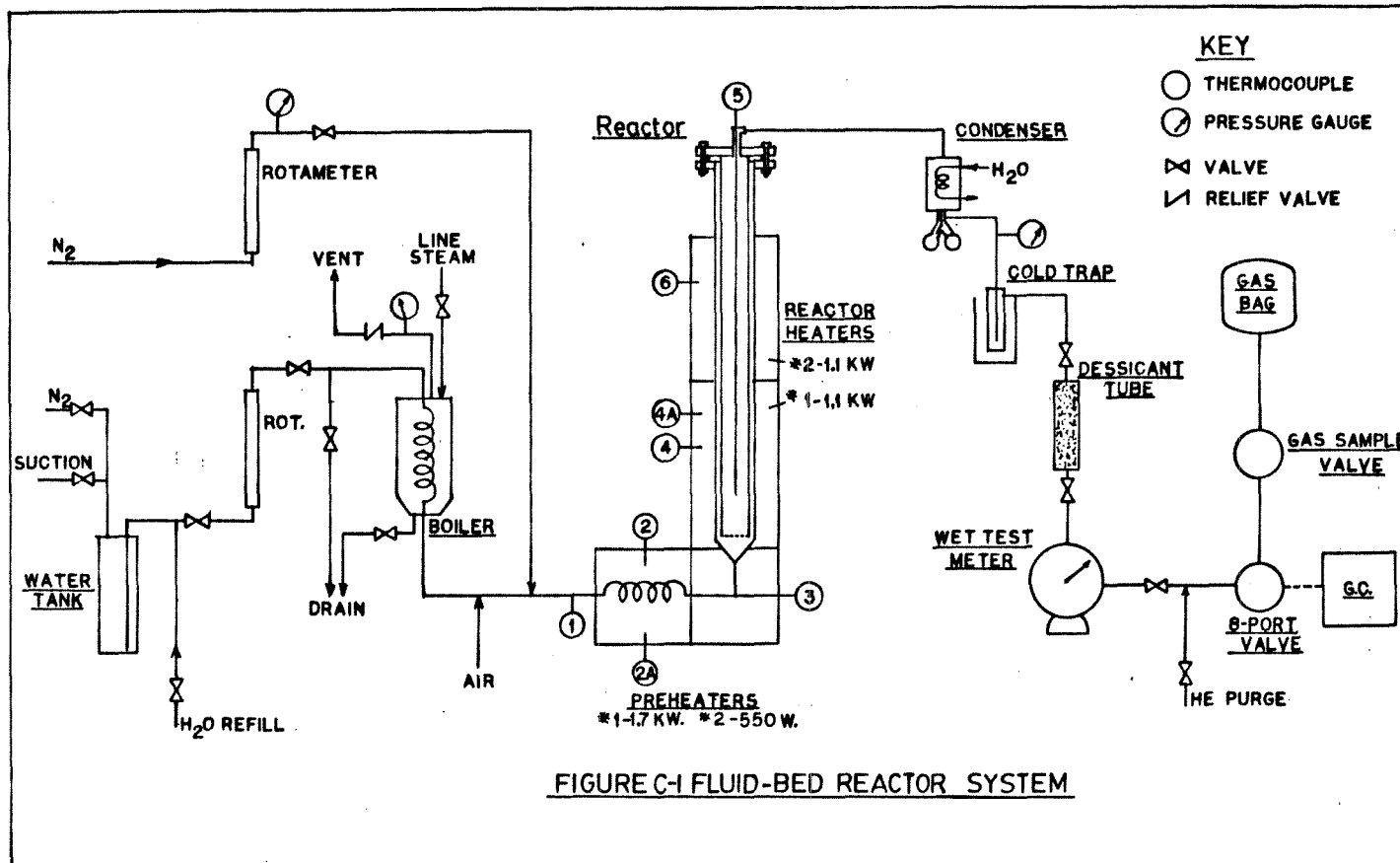
Table C.9 Material Balance for Moistened Woodex		
Sample	% of Initial Weight	
	Dry	Moistened*
Water	0.0	13.07
Char	53.26	51.74
Tar	13.62	9.57
Aqueous	22.98	29.82
Gas	4.66	7.08
Total	94.52	98.08

* - Yields are on a dry basis

Table C.10 Composition of Condensate from Moistened Woodex		
Compound	Weight % of Initial Sample	
	Untreated	Moistened
methanol	0.161	0.105
acetic acid	1.193	1.061
1-hydroxy-2-propanone	1.729	1.115
2-furfural	0.179	0.088
guaiacols	0.084	0.135

Table C.11 Material Balance for Oxidized Woodex		
Sample	% of Initial Weight	
	Acid Washed	Oxidized
Oxidized	0.0	18.78
Char	63.44	52.00
Tar	12.52	6.84
Aqueous	16.33	11.22
Gas	1.54	4.35
Total	93.84	101.71

Table C.12 Composition of Condensate from Oxidized Woodex		
Compound	Weight % of Initial Sample	
	Acid Washed	Oxidized
methanol	0.081	0.022
2-oxopropanal	0.0	0.016
acetic acid	0.221	0.247
1-hydroxy-2-propanone	0.016	0.015
2-furfural	0.175	0.094
2-furfurol	0.0	0.731
guaiacols	0.050	0.644



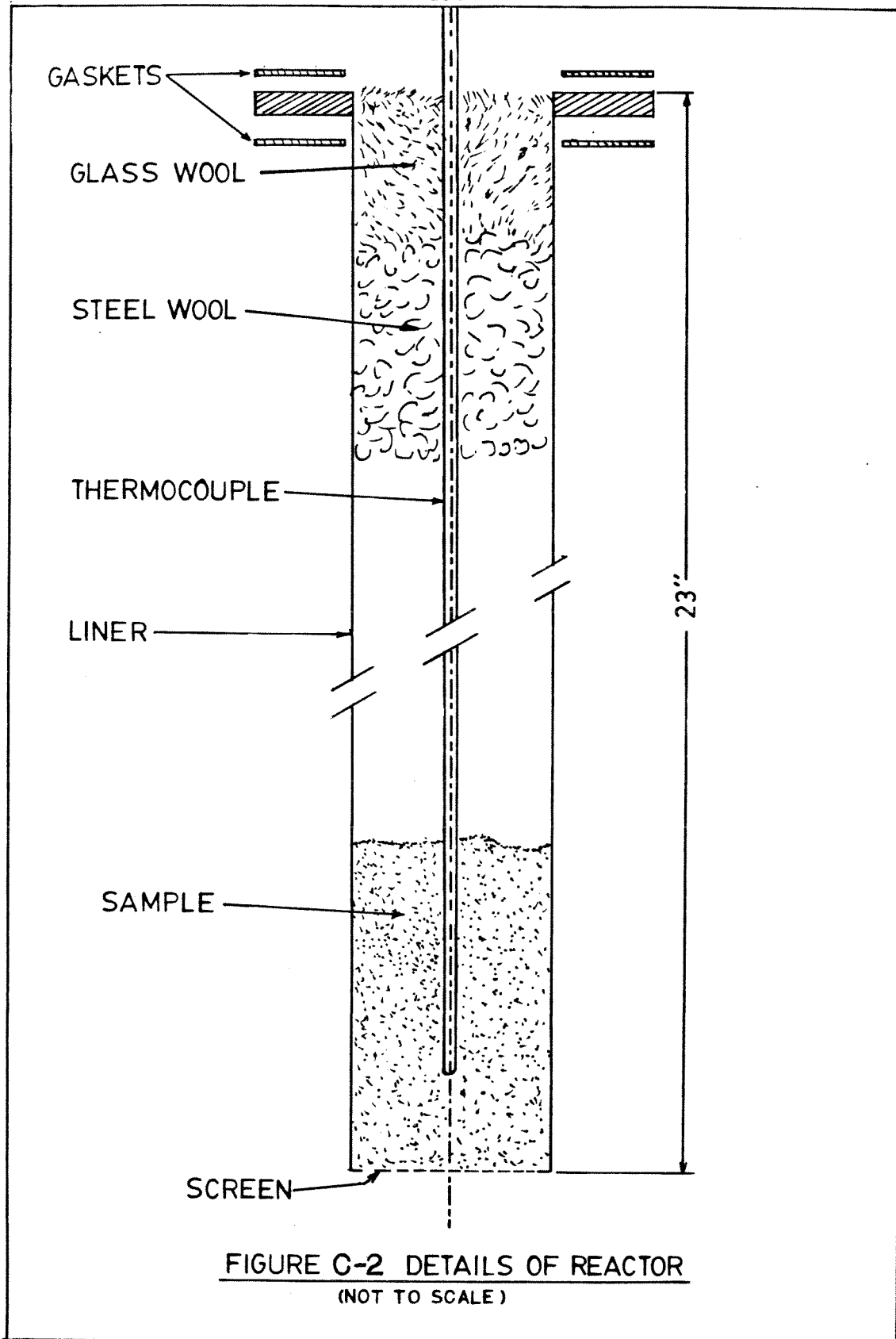
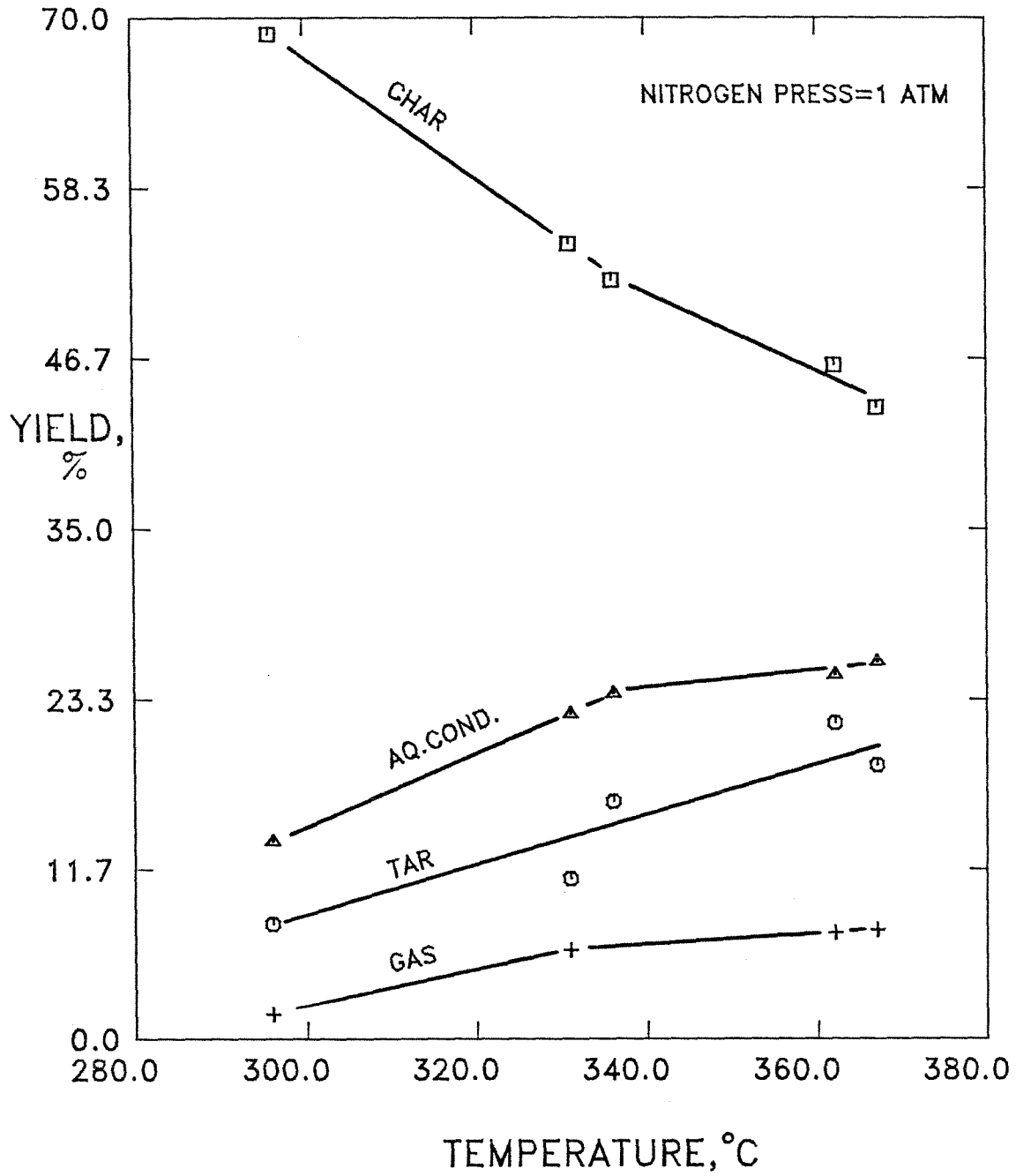


FIGURE C-3
EFFECT OF TEMPERATURE ON PRODUCT
OF PYROLYSIS OF WOODEX



APPENDIX D: FLUIDIZATION TESTS AND MATERIAL SELECTION

D.1 Prediction of Fluidization Velocity in Reactor

In the design of fluid-bed experiments it is convenient to measure the behavior of the solids under simulated conditions and then predict the fluid-bed behavior under reaction conditions. The following section outlines the relations which govern the behavior of fluid beds and provide the basis for predicting the variation of the fluidization velocity with gas properties.

Based on a balance between drag and particle weight, the fluidization velocity is given by the following relation (Kunii and Levenspiel, 1969):

$$\frac{1.75 \text{Re}_{p,mf}^2}{\varphi_s \varepsilon_{mf}^3} + 150(1 - \varepsilon_{mf}) \frac{\text{Re}_{p,mf}}{\varphi_s^2 \varepsilon_{mf}^3} = \frac{d_p^3 \rho_g (\rho_s - \rho_g) g}{\mu^2} \quad (\text{D.1})$$

where $\text{Re}_{p,mf}$ is the particle Reynolds number at the minimum fluidization velocity; φ_s is the particle sphericity; ε_{mf} is the void fraction of the particles at minimum fluidization velocity; d_p is the particle diameter; ρ is density; and μ is the fluid viscosity. For small, light particles, the equation simplifies to the form:

$$U_{mf} = \frac{K(\rho_s - \rho_p)}{\mu} \quad (\text{D.2})$$

where U_{mf} is the minimum fluidization velocity. K will be a constant for a given particle system so that equation (D.2) may be used to predict the effect of gas properties on the minimum velocity of fluidization.

At gas velocities greater than U_{mf} , additional gas flows through the particle bed as a second bubble-phase while the superficial velocity through the particle-phase remains constant. If the particles in the bed bind or clump, then the concept of minimum fluidization velocity is no longer relevant since there is no smooth transition from fixed to fluid-bed behavior. The particles may clump to form an annular ring or the gas may pass through the bed mainly in jets.

Binding and clumping depend on the particle structure and on the ratio of particle diameter to bed diameter.

Mixing in the bed will occur as rising bubbles exchange gas with the particle phase and entrain particles in their wakes. The rate of mixing will depend on the number and velocity of the bubbles in the bed. Gas-phase mixing will also depend on the rate of exchange between the particles and the surrounding gas.

D.2 Experimental

Several biomass materials were tested to determine their fluidization characteristics in a reactor having an inside diameter of one inch. Figure D-1 gives a schematic of the apparatus. Measurements were made in nitrogen at room temperature and pressure. The following materials were selected as being representative of waste materials which would be suitable for gasification:

- [1] Eco-Fuel II, a powdered, municipal-solid-waste derivative manufactured by Combustion Equipment Associates Inc. of New York. The waste is sorted to remove metal, glass, and plastic. The remaining material, largely cellulosic, is treated with an embrittling agent then ground to yield a free-flowing powder.
- [2] ROEMMC wood pellets, manufactured by Guaranty Fuels of Kansas from wood wastes.
- [3] Woodex pellets, manufactured from sawmill wastes by Bio-Solar Research of Oregon. The wastes are sieved and then heated and extruded into pellets. The combination of heat and pressure destroys much of the cellular structure of the wood and gives a denser product. The heat makes the lignin plastic so that it acts as a binder. No additives are required to hold the pellets together.

The wood pellets were ground in a Wiley mill, and all three materials were sieved to separate specific screen sizes. Harshaw Ni-0104 nickel methanation catalyst was ground and sieved and fluidized in mixtures with ground ROEMMC and Woodex pellets.

D.3 Results and Material Selection

Eco-Fuel II and Woodex particles fluidized when the particle size was less than 42 mesh. ROEMMC pellets could be fluidized only when a granular material such as catalyst was added in a 1:1 ratio.

Due to the tendency of the wood pellets to stick together, bubbling-bed behavior was not observed until the mixing effect of the flowing gas was great enough to break up clumps. For such a particulate system the velocity of interest was the minimum velocity to achieve a bubbling-bed. This velocity was correlated in the same way that the minimum fluidization velocity was treated in equation (D.2) to yield:

$$U_b = \frac{K^+ (\rho_s - \rho_g)}{\mu} \quad (D.3)$$

U_b = minimum velocity for a bubbling bed, ft./ sec.

K^+ = constant for a given material, $\left(\frac{\text{cp.} \cdot \text{ft.}^4}{\text{lb.} \cdot \text{sec.}} \right)$

ρ_s = density of solid particles, lb./ft.³

ρ_g = density of gas

μ = viscosity of gas, cp.

In the case of granular or spherical particles, K from equation (D.2) and K^+ will be related by a constant factor. Table D.1 lists the values of K^+ calculated from gas velocities in the fluid-bed apparatus.

Mixtures of Woodex ground and sized to 60-80 mesh and of Ni-0104 catalyst sized to 60-100 mesh formed a homogenous mixture at the same U_b as measured for Woodex alone, indicating that catalysts could be tested experimentally in a fluid-bed system. On the basis of the fluid-bed tests Woodex was selected as the most suitable material for further experimental work.

REFERENCES

- [1] Kunii,D. and Levenspiel,O., *Fluidization Engineering* , Wiley, New York, 1969.

Table D.1. Fluidization Velocities in Nitrogen at NTP				
Material	$\frac{\rho_s - \rho_g}{\mu}$ $\left(\frac{\text{lb.}}{\text{ft.}^3 - \text{cp.}} \right)$	US Mesh Size	U_b (ft/sec)	$K^+ \times 10^4$ $\left(\frac{\text{cp.} - \text{ft.}^4}{\text{lb.} - \text{sec.}} \right)$
ECO-FUEL II	1.67×10^3	35-48	0.642	3.85
		48-65	0.367	2.20
		65-100	0.275	1.65
		100-150	0.214	1.284
WOODEX	4.4×10^3	42-60	0.886	2.0
		60-80	0.488	1.03
		80-140	0.213	0.48
Ni-0104	1.12×10^4	24-42	0.703	0.63
		42-60	0.290	0.26
		60-100	0.138	0.124
		100-140	0.076	0.068

